NASA Contractor Report 168283

NUMERICAL SIMULATION OF TWO-DIMENSIONAL HEAT TRANSFER IN COMPOSITE BODIES WITH APPLICATION TO DE-ICING OF AIRCRAFT COMPONENTS

David Fu-Kuo Chao
The University of Toledo
Toledo, Ohio

November 1983

Prepared for

NATIONAL AERONAUTICS AND SPACE ADMINISTRATION
Lewis Research Center
Under Grant NAG3-72

TABLE OF CONTENTS

Page

NOMENCLATURE

$\hat{C}_p$	specific heat capacity (Btu/lb-°F)
E	dependent variable, H or T
H	enthalpy (Btu/lb)
h	heat transfer coefficient (Btu/ft^2-hr-°F)
K	thermal conductivity (Btu/ft-hr-°F)
KW	average thermal conductivity (Btu/ft-hr-°F)
L	the total length of the composite slab in the y-direction (ft)
L_f	latent heat of fusion for ice (Btu/lb)
q	rate of heat generation per unit volume (Btu/hr-ft^3)
q"	rate of heat generation per unit area (Btu/hr-ft^2 or Watts/in^2)
T	temperature (°F)
t	time variable (hr)
x	space coordinate in x-direction (ft)
$\bar{x}$	dimensionless space coordinate in x-direction
y	space coordinate in y-direction (ft)
$\bar{y}$	dimensionless space coordinate in y-direction

Greek Letters:

α	thermal diffusivity (ft^2/hr)
Δt	size of time step (hr)
$\Delta\bar{x}$	dimensionless grid spacing

NOMENCLATURE (CONTINUED)

Greek Letters:

$\Delta\bar{y}$	dimensionless grid spacing
θ	dimensionless temperature
ρ	density (lb/ft^3)

Subscripts:

b_1	inner ambient boundary
b_2	outer ambient boundary
g	the position in the center line of the gap
h	the position in the center line of the heater
i	grid point in x-direction
j	layer in composite blade
k	grid point in y-direction
l	liquid (water)
lm	liquid at the melting point
m	melting point
s	solid (ice)
sm	solid at the melting point

Superscripts:

Δ	evaluated at the previous time level
o	evaluated halfway between the previous and present time levels
N	value from previous iteration
N+1	value from current iteration

I. INTRODUCTION

Many practical transient heat conduction problems involve phase changes, e.g., the melting of a solid or the solidification of a liquid. These types of phase change problems are known as Stefan problems, after the early work done by Stefan (1889), and they have recently received considerable attention. Two of the oldest examples of this type of problem are the formation of ice on a solid body and the solidification of lava streams. Other applications include ablation of missile skins under aerodynamic heating, casting of metals and glass in molds, freeze drying of foodstuffs, heat exchangers using cryogenics, and the freezing and thawing of soil. The number and diversity of melting/freezing applications has motivated much research, which has been extensively reported in the literature [1].

The formation of ice on aircraft components has a considerable effect on aircraft performance as it increases drag and decreases lift. Thus, an aircraft must be designed with the necessary equipment required for ice removal or prevention. Basically, ice protection systems can be classified as either anti-icing or de-icing.

The anti-icing (or ice prevention) principle involves the prevention of ice formation on the protected area at all times. Typical methods of anti-icing employ the use of chemical systems (freezing point depressants) or the passage of hot, compressed bleed air from the engine

through passages below the surface on which ice formation is to be prevented. Anti-icing methods usually utilize large amounts of energy. On the other hand, the de-icing (or ice removal) principle involves the periodic removal of a layer of ice by mechanical or thermal means. This is accomplished by destroying the adhesion strength between the ice and the aircraft surfaces. Various de-icing techniques that have been investigated and reported upon [2, 3] are pneumatic boots and thermal techniques, the latter comprising cyclic heating of discrete elements by hot fluid or electrothermal means. For de-icing systems, the energy requirements are significantly less than those required for anti-icing systems.

The choice between anti-icing and de-icing techniques depends upon the component geometry and its function, and upon other factors such as the energy source utilized, the sensitivity of the component and the total energy available for ice protection. The advantages and pitfalls of anti-icing and de-icing systems have been reviewed by Baliga [4]. Stallabrass [5] has concluded from his experimental studies that the electrothermal method has the most advantages as a de-icing mechanism, although it does have maintainability/reliability problems. Werner [3] also reported that the electrothermal de-icing technique is the method most commonly used, and it has been applied to both fixed and rotary wing aircraft. For these reasons, the electrothermal means of de-icing will be the major topic of the present work.

The electrothermal de-icing principle was first successfully applied to propeller blades. The purpose of this thermal technique is to raise the composite blade surface-ice interface temperature to above

the melting point of ice, resulting in a very thin liquid interface layer which reduces the ice adhesion to the blade surface. Aerodynamic and/or centrifugal forces can then sweep the unmelted ice from the surface. The basic two-dimensional electrothermal de-icing pad employed in this study is shown in Figure 1. It is essentially a composite body consisting of: (1) a metal substrate (aircraft blade); (2) an inner insulation layer; (3) a heater element; (4) an outer insulation layer; and (5) an abrasion shield. A layer of ice is shown attached to the abrasion shield.

The design of the heating elements is either spanwise on the blade to cause chordwise shedding, or chordwise to cause spanwise shedding. The heater element usually consists either of a woven mat of wires and glass fibers or of multiple strips of resistance ribbon. As pointed out by Werner [3], the key factors in the design of an electrical heating element for a cyclic de-icing system are: (1) the uniformity of the obtained surface temperature at the abrasion shield-ice interface; (2) the amount of insulation required between the heater element and the ice surface; and (3) the amount of insulation required between the heater element and the aircraft blade. Stallabrass [5] has mentioned that heater element configurations may vary considerably. One such configuration consists of an array of parallel wires, woven or knitted with nylon or glass filaments to a surface or plane heater mat; the wires might be 0.02" in diameter, and spaced 24 to the inch, whereas metal ribbons usually have a thickness between 0.001" and 0.005". The gaps which exist between these heating elements can reduce the heater pad de-icing effectiveness, causing non-uniform melting of the ice. The gap width is

approximately 0.040" for metal ribbons and 0.080" for wires.

The two insulation layers, which usually consist of resin impregnated glass cloth, serve to provide electrical insulation for the heating element. In order to direct more heat flow toward the ice layer, it is necessary to use a much greater thickness for the inner insulation than for the outer insulation. A minimum thickness ratio of at least 2:1 has been suggested by Stallabrass [5]. The thickness of the outer insulation typically ranges from 0.010" to 0.020".

The purposes of the abrasion shield, which is generally made of stainless steel, are: (1) to protect the de-icer pad from rain erosion or sand and stone abrasion (especially when flying at high speeds); and (2) to diffuse the heat from the heater element so as to provide more uniform heating, thus minimizing cold spots above the heater gaps. The range of abrasion shield thickness is from 0.010" to 0.020". The material of construction of the substrate may vary widely depending upon the application. An aluminum alloy is considered in this study.

A two-dimensional model of the de-icing pad is the subject of this investigation. The model, which represents a cross-section of the heater pad normal to the run of the heater elements, is shown in Figure 1. It can be seen in the figure that natural boundary lines have been formed by lines of symmetry of the centerlines of the heater strip and the gap between the heater strips. It is assumed that there is perfect adhesion between each layer and therefore no contact resistance to heat flow shall be introduced into the analysis. A point heat source or a finite thickness heater providing either a constant or a time dependent heat supply will be included in this study. A wide range of parametric

studies have been conducted using the model to investigate such phenomena as the effect due to different heating functions on the rate and depth of ice melting, the effect of the abrasion shield toward evening out the temperature field due to non-uniform heating, and the effect of the gap width on the heater pad de-icing performance. A finite difference numerical analysis using the Enthalpy method to simulate the phase change in the ice layer is employed in the model solution.

II. LITERATURE REVIEW

A comprehensive review of the recent literature reveals that the study of electrothermal de-icer pads has either been ignored or that relevant information has not been published in the open literature. Of the investigations found, only the works of Stallabrass [5], Baliga [4] and Marano [6] have considered the effect of the phase change in the ice layer. All of the models have been one-dimensional except for that of Stallabrass, who proposed both one-dimensional and two-dimensional models. A two-dimensional electrothermal de-icer pad accounting for the phase change in the ice layer has been considered in the present study.

Temperature distributions in composite bodies consisting of several layers of material have numerous applications in heat transfer problems, such as in rocket thrust chamber liners, fuel elements for nuclear reactors, and in reentry spacecraft. Several analytical methods may be used to obtain solutions for a limited number of layers with various boundary conditions. The Laplace transform technique, as presented in Carslaw and Jaeger [7], is the most common analytical technique used to solve transient heat conduction problems in composite bodies. In principle, this technique will yield the temperature distribution in any composite slab, but, in practice, if the number of layers exceeds two, the inverse Laplace transform becomes quite difficult. Scott [8] applied this method to determine the temperature distribution in a symmetrical

five-component slab problem, and obtained a complicated solution which is limited to constant physical properties within each slab. Goodman [9] introduced the adjoint-solution technique, which is a method of obtaining the solution to a large class of heat conduction problems in composite bodies from the solution of but one adjoint problem. The adjoint solution arises from consideration of an auxiliary function with the application of Green's theorem to transform the problem from a volume to a surface integral. The primary disadvantages of this method are that the solution provides just the interfacial temperatures and not the temperature profiles within each layer in the composite body, and that only steady state cases were evaluated. The extension of this method to handle the transient case has been done by Bouchillon [10]. Campbell [11] proposed a method analogous to electric transmission line theory to calculate the temperature profile in a composite body. Stallabrass [5] applied Campbell's method to check the accuracy of his numerical method.

Tittle [12, 13] has shown that a one-dimensional multilayer problem can be solved by applying the Orthogonal-Expansion technique. This technique basically involves constructing orthogonal sets from the solutions of each of the layers. An orthogonality factor, called the discontinuous weighting function, is used such that the resulting orthogonal set is applicable to the entire composite media.

The disadvantage of using an analytical technique is that an excessive number of calculations must be done for each temperature desired. Hence, as the number of layers within the body increases, the calculations become prohibitively cumbersome. In addition, analytical methods can not be applied when a phase change is considered.

The most commonly used numerical technique for solving partial differential equations is the finite difference method, or, alternatively, the grid method. From a study of the recent literature, it appears that almost all of the numerical models for de-icer pads have used finite difference methods. The method is considered approximate in that the continuous space domain is replaced by a grid composed of nodal points, and the derivative at a given point is represented by a derivative taken over a finite interval across the point. The differential equation is replaced by a system of difference equations. The difference equations are then solved by algebraic or arithmetic procedures. Using this method, the temperature at any or all of the nodal points within the composite body may be obtained at any or all time steps. The disadvantages of the analytical methods are thus overcome by the use of finite difference numerical methods.

Two types of difference equations have previously been studied [14]: (1) explicit difference equations, which are simple to solve, but which require an uneconomically large number of time steps of limited size; and (2) implicit difference equations, which do not limit the time step, but which require at each time step the solution by iteration of a large set of simultaneous equations. Various finite differencing methods have been presented and are discussed in detail by Rosenberg [15] and Nogotov [16]. Convergence and stability are two important considerations in using a finite difference scheme. The accuracy of any finite difference scheme can be controlled by choosing the space and/or time interval as small as possible at the expense of increased computation time in solving the resulting increased number of algebraic equations. A finite

difference representation of the de-icer pad is shown in Figure 2.

Stallabrass [5] and Gent and Canedale [17] employed the explicit forward time, central space finite difference technique in their de-icer investigation. In this numerical method, the temperature at each node is calculated directly from the value of the temperature at the previous time step. This method is stable only if certain criteria relating the time step and the grid size are satisfied. The criteria requires that the ratio of $\alpha\Delta t$ to $(\Delta x)^2$ must remain less than or equal to 1/2, i.e., the size of $\alpha\Delta t$ must be of the same order of magnitude as $(\Delta x)^2$ for the solution to be stable. A time step of 0.001 sec. or smaller is normally used so that the stability criterion at the most sensitive of the nodal points is satisfied. The excessive number of calculations needed because of this small time step can, however, cause an accumulation of truncation and round-off error. The truncation error for the forward differencing scheme is first order for the time differential and second order for the space differential. Stallabrass [5] used the above method to solve a square grid (i.e., $\Delta x = \Delta y$) two-dimensional model with a point source or a finite thickness heater with constant heat output.

Kaliga [4], Marano [6] and the present study have employed the Crank-Nicolson implicit finite difference scheme in the electrothermal de-icer pad analysis. This numerical scheme is unconditionally stable, and consequently permits an independent choice of the time and space parameters of the grid. The truncation error of this method is second order for both the time and space differential. This allows a time step of 0.1 sec. to be used. In addition, Rosenberg [15] has pointed out that the Crank-Nicolson implicit finite difference scheme is the

preferred method for obtaining numerical solutions to parabolic partial differential equations. Baliga [4] used the Gaussian Elimination method to solve the resulting set of linear algebraic equations for a one-dimensional model of the de-icer problem. In order to obtain the temperature profile at any time step with the effect of the phase change, the Gauss-Seidel method, which is also known as the Liebmann method, is recommended. This method is best suited to the solution of systems whose matrix is sparse but not tridiagonal, i.e., for systems of two- and three-dimensional problems.

Phase change or moving-boundary problems are important in many engineering applications, and have been studied by several investigators over the last two decades. Most studies have been restricted to one-dimensional cases. The few investigations that do deal with two-dimensional problems are restricted to specific problems and to a limited range of parameters. The solution of Stefan problems is inherently difficult because the interface between the solid and liquid phase is moving as the latent heat is absorbed or released at the interface; as a result the location of the solid-liquid interface is not known apriori and must be determined as a part of the solution. Many solution approaches such as Integral methods [18], Successive approximation [19], Series solution [20], Green's function [2]] and Perturbation techniques [22] have been proposed for solving one-dimensional problems with a number of simplifying assumptions. The exact solution of a more general phase change problem was discussed by F. Neumann in his lectures in the 1860's, but his lecture notes containing these solutions were not published

until 1912. Since then, many phase change problems have appeared in the literature, but the exact solutions are limited to a few idealized cases involving semi-infinite or infinite regions, subject to simple boundary and initial conditions [7]. Because of the non-linear nature of such problems, the superposition principle is not applicable and each case must be treated separately. Since exact solutions are not available for these problems, approximate, semi-analytical, and numerical methods are used to solve phase change problems. An extensive review of these techniques has been presented in References [23, 24, 25, 26].

Numerically, the major difficulties are caused by the need to track a continuously moving phase change boundary through a region approximated by a finite number of points. Various methods have been proposed in Reference [23] to overcome this problem, including moving grid points, isotherm migration, reformulation of the problem into integral form, etc. A time dependent grid spacing scheme, also requiring nodal iteration, has been presented by Heitz and Westwater [27] and by Murray and Landis [28]. Crank [29] and Ehrlich [30] employed higher order space differences for the phase change equation. The drawback with this method is the requirement that the media be homogeneous, thus necessitating intricate programming in order to simulate the movement of the phase interface across element boundaries.

Most of these methods use predictor-corrector techniques to locate the position of the solid-liquid interface. In general, such procedures require a large number of trial and error computations. In order to circumvent these difficulties, the Enthalpy method, which is also called

the method of weak solution, has been employed frequently in the recent literature, e.g., see [23, 31, 32, 33]. In this technique, enthalpy is used as a dependent variable along with the temperature, the interface is eliminated from consideration in the calculations, and the problem is made equivalent to one of nonlinear heat conduction without change of phase. Hence, the advantages of this method are: (1) that the problem to be solved is formulated in a fixed region; (2) that no modification of the numerical scheme is necessary in order to satisfy the requirement of accurately tracking the moving phase change interface; (3) that the temporal derivative of the temperature no longer appears in the governing equation; and (4) that it is not necessary to consider the solid and liquid regions separately. In addition, Fox [34] asserts that weak solution techniques are by far the best of the finite difference techniques for any significant problem, and especially those in more than one space dimension. It is shown in Reference [33] that the mathematical representation of the Enthalpy method is equivalent to the conventional formulation of the conservation equations for the solid and liquid regions and the movement of the solid-liquid interface.

Kamenomostskaja [35] and Atthey [32] have applied the Enthalpy method to one-dimensional phase change problems using a finite difference scheme. The latter applied the method to a one-dimensional spot-welding problem. Crowley [36] applied the method to Stefan problems in more than one dimension. Marano [6] used the Enthalpy method in a one-dimensional deicer pad analysis.

Bonacina et al. [37] and Goodrich [38] have proposed a heat capacity formulation of the Stefan problem by associating the latent heat effect with a finite temperature interval about the phase change isotherm. Baliga [4] employed this method in a one-dimensional electrothermal de-icer pad analysis. Stallabrass [5] implemented the phase change process by holding the desired node at the melting point until enough heat had been transferred into the nodal volume to completely melt all of the ice in the volume. Both Baliga's [4] and Stallabrass' [5] techniques are equivalent but less rigorous than the Enthalpy method. Meyer [39] and Shamsunder and Sparrow [33] have used an Enthalpy technique to solve two-dimensional phase change problems.

In the present study, a transient, two-dimensional solution is obtained for the de-icer pad by the use of finite-difference techniques which employ the Enthalpy method to simulate the phase change occurring in the ice layer.

III. FORMULATION OF NUMERICAL METHOD

A. GOVERNING EQUATIONS AND BOUNDARY CONDITIONS

The following assumptions were made in the development of a two-dimensional, transient, mathematical model for heat conduction in a composite blade with an ice layer:

(1) The thermal physical properties of the material composing each layer of the blade are different, but do not depend on temperature;

(2) The ambient temperature, blade air temperature and all heat transfer coefficients are constants;

(3) There is perfect thermal contact between each layer; and

(4) The density change due to melting is negligible, i.e., the effect of the volume contraction of the ice as it melts is neglected.

With the above assumptions, the mathematical formulation for the problem of unsteady heat conduction in a chordwise two-dimensional section with electrothermal heating can be represented as

$$\rho_j \hat{C}_{pj} \frac{\partial T_j}{\partial t} = K_j \left(\frac{\partial^2 T_j}{\partial x^2} + \frac{\partial^2 T_j}{\partial y^2} \right) + q_j \qquad (1)$$

where j stands for the material in question, as given by

$j = 1$: blade or substrate $q_1 = 0$

$j = 2$: lower or inner insulation $q_2 = 0$ (2)

$j = 3$: heater $q_3 = q_3(t)$

$j = 4$: upper or outer insulation $q_4 = 0$

$j = 5$: abrasion shield $q_5 = 0$

and where

ρ_j = density of the j^{th} layer;

$\hat{C}_{pj}$ = specific heat capacity of the j^{th} layer;

T_j = temperature in j^{th} layer;

K_j = thermal conductivity of the j^{th} layer;

q_j = rate of heat generation per unit volume in j^{th} layer;

t = time variable; and

x,y = space coordinates.

For the ice layer ($j = 6$), the governing equation for the Enthalpy method is:

$$\frac{\partial H_6}{\partial t} = \frac{\partial}{\partial x}\left(K_6 \frac{\partial T_6}{\partial x}\right) + \frac{\partial}{\partial y}\left(K_6 \frac{\partial T_6}{\partial y}\right) \qquad (3)$$

where

H_6 = enthalpy per unit volume within the ice-water layer;

T_6 = temperature within the ice-water layer; and

K_6 = thermal conductivity within the ice-water layer.

The enthalpy within both phases (ice and water) can be found from

equation (3). The temperature T_6 can then be determined from the following relationship between H_6 and T_6:

$$H_6 = \begin{cases} \rho_s \hat{C}_{ps} T_6 & , T_6 < T_m \\ \rho_l \hat{C}_{pl} (T_6 - T_m) + \rho_l (\hat{C}_{ps} T_m + L_f), & T_6 > T_m \end{cases} \quad (4)$$

where

ρ_s, $\hat{C}_{ps}$ = physical properties of the solid phase;

ρ_l, $\hat{C}_{pl}$ = physical properties of the liquid phase;

T_m = melting temperature; and

L_f = latent heat of fusion per unit mass.

From equation (4),

$$T_6 = \begin{cases} H_6/\rho_s \hat{C}_{ps} & , H_6 \leq H_{sm} \\ T_m & , H_{sm} < H_6 < H_{lm} \\ (H_6 - H_{lm})/\rho_l \hat{C}_{pl} + T_m & , H_6 \geq H_{lm} \end{cases} \quad (5)$$

with

$$H_{sm} = \rho_s \hat{C}_{ps} T_m$$

$$H_{lm} = \rho_l (\hat{C}_{ps} T_m + L_f)$$

where H_{sm} and H_{lm} are the enthalpies of the ice and water at the melting point, respectively.

The boundary and initial conditions are as follows:

(i) At interior interfaces, the temperatures and heat fluxes are continuous, i.e.,

$$T_j\Big|_I = T_{j+1}\Big|_I \qquad j = 1, \ldots, 5$$

$$-K_j \frac{\partial T_j}{\partial y_j}\Big|_I = -K_{j+1} \frac{\partial T_{j+1}}{\partial y_{j+1}}\Big|_I \qquad j = 1, \ldots, 5 \tag{6}$$

where I denotes the interface.

(ii) At the interior and exterior surfaces of the composite body, Newton's law of cooling can be used to represent the convective heat exchange.

For the lower or inner boundary:

$$K_j \frac{\partial T_j}{\partial y_j}\Big|_1 = h_{b1} \left(T_j\Big|_1 - T_{b1}\right), \quad j = 1 \tag{7a}$$

Where 1 denotes the lower or inner ambient boundary, h_{b1} is the convective heat transfer coefficient at the boundary and T_{b1} is the lower ambient (blade air) temperature.

For the upper or outer boundary:

$$-K_j \frac{\partial T_j}{\partial y_j}\Big|_2 = h_{b2} \left(T_j\Big|_2 - T_{b2}\right), \quad j = 6 \tag{7b}$$

where 2 denotes the upper or outer ambient boundary, h_{b2} is the convective heat transfer coefficient at the boundary and T_{b2} is the upper ambient temperature.

(iii) At the centerline of the heater and the gap, insulated boundary conditions can be used to represent the symmetry, i.e.,

$$\left.\frac{\partial T_j}{\partial x}\right|_{g,j} = 0 \qquad , j = 1, \ldots, 6 \tag{8a}$$

$$\left.\frac{\partial T_j}{\partial x}\right|_{h,j} = 0 \qquad , j = 1, \ldots, 6 \tag{8b}$$

where g denotes the position of the centerline of the gap, and h denotes the position of the centerline of the heater.

In addition to the above, the initial temperature distribution in the composite blade can be constant or a function of position, and, if desired, constant temperature boundary conditions can be used for the lower and upper surfaces of the composite blade.

To formulate the above equations in terms of dimensionless temperature and distance, the following definitions are made:

$$\theta \equiv \frac{T}{T_{ref}} , \quad \bar{x} \equiv \frac{x}{L} , \quad \bar{y} \equiv \frac{y}{L} , \quad \alpha_j \equiv \frac{K_j}{\rho_j \hat{C}_{pj}}$$

where

T_{ref} = the reference temperature (taken to be 32°F in this study);

L = the total length of the composite slab in the y direction; and

α_j = the thermal diffusivity of the j^{th} layer.

Using these definitions, equations (1) through (8) take the following form:

For each layer in the composite blade:

$$\frac{\partial \theta_j}{\partial t} = \frac{\alpha_j}{L^2}\left[\frac{\partial^2 \theta_j}{\partial \bar{x}^2} + \frac{\partial^2 \theta_j}{\partial \bar{y}^2}\right] + \frac{q_j}{\rho_j \hat{C}_{pj} T_{ref}} \tag{9}$$

For the ice layer:

$$\frac{\partial H_6}{\partial t} = \frac{T_{ref}}{L}\left[\frac{\partial}{\partial \bar{x}}\left(K_6 \frac{\partial \theta_6}{\partial \bar{x}}\right) + \frac{\partial}{\partial \bar{y}}\left(K_6 \frac{\partial \theta_6}{\partial \bar{y}}\right)\right] \tag{10}$$

$$H_6 = \begin{cases} \rho_s \hat{C}_{ps} \theta_6 T_{ref} & , \theta_6 < T_m \\ \rho_l \hat{C}_{pl} T_{ref} (\theta_6 - \theta_m) + \rho_l (\hat{C}_{ps} \theta_m T_{ref} + L_f), & \theta_6 > T_m \end{cases} \tag{11}$$

$$\theta_6 = \begin{cases} H_6/\rho_s \hat{C}_{ps} T_{ref} & , H_6 \leq H_{sm} \\ \theta_m & , H_{sm} < H_6 < H_{lm} \\ H_6/\rho_l \hat{C}_{pl} T_{ref} - \frac{1}{\hat{C}_{pl}}\left(\hat{C}_{ps} \theta_m + \frac{L_f}{T_{ref}}\right) + \theta_m & , H_6 \geq H_{lm} \end{cases} \tag{12}$$

At the interfacial points:

$$\theta_j\Big|_I = \theta_{j+1}\Big|_I \quad , j = 1, \ldots, 5 \tag{13a}$$

$$-K_j \frac{\partial \theta_j}{\partial \bar{y}_j}\Big|_I = -K_{j+1} \frac{\partial \theta_{j+1}}{\partial \bar{y}_{j+1}}\Big|_I \quad , j = 1, \ldots, 5 \tag{13b}$$

At the lower and upper boundaries:

$$K_j \frac{\partial \theta_j}{\partial \bar{y}_j}\Big|_1 = h_{b1} L (\theta_j\Big|_1 - \theta_{b1}) \quad , j = 1 \tag{14a}$$

$$-K_j \frac{\partial \theta_j}{\partial \bar{y}_j}\Big|_2 = h_{b2} L (\theta_j\Big|_2 - \theta_{b2}) \quad , j = 6 \tag{14b}$$

Finally, the insulated boundary conditions at the centerlines of the gap and the heater are:

$$\left.\frac{\partial \theta_j}{\partial \bar{x}}\right|_{g,j} = 0 \qquad j = 1, \ldots, 6 \tag{15a}$$

$$\left.\frac{\partial \theta_j}{\partial \bar{x}}\right|_{h,j} = 0 \qquad j = 1, \ldots, 6 \tag{15b}$$

Next the above equations will be expressed in finite difference form and arranged for numerical solution.

B. NUMERICAL TECHNIQUE AND CRANK-NICOLSON FINITE DIFFERENCE FORMULATION

Formulation of a difference problem begins with the choice of a difference grid (a discrete set of points), on which a discretized or finite difference version of the original differential equation is to be solved. A significant feature of this technique is associated with the optional choice of grid parameters for characterizing the mesh spacing. For this study, there are three independent variables: two spacial coordinates x and y, and time t. The respective grid spacings and time increment are Δx, Δy and Δt. Let $E_{i,k}$ stand for the value of a dependent variable at the point (i, k), i.e., either T, θ or H. The central difference approximations of $\partial^2 E/\partial \bar{x}^2$ and $\partial E/\partial \bar{x}$ are:

$$\left.\frac{\partial^2 E_{i,k}}{\partial \bar{x}^2}\right|_j = \frac{E_{i+1,k} - 2E_{i,k} + E_{i-1,k}}{(\Delta \bar{x})^2} + 0\,(\Delta \bar{x})^2 \tag{16}$$

$$\left.\frac{\partial E_{i,k}}{\partial \bar{x}}\right|_j = \frac{E_{i+1,k} - E_{i-1,k}}{2\,\Delta\bar{x}} + 0\,(\Delta\bar{x})^2 \qquad (17)$$

These are second-order finite difference analogs. The second order finite difference analog for the time derivative, $\partial E/\partial t$, is:

$$\left.\frac{\partial E_{i,k}}{\partial t}\right|_j^o = \frac{E_{i,k} - E^{\Delta}_{i,k}}{\Delta t} + 0\,(\Delta t)^2 \qquad (18)$$

where the superscript Δ denotes the value at the previous time level and the superscript o denotes the value at a half-time step between the previous and present time levels. Equation (18) represents the Crank-Nicolson formulation of the time derivative. The real key to the Crank-Nicolson formulation is the manner of approximating $\partial^2 E/\partial\bar{x}^2$ and $\partial E/\partial\bar{x}$ without requiring the evaluation of the dependent variable at a time level half-way between the known and the unknown time levels. These derivatives are approximated by the arithmetic average of the finite difference analogs at the previous time level and the present time level. Equations (16) and (17) are approximated as:

$$\left.\frac{\partial^2 E_{i,k}}{\partial\bar{x}^2}\right|_j^o = 1/2\left(\left.\frac{\partial^2 E_{i,k}}{\partial\bar{x}^2}\right|_j + \left.\frac{\partial^2 E_{i,k}}{\partial\bar{x}^2}\right|_j^{\Delta}\right)$$

$$= \frac{E_{i+1,k} - 2E_{i,k} + E_{i-1,k} + E^{\Delta}_{i+1,k} - 2E^{\Delta}_{i,k} + E^{\Delta}_{i-1,k}}{2\,(\Delta\bar{x})^2} + 0\,(\Delta\bar{x})^2 \qquad (19)$$

$$\left.\frac{\partial E_{i,k}}{\partial\bar{x}}\right|_j^o = 1/2\left(\left.\frac{\partial E_{i,k}}{\partial\bar{x}}\right|_j + \left.\frac{\partial E_{i,k}}{\partial\bar{x}}\right|_j^{\Delta}\right)$$

$$= \frac{E_{i+1,k} - E_{i-1,k} + E^{\Delta}_{i+1,k} - E^{\Delta}_{i-1,k}}{4\,\Delta\bar{x}} + 0\,(\Delta\bar{x})^2 \qquad (20)$$

The Crank-Nicolson finite difference equations for the present problem are obtained by substituting the analogs of the above derivatives into the governing equations and boundary conditions.

1. Finite Difference Equations for the Composite Body

Substituting equations (19) and (20) into equation (9) yields:

$$\frac{\theta_{i,k,j} - \overset{\Delta}{\theta}_{i,k,j}}{\Delta t} = \frac{\alpha_j}{2L^2}\left[\frac{\theta_{i+1,k,j} - 2\theta_{i,k,j} + \theta_{i-1,k,j} + \overset{\Delta}{\theta}_{i+1,k,j} - 2\overset{\Delta}{\theta}_{i,k,j} + \overset{\Delta}{\theta}_{i-1,k,j}}{(\Delta\bar{x})^2} + \frac{\theta_{i,k+1,j} - 2\theta_{i,k,j} + \theta_{i,k-1,j} + \overset{\Delta}{\theta}_{i,k+1,j} - 2\overset{\Delta}{\theta}_{i,k,j} + \overset{\Delta}{\theta}_{i,k-1,j}}{(\Delta\bar{y}_j)^2}\right] + \frac{q_j}{\rho_j C_{pj} T_{ref}} \qquad j = 1, \ldots, 5 \qquad (21a)$$

Solving for the unknown temperature at node (i, k) in the j^{th} layer gives:

$$\theta_{i,k,j} = A_j \left\{\frac{\alpha_j}{2(L\Delta\bar{x})^2}\left[\theta_{i+1,k,j} + \theta_{i-1,k,j} + \overset{\Delta}{\theta}_{i+1,k,j} + \overset{\Delta}{\theta}_{i-1,k,j}\right] + \frac{\alpha_j}{2(L\Delta\bar{y}_j)^2}\left[\theta_{i,k+1,j} + \theta_{i,k-1,j} + \overset{\Delta}{\theta}_{i,k+1,j} + \overset{\Delta}{\theta}_{i,k-1,j}\right] + B_j \overset{\Delta}{\theta}_{i,k,j} + \frac{q_j''/L\Delta\bar{y}_j}{\rho_j C_{pj} T_{ref}}\right\} \qquad i = 2, \ldots, n-1, \quad j = 1, \ldots, 5 \qquad (21b)$$

where

$$A_j = \frac{1}{\frac{1}{\Delta t} + \frac{\alpha_j}{(L\Delta\bar{x})^2} + \frac{\alpha_j}{(L\Delta\bar{y}_j)^2}}$$

$$B_j = \frac{1}{\Delta t} - \frac{\alpha_j}{(L\Delta\bar{x})^2} - \frac{\alpha_j}{(L\Delta\bar{y}_j)^2} \quad \text{and}$$

q''_j = the heat source per unit area, and equals $q_j L\Delta\bar{y}_j$.

Equation (21b) is valid for all grid points within each of the layers of the composite aircraft blade, except at the centerlines of the gap and the heater, i.e., at i = 1 and i = n. Finite differencing equation (15) gives:

$$\theta_{0,k,j} = \theta_{2,k,j} \qquad j = 1, \ldots, 6 \tag{22a}$$

$$\theta_{n+1,k,j} = \theta_{n-1,k,j} \qquad j = 1, \ldots, 6 \tag{22b}$$

The grid points within each of the layers of the composite body at the centerlines of the gap and the heater are shown in Figures 3a and 3b, respectively. The equations for these points can be determined by substituting equation (22) into equation (21b), producing the following:

At the centerline of the gap:

$$i = 1, \ \theta_{1,k,j} = A_j \left\{\frac{\alpha_j}{2(L\Delta\bar{x})^2}\left[2\,\theta_{2,k,j} + 2\,\theta^{\Delta}_{2,k,j}\right] + \frac{\alpha_j}{2(L\Delta\bar{y}_j)^2}\left[\theta_{1,k+1,j} + \theta_{1,k-1,j} + \theta^{\Delta}_{1,k+1,j} + \theta^{\Delta}_{1,k-1,j}\right] + B_j\,\theta^{\Delta}_{1,k,j} + \frac{q''_j/L\Delta\bar{y}_j}{\rho_j \hat{C}_{pj} T_{ref}}\right\}$$

$$j = 1, \ldots, 5 \tag{23a}$$

At the centerline of the heater:

$$i = n,\ \theta_{n,k,j} = A_j\{\frac{\alpha_j}{2(L\Delta\bar{x})^2}\,[2\,\theta_{n-1,k,j} + 2\theta^{\Delta}_{n-1,k,j}] + \frac{\alpha_j}{2(L\Delta\bar{y}_j)^2}\,[\theta_{n,k+1,j} + \theta_{n,k-1,j} + \theta^{\Delta}_{n,k+1,j} + \theta^{\Delta}_{n,k-1,j}] + B_j\,\theta^{\Delta}_{n,k,j}\}\quad j = 1, \ldots, 5 \tag{23b}$$

2. Finite Difference Equations at Interfacial Points of the Composite Body

Let (i, k) denote one of the interfacial nodal points between the slab layers j and j+1, as shown in Figure 3c. Substitution of equation (20) into equation (13b), with the aid of analog (13a), yields:

$$\theta_{i,k,j} = \theta_{i,k,j+1}\ ,\quad \theta^{\Delta}_{i,k,j} = \theta^{\Delta}_{i,k,j+1}\ ,\quad j = 1, \ldots, 5 \tag{24a}$$

and

$$-K_j\,\left(\frac{\theta_{i,k+1,j} - \theta_{i,k-1,j} + \theta^{\Delta}_{i,k+1,j} - \theta^{\Delta}_{i,k-1,j}}{4\,\Delta\bar{y}_j}\right) = -K_{j+1}\,\left(\frac{\theta_{i,k+1,j+1} - \theta_{i,k-1,j+1} + \theta^{\Delta}_{i,k+1,j+1} - \theta^{\Delta}_{i,k-1,j+1}}{4\,\Delta\bar{y}_{j+1}}\right) \tag{24b}$$

The temperatures $\theta_{i,k+1,j}$, $\theta^{\Delta}_{i,k+1,j}$, $\theta_{i,k-1,j+1}$ and $\theta^{\Delta}_{i,k-1,j+1}$ are fictitious and can be eliminated by equation (21b) when applied to the layers j and j+1:

$$\theta_{i,k+1,j} + \theta^{\Delta}_{i,k+1,j} = \frac{2(L\Delta\bar{y}_j)^2}{A_j\,\alpha_j}\{\theta_{i,k,j} - A_j\,[\frac{\alpha_j}{2(L\Delta\bar{x})^2}\,(\theta_{i+1,k,j} +$$

$$\theta_{i-1,k,j} + \theta^{\Delta}_{i+1,k,j} + \theta^{\Delta}_{i-1,k,j}) + \frac{\alpha_j}{2(L\Delta\bar{y}_j)^2}(\theta_{i,k-1,j} + \theta^{\Delta}_{i,k-1,j})$$

$$+ B_j\,\theta^{\Delta}_{i,k,j} + \frac{q''_j/L\Delta\bar{y}_j}{\rho_j \hat{C}_{pj} T_{ref}}]\} \qquad (25)$$

$$\theta_{i,k-1,j+1} + \theta^{\Delta}_{i,k-1,j+1} = \frac{2(L\Delta\bar{y}_{j+1})^2}{A_{j+1}\,\alpha_{j+1}}\{\theta_{i,k,j+1} - A_{j+1}[\frac{\alpha_{j+1}}{2(L\Delta\bar{x})^2}$$

$$(\theta_{i+1,k,j+1} + \theta_{i-1,k,j+1} + \theta^{\Delta}_{i+1,k,j+1} + \theta^{\Delta}_{i-1,k,j+1})$$

$$+ \frac{\alpha_{j+1}}{2(L\Delta\bar{y}_{j+1})^2}(\theta_{i,k+1,j+1} + \theta^{\Delta}_{i,k+1,j+1})$$

$$+ B_{j+1}\theta^{\Delta}_{i,k,j+1} + \frac{q''_{j+1}/L\Delta\bar{y}_{j+1}}{\rho_{j+1}\hat{C}_{pj+1}T_{ref}}]\} \qquad (26)$$

Eliminating the fictitious temperatures by combining equations (24a), (25) and (26) yields:

$$\theta_{i,k,j} = \frac{1}{\frac{2(L\Delta\bar{y}_j)^2}{A_j\,\alpha_j} + \frac{K_{j+1}\,\Delta\bar{y}_j\,2(L\Delta\bar{y}_{j+1})^2}{K_j\,\Delta\bar{y}_{j+1}\,A_{j+1}\,\alpha_{j+1}}}\{[\frac{(\Delta\bar{y}_j)^2}{(\Delta\bar{x})^2} + \frac{K_{j+1}\,\Delta\bar{y}_j(\Delta\bar{y}_{j+1})^2}{K_j\,\Delta\bar{y}_{j+1}\,(\Delta\bar{x})^2}]$$

$$[\theta_{i+1,k,j} + \theta_{i-1,k,j} + \theta^{\Delta}_{i+1,k,j} + \theta^{\Delta}_{i-1,k,j}] + 2[\theta_{i,k-1,j} + \theta^{\Delta}_{i,k-1,j}]$$

$$+ \frac{2\,K_{j+1}\,\Delta\bar{y}_j}{K_j\,\Delta\bar{y}_{j+1}}[\theta_{i,k+1,j+1} + \theta^{\Delta}_{i,k+1,j+1}] + [\frac{2(L\Delta\bar{y}_j)^2}{\alpha_j}\,B_j$$

$$+ \frac{2(L\Delta\bar{y}_{j+1})^2\,K_{j+1}\,\Delta\bar{y}_j}{\alpha_{j+1}\,K_j\,\Delta\bar{y}_{j+1}}\,B_{j+1}]\,\theta^{\Delta}_{i,k,j} + \frac{2(L\Delta\bar{y}_j)^2}{\alpha_j}\,\frac{q''_j/L\Delta\bar{y}_j}{\rho_j\hat{C}_{pj}T_{ref}}$$

$$+ \frac{2(L\Delta\bar{y}_{j+1})^2 \; K_{j+1} \; \Delta\bar{y}_j \; q''_{j+1}/L\Delta\bar{y}_{j+1}}{\alpha_{j+1} \; \rho_{j+1} \; \hat{C}_{pj+1} \; T_{ref}} \Big\} \quad i=2, \ldots, n-1, \; j=1, \ldots, 5 \tag{27}$$

Equation (27) is applicable for the interfacial points within the composite blade, except at the centerlines of the gap and the heater. Applicable equations for the interfacial points at the centerlines of the gap and the heater, as shown in Figure 3c with i = 1, and i = n, can be determined by substituting equation (22) into equation (27):

At the centerline of the gap:

$$i=1, \; \theta_{1,k,j} = \frac{1}{\frac{2(L\Delta\bar{y}_j)^2}{A_j \; \alpha_j} + \frac{K_{j+1} \; \Delta\bar{y}_j \; 2(L\Delta\bar{y}_{j+1})^2}{K_j \; \Delta\bar{y}_{j+1} \; A_{j+1} \; \alpha_{j+1}}} \Big\{ 2 \Big[\frac{(\Delta\bar{y}_j)^2}{(\Delta\bar{x})^2}$$

$$+ \frac{(\Delta\bar{y}_{j+1})^2 \; K_{j+1} \; \Delta\bar{y}_j}{(\Delta\bar{x})^2 \; K_j \; \Delta\bar{y}_{j+1}}\Big] \left[\theta_{2,k,j} + \theta^{\Delta}_{2,k,j}\right] + 2 \left[\theta_{1,k-1,j} + \theta^{\Delta}_{1,k-1,j}\right]$$

$$+ 2 \frac{K_{j+1} \; \Delta\bar{y}_j}{K_j \; \Delta\bar{y}_{j+1}} \left[\theta_{1,k+1,j+1} + \theta^{\Delta}_{1,k+1,j+1}\right] + \Big[\frac{2(L\Delta\bar{y}_j)^2}{\alpha_j} \; B_j$$

$$+ \frac{2(L\Delta\bar{y}_{j+1})^2 \; K_{j+1} \; \Delta\bar{y}_j}{\alpha_{j+1} \; K_j \; \Delta\bar{y}_{j+1}} \; B_{j+1}\Big] \; \theta^{\Delta}_{1,k,j} + \frac{2(L\Delta\bar{y}_j)^2}{\alpha_j} \; \frac{q''_j/L\Delta\bar{y}_j}{\rho_j \hat{C}_{pj} T_{ref}}$$

$$+ \frac{2(L\Delta\bar{y}_{j+1}) \; K_{j+1} \; \Delta\bar{y}_j \; q''_{j+1}/L\Delta\bar{y}_{j+1}}{\alpha_{j+1} \; K_j \; \Delta\bar{y}_{j+1} \; \rho_{j+1} \; \hat{C}_{pj+1} \; T_{ref}} \Big\} \tag{27a}$$

At the centerline of the heater:

$$i=n, \; \theta_{n,k,j} = \frac{1}{\frac{2(L\Delta\bar{y}_j)^2}{A_j \; \alpha_j} + \frac{2(L\Delta\bar{y}_{j+1})^2 \; K_{j+1} \; \Delta\bar{y}_j}{\alpha_{j+1} \; A_{j+1} \; K_j \; \Delta\bar{y}_{j+1}}} \Big\{ 2 \Big[\frac{(\Delta\bar{y}_j)^2}{(\Delta\bar{x})^2}$$

$$+ \frac{(\Delta\bar{y}_{j+1})^2 \; K_{j+1} \; \Delta\bar{y}_j}{(\Delta\bar{x})^2 \; K_j \; \Delta\bar{y}_{j+1}}] \; [\theta_{n-1,k,j} + \theta^{\Delta}_{n-1,k,j}] + 2 \; [\theta_{n,k-1,j} + \theta^{\Delta}_{n,k-1,j}]$$

$$+ \frac{2K_{j+1}\Delta\bar{y}_j}{K_j\Delta\bar{y}_{j+1}} \; [\theta_{n-1,k,j} + \theta^{\Delta}_{n-1,k,j}] + [\frac{2(L\Delta\bar{y}_j)^2}{\alpha_j} \; B_j + \frac{2(L\Delta\bar{y}_{j+1})^2}{\alpha_{j+1}} \; \frac{K_{j+1} \; \Delta\bar{y}_j}{K_j \; \Delta\bar{y}_{j+1}}$$

$$B_{j+1}] \; \theta^{\Delta}_{n,k,j} + \frac{2(L\Delta\bar{y}_j)^2}{\alpha_j} \; \frac{q''_j/L\Delta\bar{y}_j}{\rho_j \hat{C}_{pj} T_{ref}} + \frac{2(L\Delta\bar{y}_{j+1})^2 \; K_{j+1} \; \Delta\bar{y}_j}{\alpha_{j+1} \; K_j \; \Delta\bar{y}_{j+1}} \; \frac{q''_{j+1}/L\Delta\bar{y}_{j+1}}{\rho_{j+1} \hat{C}_{pj+1} T_{ref}} \} \tag{27b}$$

3. Finite Difference Equations for the Substrate-Ambient Interface

The grid under consideration is shown in Figure 4a. At this surface j = 1, and (i, k) is taken to be the interfacial node. The finite difference representation of equation (14a) is:

$$K_1 \; (\frac{\theta_{i,2,1} - \theta_{i,0,1} + \theta^{\Delta}_{i,2,1} - \theta^{\Delta}_{i,0,1}}{4 \; \Delta\bar{y}_1}) = h_{b1} \; L \; (\frac{\theta_{i,1,1} + \theta^{\Delta}_{i,1,1}}{2} - \theta_{b1}) \tag{28}$$

Temperatures $\theta_{i,0,1}$ and $\theta^{\Delta}_{i,0,1}$ are fictitious and must be eliminated. Applying equation (21b) with k = 1, j = 1 and $q''_j = 0$, gives:

$$\theta_{i,1,1} = A_1 \; \{\frac{\alpha_1}{2(L\Delta\bar{x})^2} \; [\theta_{i+1,1,1} + \theta_{i-1,1,1} + \theta^{\Delta}_{i+1,1,1} + \theta^{\Delta}_{i-1,1,1}]$$

$$+ \frac{\alpha_1}{2(L\Delta\bar{y}_1)^2} \; [\theta_{i,2,1} + \theta_{i,0,1} + \theta^{\Delta}_{i,2,1} + \theta^{\Delta}_{i,0,1}] + B_1 \; \theta^{\Delta}_{i,1,1}\} \tag{29}$$

The fictitious temperatures are eliminated by substituting equation (29) into equation (28):

$$\theta_{i,1,1} = \frac{1}{\frac{2(L\Delta\bar{y}_1)^2}{A_1\,\alpha_1} + \frac{2h_{b1}L\Delta\bar{y}_1}{K_1}} \left\{\frac{(\Delta\bar{y}_1)^2}{(\Delta\bar{x})^2}\,(\theta_{i+1,1,1} + \theta_{i-1,1,1} + \theta^{\Delta}_{i+1,1,1} + \theta^{\Delta}_{i-1,1,1})\right.$$

$$+ 2(\theta_{i,2,1} + \theta^{\Delta}_{i,2,1}) + \left[\frac{2(L\Delta\bar{y}_1)^2}{\alpha_1} B_1 - \frac{2\,h_{b1}\,L\Delta\bar{y}_1}{K_1}\right]\,\theta^{\Delta}_{i,1,1} +$$

$$\left.\frac{4\,h_{b1}\,L\Delta\bar{y}_1}{K_1}\,\theta_{b1}\right\} \quad i = 2, \ldots, n-1 \qquad (30)$$

Again, the interfacial points for the substrate-ambient boundary at the centerlines of the gap and the heater are shown in Figure 4a with $i = 1$ and $i = n$, respectively. The equations for these points can be determined by substituting equation (22) into equation (30):

At the centerline of the gap:

$$i=1,\ \theta_{1,1,1} = \frac{1}{\frac{2(L\Delta\bar{y}_1)^2}{A_1\,\alpha_1} + \frac{2h_{b1}L\Delta\bar{y}_1}{K_1}} \left\{2\,\frac{(\Delta\bar{y}_1)^2}{(\Delta\bar{x})^2}\,[\theta_{2,1,1} + \theta^{\Delta}_{2,1,1}] + \right.$$

$$\left. 2\,[\theta_{1,2,1} + \theta^{\Delta}_{1,2,1}] + \left[\frac{2(L\Delta\bar{y}_1)^2}{\alpha_1} B_1 - \frac{2h_{b1}L\Delta\bar{y}_1}{K_1}\right]\,\theta^{\Delta}_{1,1,1} + \frac{4h_{b1}L\Delta\bar{y}_1}{K_1}\,\theta_{b1}\right\} \qquad (31a)$$

At the centerline of the heater:

$$i=n,\ \theta_{n,1,1} = \frac{1}{\frac{2(L\Delta\bar{y}_1)^2}{A_1\,\alpha_1} + \frac{2h_{b1}L\Delta\bar{y}_1}{K_1}} \left\{2\,\frac{(\Delta\bar{y}_1)^2}{(\Delta\bar{x})^2}\,[\theta_{n-1,1,1} + \theta^{\Delta}_{n-1,1,1}]\right.$$

$$+ 2\,[\theta_{n,2,1} + \theta^{\Delta}_{n,2,1}] + \left[\frac{2(L\Delta\bar{y}_1)^2}{\alpha_1} B_1 - \frac{2h_{b1}L\Delta\bar{y}_1}{K_1}\right]\,\theta^{\Delta}_{n,1,1}$$

$$\left. + \frac{4h_{b1}L\Delta\bar{y}_1}{K_1}\,\theta_{b1}\right\} \qquad (31b)$$

4. Finite Difference Equations for the Abrasion Shield-Ambient Interface

When the ice layer is not present or when the ice is shed, the grid under consideration is shown in Figure 4b. At this surface, j = 5, and (i, m) is taken to be the interfacial node. Finite differencing equation (14b) yields:

$$-K_5 \left(\frac{\theta_{i,m+1,5} - \theta_{i,m-1,5} + \theta^{\Delta}_{i,m+1,5} - \theta^{\Delta}_{i,m-1,5}}{4\,\Delta\bar{y}_5}\right)$$

$$= h_{b2}\, L \left(\frac{\theta_{i,m,5} + \theta^{\Delta}_{i,m,5}}{2} - \theta_{b2}\right) \qquad (32)$$

Temperatures $\theta_{i,m+1,5}$ and $\theta^{\Delta}_{i,m+1,5}$ are fictitious and are eliminated by the same procedure as used for the previous substrate-ambient interface boundary:

$$\theta_{i,m,5} = \frac{1}{\dfrac{2(L\Delta\bar{y}_5)^2}{A_5\,\alpha_5} + \dfrac{2h_{b2}L\Delta\bar{y}_5}{K_5}} \left\{\frac{(\Delta\bar{y}_5)^2}{(\Delta\bar{x})^2}\left[\theta_{i+1,m,5} + \theta_{i-1,m,5} + \theta^{\Delta}_{i+1,m,5} + \theta^{\Delta}_{i-1,m,5}\right] + 2\left[\theta_{i,m-1,5} + \theta^{\Delta}_{i,m-1,5}\right] + \left[\frac{2(L\Delta\bar{y}_5)^2}{\alpha_5} B_5 - \frac{2h_{b2}L\Delta\bar{y}_5}{K_5}\right] \theta^{\Delta}_{i,m,5} + \frac{4h_{b2}L\Delta\bar{y}_5}{K_5}\,\theta_{b2}\right\} \quad i=2, \ldots, n-1 \qquad (33)$$

At the centerline of the gap:

$$i=1,\ \theta_{1,m,5} = \frac{1}{\dfrac{2(L\Delta\bar{y}_5)^2}{A_5\,\alpha_5} + \dfrac{2h_{b2}L\Delta\bar{y}_5}{K_5}} \left\{2\,\frac{(\Delta\bar{y}_5)^2}{(\Delta\bar{x})^2}\left[\theta_{2,m,5} + \theta^{\Delta}_{2,m,5}\right]\right.$$

$$+ 2[\theta_{1,m-1,5} + \theta^{\Delta}_{1,m-1,5}] + [\frac{2(L\Delta\bar{y}_5)^2}{\alpha_5}B_5 - \frac{2h_{b2}L\Delta\bar{y}_5}{K_5}]\ \theta^{\Delta}_{1,m,5}$$

$$+ \frac{4h_{b2}L\Delta\bar{y}_5}{K_5}\ \theta_{b2}\ \} \qquad (34a)$$

At the centerline of the heater:

$$i=n,\ \theta_{n,m,5} = \frac{1}{\frac{2(\Delta\bar{y}_5)^2}{A_5\ \alpha_5} + \frac{2h_{b2}L\Delta\bar{y}_5}{K_5}}\ \{\ 2\ \frac{(\Delta\bar{y}_5)^2}{(\Delta\bar{x})^2}\ [\theta_{n-1,m,5} + \theta^{\Delta}_{n-1,m,5}]$$

$$+ 2[\theta_{n,m-1,5} + \theta^{\Delta}_{n,m-1,5}] + [\frac{2(L\Delta\bar{y}_5)^2}{\alpha_5} B_5 - \frac{2h_{b2}L\Delta\bar{y}_5}{K_5}]\ \theta_{n,m,5}$$

$$+ \frac{4h_{b2}L\Delta\bar{y}_5}{K_5}\ \theta_{b2}\ \} \qquad (34b)$$

5. Finite Difference Equations for the Ice Layer

As mentioned before, two equations are needed in the formulation of the Enthalpy method within the ice-water layer (j = 6), one to calculate enthalpy and one to calculate temperature at each nodal point in the ice layer. Substitution of analogs (18) and (19) into equation (10) gives:

$$\frac{H_{i,k,6} - H^{\Delta}_{i,k,6}}{\Delta t} = \frac{K_6\ T_{ref}}{2L^2}\ [\frac{\theta_{i+1,k,6} - 2\theta_{i,k,6} + \theta_{i-1,k,6}}{(\Delta\bar{x})^2}$$

$$+ \frac{\theta^{\Delta}_{i+1,k,6} - 2\theta^{\Delta}_{i,k,6} + \theta^{\Delta}_{i-1,k,6}}{} + \frac{\theta_{i,k+1,6} - 2\theta_{i,k,6} + \theta_{i,k-1,6} + \theta^{\Delta}_{i,k+1,6}}{(\Delta\bar{y}_6)^2}$$

$$\frac{- 2\theta^{\Delta}_{i,k,6} + \theta^{\Delta}_{i,k-1,6}}{}] \qquad (35)$$

Equation (35) can be solved explicitly for $H_{i,k,6}$ by using equation (12) to relate $\theta_{i,k,6}$ to $H_{i,k,6}$. Thus, there are three sets of equations

pertaining to the solid phase, the melting point and the liquid phase. Since the thermal conductivity for each node within the ice-water layer is a function of position, average values of the thermal conductivity have been used. The quantity KW_1 is the average value of the thermal conductivity between two adjacent nodes (i-1, k) and (i, k); KW_2 is the average value of the thermal conductivity between two adjacent nodes (i, k) and (i+1, k); KW_3 is the average value of the thermal conductivity between two adjacent nodes (i, k) and (i, k+1); and KW_4 is the average value of the thermal conductivity between two adjacent nodes (i, k-1) and (i, k). Employing this averaging approach and substituting equation (12) into equation (35), we obtain, upon rearrangement, the governing finite difference equation for each phase.

For the solid phase:

$$H_{i,k,6} = \{1 + \frac{\Delta t}{2L^2 \hat{C}_{ps} \rho_s} [\frac{KW_1 + KW_2}{(\Delta \bar{x})^2} + \frac{KW_3 + KW_4}{(\Delta \bar{y}_6)^2}]\}^{-1} \times$$

$$\{H^{\Delta}_{i,k,6} + \frac{\Delta t\ T_{ref}}{2L^2} [\frac{KW_2\ \theta_{i+1,k,6} + KW_1\ \theta_{i-1,k,6}}{(\Delta \bar{x})^2} + \frac{KW_3\ \theta_{i,k+1,6}}{(\Delta \bar{y}_6)^2}$$

$$\frac{+ KW_4\ \theta_{i,k-1,6}}{} + \frac{KW_1^{\Delta}}{(\Delta \bar{x})^2} (\theta^{\Delta}_{i-1,k,6} - \theta^{\Delta}_{i,k,6}) - \frac{KW_2^{\Delta}}{(\Delta \bar{x})^2} (\theta^{\Delta}_{i,k,6} - \theta^{\Delta}_{i+1,k,6})$$

$$+ \frac{KW_3^{\Delta}}{(\Delta \bar{y}_6)^2} (\theta^{\Delta}_{i,k+1,6} - \theta^{\Delta}_{i,k,6}) - \frac{KW_4^{\Delta}}{(\Delta \bar{y}_6)^2} (\theta^{\Delta}_{i,k,6} - \theta^{\Delta}_{i,k-1,6})]\}$$

$$i = 2, \ldots, n-1 \qquad H_{i,k,6} \leq H_{sm} \tag{36}$$

Substitution of equation (22) into equation (36) yields:

At the centerline of the gap:

$$i=1,\quad H_{1,k,6} = \{1 + \frac{\Delta t}{2L^2 \hat{C}_{ps}\rho_s}\left[\frac{KW_1 + KW_2}{(\Delta\bar{x})^2} + \frac{KW_3 + KW_4}{(\Delta\bar{y}_6)^2}\right]\}^{-1} \times$$

$$\{H^{\Delta}_{1,k,6} + \frac{\Delta t\ T_{ref}}{2L^2}\left[\frac{2KW_2\ \theta_{2,k,6}}{(\Delta\bar{x})^2} + \frac{KW_3\ \theta_{1,k+1,6} + KW_4\ \theta_{1,k-1,6}}{(\Delta\bar{y}_6)^2}\right.$$

$$+ \frac{2KW_2^{\Delta}(\theta^{\Delta}_{2,k,6} - \theta^{\Delta}_{1,k,6})}{(\Delta\bar{x})^2} + \frac{KW_3^{\Delta}}{(\Delta\bar{y}_6)^2}(\theta^{\Delta}_{1,k+1,6} - \theta^{\Delta}_{1,k,6})$$

$$\left. - \frac{KW_4^{\Delta}}{(\Delta\bar{y}_6)^2}(\theta^{\Delta}_{1,k,6} - \theta^{\Delta}_{1,k-1,6})\right]\} \qquad H_{1,k,6} \le H_{sm} \tag{37a}$$

At the centerline of the heater:

$$i=n,\quad H_{n,k,6} = \{1 + \frac{\Delta t}{2L^2 \hat{C}_{ps}\rho_s}\left[\frac{KW_1 + KW_2}{(\Delta\bar{x})^2} + \frac{KW_3 + KW_4}{(\Delta\bar{y}_6)^2}\right]\}^{-1} \times$$

$$\{H^{\Delta}_{n,k,6} + \frac{\Delta t\ T_{ref}}{2L^2}\left[\frac{2KW_1\ \theta_{n-1,k,6}}{(\Delta\bar{x})^2} + \frac{KW_3\ \theta_{n,k+1,6} + KW_4\ \theta_{n,k-1,6}}{(\Delta\bar{y}_6)^2}\right.$$

$$+ \frac{2KW_1^{\Delta}(\theta^{\Delta}_{n-1,k,6} - \theta^{\Delta}_{n,k,6})}{(\Delta\bar{x})^2} + \frac{KW_3^{\Delta}}{(\Delta\bar{y}_6)^2}(\theta^{\Delta}_{n,k+1,6} - \theta^{\Delta}_{n,k,6})$$

$$\left. - \frac{KW_4^{\Delta}}{(\Delta\bar{y}_6)^2}(\theta^{\Delta}_{n,k,6} - \theta^{\Delta}_{n,k-1,6})\right]\} \qquad H_{n,k,6} \le H_{sm} \tag{37b}$$

with $\theta_{i,k,6} = H_{i,k,6}/\hat{C}_{ps}\rho_s T_{ref}$ $\quad i = 1, \ldots, n$

<u>For the melting point:</u>

$$H_{i,k,6} = H^{\Delta}_{i,k,6} + \frac{\Delta t\ T_{ref}}{2L^2}\{-\left[\frac{KW_1 + KW_2}{(\Delta\bar{x})^2} + \frac{KW_3 + KW_4}{(\Delta\bar{y}_6)^2}\right]\theta_m$$

$$+\frac{KW_2\,\theta_{i+1,k,6}+KW_1\,\theta_{i-1,k,6}}{(\Delta\bar{x})^2}+\frac{KW_3\,\theta_{i,k+1,6}+KW_4\,\theta_{i,k-1,6}}{(\Delta\bar{y}_6)^2}$$

$$+\frac{KW_i^{\Delta}}{(\Delta\bar{x})^2}[\theta^{\Delta}_{i-1,k,6}-\theta^{\Delta}_{i,k,6}]-\frac{KW_2^{\Delta}}{(\Delta\bar{x})^2}[\theta^{\Delta}_{i,k,6}-\theta^{\Delta}_{i+1,k,6}]+\frac{KW_3^{\Delta}}{(\Delta\bar{y}_6)^2}$$

$$[\theta^{\Delta}_{i,k+1,6}-\theta^{\Delta}_{i,k,6}]-\frac{KW_4^{\Delta}}{(\Delta\bar{y}_6)^2}[\theta^{\Delta}_{i,k,6}-\theta^{\Delta}_{i,k-1,6}]\ \}$$

$$i=2,\ \ldots,\ n-1,\qquad H_{sm}<H_{i,k,6}<H_{1m} \tag{38}$$

Substitution of equation (22) into the above equation gives

At the centerline of the gap:

$$i=1,\ H_{1,k,6}=H^{\Delta}_{1,k,6}+\frac{\Delta t\ T_{ref}}{2L^2}\{-[\frac{KW_1+KW_2}{(\Delta\bar{x})^2}+\frac{KW_3+KW_4}{(\Delta\bar{y}_6)^2}]\ \theta_m$$

$$+\frac{2KW_2\,\theta_{2,k,6}}{(\Delta\bar{x})^2}+\frac{KW_3\,\theta_{1,k+1,6}+KW_4\,\theta_{1,k-1,6}}{(\Delta\bar{y}_6)^2}+\frac{2KW_2^{\Delta}(\theta^{\Delta}_{2,k,6}-\theta^{\Delta}_{1,k,6})}{(\Delta\bar{x})^2}$$

$$+\frac{KW_3^{\Delta}}{(\Delta\bar{y}_6)^2}[\theta^{\Delta}_{1,k+1,6}-\theta^{\Delta}_{1,k,6}]-\frac{KW_4^{\Delta}}{(\Delta\bar{y}_6)^2}[\theta^{\Delta}_{1,k,6}-\theta^{\Delta}_{1,k-1,6}]\}$$

$$H_{sm}<H_{1,k,6}<H_{1m} \tag{39a}$$

At the centerline of the heater:

$$i=n,\ H_{n,k,6}=H^{\Delta}_{n,k,6}+\frac{\Delta t\ T_{ref}}{2L^2}\{-[\frac{KW_1+KW_2}{(\Delta\bar{x})^2}+\frac{KW_3+KW_4}{(\Delta\bar{y}_6)^2}]\ \theta_m$$

$$+\frac{2KW_1\,\theta_{n-1,k,6}}{(\Delta\bar{x})^2}+\frac{KW_3\,\theta_{n,k+1,6}+KW_4\,\theta_{n,k-1,6}}{(\Delta\bar{y}_6)^2}+\frac{2KW_1^{\Delta}}{(\Delta\bar{x})^2}[\theta^{\Delta}_{n-1,k,6}$$

$$-\theta^{\Delta}_{n,k,6}]+\frac{KW_3}{(\Delta\bar{y}_6)^2}[\theta^{\Delta}_{n,k+1,6}-\theta^{\Delta}_{n,k,6}]-\frac{KW_4}{(\Delta\bar{y}_6)^2}[\theta^{\Delta}_{n,k,6}-\theta^{\Delta}_{n,k-1,6}]\}$$

$$H_{sm} < H_{n,k,6} < H_{lm} \tag{39b}$$

with $\theta_{i,k,6} = \theta_m \qquad i = 1, \ldots, n$

For the liquid phase:

$$H_{i,k,6} = \{1 + \frac{\Delta t}{2L^2 \hat{C}_{pl}\rho_l}\left[\frac{KW_1 + KW_2}{(\Delta\bar{x})^2} + \frac{KW_3 + KW_4}{(\Delta\bar{y}_6)^2}\right]\}^{-1} \times$$

$$\{H^{\Delta}_{i,k,6} + \frac{\Delta t\, T_{ref}}{2L^2}\left[\left(\frac{KW_1 + KW_2}{(\Delta\bar{x})^2} + \frac{KW_3 + KW_4}{(\Delta\bar{y}_6)^2}\right)\left(\frac{\hat{C}_{ps}\theta_m}{\hat{C}_{pl}} + \frac{L_f}{\hat{C}_{pl}T_{ref}} - \theta_m\right)\right.$$

$$+ \frac{KW_2\,\theta_{i+1,k,6} + KW_1\,\theta_{i-1,k,6}}{(\Delta\bar{x})^2} + \frac{KW_3\,\theta_{i,k+1,6} + KW_4\,\theta_{i,k-1,6}}{(\Delta\bar{y}_6)^2}$$

$$+ \frac{KW_1}{(\Delta\bar{x})^2}(\theta^{\Delta}_{i-1,k,6} - \theta^{\Delta}_{i,k,6}) - \frac{KW_2}{(\Delta\bar{x})^2}(\theta^{\Delta}_{i,k,6} - \theta^{\Delta}_{i+1,k,6})$$

$$\left. + \frac{KW_3}{(\Delta\bar{y}_6)^2}(\theta^{\Delta}_{i,k+1,6} - \theta^{\Delta}_{i,k,6}) - \frac{KW_4}{(\Delta\bar{y}_6)^2}(\theta^{\Delta}_{i,k,6} - \theta^{\Delta}_{i,k-1,6})\right]\}$$

$$i = 2, \ldots, n-1 \qquad H_{i,k,6} \geq H_{lm} \tag{40}$$

By substituting equation (22) into equation (39), the following are obtained:

At the centerline of the gap:

$$i=1,\ H_{1,k,6} = \{1 + \frac{\Delta t}{2L^2 \hat{C}_{pl}\rho_l}\left[\frac{KW_1 + KW_2}{(\Delta\bar{x})^2} + \frac{KW_3 + KW_4}{(\Delta\bar{y}_6)^2}\right]\}^{-1}$$

$$\times \{H^{\Delta}_{1,k,6} + \frac{\Delta t T_{ref}}{2L^2}\left[\left(\frac{KW_1 + KW_2}{(\Delta\bar{x})^2} + \frac{KW_3 + KW_4}{(\Delta\bar{y}_6)^2}\right)\left(\frac{\hat{C}_{ps}\rho_m}{\hat{C}_{pl}} + \frac{L_f}{\hat{C}_{pl}T_{ref}} - \theta_m\right)\right.$$

$$+ \frac{2KW_2\,\theta_{2,k,6}}{(\Delta\bar{x})^2} + \frac{KW_3\,\theta_{1,k+1,6} + KW_4\,\theta_{1,k-1,6}}{(\Delta\bar{y}_6)^2} + \frac{2KW_2^{\Delta}}{(\Delta\bar{x})^2}(\theta^{\Delta}_{2,k,6} - \theta^{\Delta}_{1,k,6})$$

$$+ \frac{KW_3^{\Delta}}{(\Delta\bar{y}_6)^2}(\theta^{\Delta}_{1,k+1,6} - \theta^{\Delta}_{1,k,6}) - \frac{KW_4^{\Delta}}{(\Delta\bar{y}_6)^2}(\theta^{\Delta}_{1,k,6} - \theta^{\Delta}_{1,k-1,6})]\}$$

$$H_{1,k,6} \geq H_{1m} \qquad (41a)$$

At the centerline of the heater:

$$i=n,\ H_{n,k,6} = \{1 + \frac{\Delta t}{2L^2\hat{C}_{p1}\rho_1}[\frac{KW_1 + KW_2}{(\Delta\bar{x})^2} + \frac{KW_3 + KW_4}{(\Delta\bar{y}_6)^2}]\}^{-1}$$

$$\times \{H^{\Delta}_{n,k,6} + \frac{\Delta t T_{ref}}{2L^2}[(\frac{KW_1 + KW_2}{(\Delta\bar{x})^2} + \frac{KW_3 + KW_4}{(\Delta\bar{y}_6)^2})(\frac{\hat{C}_{ps}\theta_m}{\hat{C}_{p1}} + \frac{L_f}{\hat{C}_{p1}T_{ref}} - \theta_m)$$

$$+ \frac{2KW_1\,\theta_{n-1,k,6}}{(\Delta\bar{x})^2} + \frac{KW_3\,\theta_{n,k+1,6} + KW_4\,\theta_{n,k-1,6}}{(\Delta\bar{y}_6)^2} + \frac{2KW_1^{\Delta}}{(\Delta\bar{x})^2}(\theta^{\Delta}_{n-1,k,6} - \theta^{\Delta}_{n,k,6})$$

$$+ \frac{KW_3^{\Delta}}{(\Delta\bar{y}_6)^2}(\theta^{\Delta}_{n,k+1,6} - \theta^{\Delta}_{n,k,6}) - \frac{KW_4^{\Delta}}{(\Delta\bar{y}_6)^2}(\theta^{\Delta}_{n,k,6} - \theta^{\Delta}_{n,k-1,6})]\}$$

$$H_{n,k,6} \geq H_{1m} \qquad (41b)$$

with

$$\theta_{i,k,6} = \frac{H_{i,k,6}}{T_{ref}\hat{C}_{p1}\rho_1} - \frac{1}{\hat{C}_{p1}}(\hat{C}_{ps}\,\theta_m + \frac{L_f}{T_{ref}}) + \theta_m \qquad i=1,\ \ldots,\ n$$

a. Abrasion Shield-Ice Interface

Let (i, k) be one of the abrasion shield-ice interface nodes as shown in Figure 3c (j = 5). Substitution of analog equation (20) into equation (13b) with the aid of analog equation (13a) and with j = 5 yields:

$$\theta_{i,k,5} = \theta_{i,k,6} \, , \; \theta^{\Delta}_{i,k,5} = \theta^{\Delta}_{i,k,6} \tag{42a}$$

and

$$-K_5 \left(\frac{\theta_{i,k+1,5} - \theta_{i,k-1,5} + \theta^{\Delta}_{i,k+1,5} + \theta^{\Delta}_{i,k-1,5}}{4\,\Delta\bar{y}_5}\right)$$

$$= -K_6 \left(\frac{\theta_{i,k+1,6} - \theta_{i,k-1,6} + \theta^{\Delta}_{i,k+1,6} + \theta^{\Delta}_{i,k-1,6}}{4\,\Delta\bar{y}_6}\right) \tag{42b}$$

Equation (21b) with j = 5 is used to eliminate the fictitious temperatures $\theta_{i,k+1,5}$ and $\theta^{\Delta}_{i,k+1,5}$, and equation (35) is used to eliminate to fictitious temperature $\theta_{i,k-1,6}$ and $\theta^{\Delta}_{i,k-1,6}$. Combining the resulting equation with equations (12) and (42a) yields the following equations for the solid phase, the melting point and the liquid phase.

<u>For the solid phase:</u>

$$H_{i,k,6} = \left\{\frac{\Delta t\, K_5\, \Delta\bar{y}_5}{\hat{C}_{ps}\rho_s \Delta\bar{y}_6 A_5 \alpha_5} + \frac{\Delta t}{2\hat{C}_{ps}\rho_s L^2}\left[\frac{KW_1 + KW_2}{(\Delta\bar{x})^2} + \frac{2KW_3}{(\Delta\bar{y}_6)^2}\right] + 1\right\}^{-1} \times$$

$$\left\{H^{\Delta}_{i,k,6} + \frac{\Delta t T_{ref}}{2L^2}\left[(\theta_{i+1,k,5} + \theta_{i-1,k,5} + \theta^{\Delta}_{i+1,k,5} + \theta^{\Delta}_{i-1,k,5})\,\frac{K_5 \Delta\bar{y}_5}{\Delta\bar{y}_6 (\Delta\bar{x})^2}\right.\right.$$

$$+ \frac{KW_2\,\theta_{i+1,k,6} + KW_1\,\theta_{i-1,k,6}}{(\Delta\bar{x})^2} + \frac{2K_5}{\Delta\bar{y}_5 \Delta\bar{y}_6}(\theta_{i,k-1,5} + \theta^{\Delta}_{i,k-1,5}) + \frac{KW^{\Delta}_1}{(\Delta\bar{x})^2}$$

$$(\theta^{\Delta}_{i-1,k,6} - \theta^{\Delta}_{i,k,6}) - \frac{KW^{\Delta}_2}{(\Delta\bar{x})^2}(\theta^{\Delta}_{i,k,6} - \theta^{\Delta}_{i+1,k,6}) + \frac{2KW_3\,\theta_{i,k+1,6}}{(\Delta\bar{y}_6)^2} +$$

$$\left.\left.\frac{2KW^{\Delta}_3}{(\Delta\bar{y}_6)^2}(\theta^{\Delta}_{i,k+1,6} - \theta^{\Delta}_{i,k,6}) + \frac{2L^2 \Delta\bar{y}_5 B_5 K_5}{\alpha_5 \Delta\bar{y}_6}\,\theta^{\Delta}_{i,k,5}\right]\right\}$$

$$i = 2, \ldots, n-1 \qquad H_{i,k,6} \leq H_{sm} \tag{43}$$

Substituting equation (22) into equation (43) gives

At the centerline of the gap:

$$i=1,\quad H_{1,k,6} = \{\frac{\Delta t\ K_5\ \Delta\bar{y}_5}{\hat{C}_{ps}\rho_s\Delta\bar{y}_6 A_5\alpha_5} + \frac{\Delta t}{2\hat{C}_{ps}\rho_s L^2}\left[\frac{2KW_2}{(\Delta\bar{x})^2} + \frac{2KW_3}{(\Delta\bar{y}_6)^2}\right] + 1\}^{-1} \times$$

$$\{ H_{1,k,6}^{\Delta} + \frac{\Delta t T_{ref}}{2L^2}\left[\frac{2K_5\ \Delta\bar{y}_5}{\Delta\bar{y}_6(\Delta\bar{x})^2}(\theta_{2,k,5} + \theta_{2,k,5}^{\Delta}) + \frac{2KW_2\ \theta_{2,k,6}}{(\Delta\bar{x})^2}\right.$$

$$+ \frac{2K_5}{\Delta\bar{y}_5\Delta\bar{y}_6}(\theta_{1,k-1,5} + \theta_{1,k-1,5}^{\Delta}) + \frac{2KW_3\theta_{1,k+1,6}}{(\Delta\bar{y}_6)^2} + \frac{2KW_2^{\Delta}}{(\Delta\bar{x})^2}(\theta_{2,k,6}^{\Delta} - \theta_{1,k,6}^{\Delta})$$

$$\left. + \frac{2KW_3^{\Delta}}{(\Delta\bar{y}_6)^2}(\theta_{1,k+1,6}^{\Delta} - \theta_{1,k,6}^{\Delta}) + \frac{2L^2\Delta\bar{y}_5 B_5 K_5}{\alpha_5\ \Delta\bar{y}_6}\theta_{1,k,5}^{\Delta}\right] \}$$

$$H_{1,k,6} \leq H_{sm} \tag{44a}$$

At the centerline of the heater:

$$i=n,\quad H_{n,k,6} = \{\frac{\Delta t\ K_5\ \Delta\bar{y}_5}{\hat{C}_{ps}\rho_s\Delta\bar{y}_6 A_5\ \alpha_5} + \frac{\Delta t}{2\hat{C}_{ps}\ \rho_s L^2}\left[\frac{2KW_1}{(\Delta\bar{x})^2} + \frac{2KW_3}{(\Delta\bar{y}_6)^2}\right] + 1\}^{-1} \times$$

$$\{H_{n,k,6}^{\Delta} + \frac{\Delta t T_{ref}}{2L^2}\left[\frac{2K_5\ \Delta\bar{y}_5}{\Delta\bar{y}_6(\Delta\bar{x})^2}(\theta_{n-1,k,5} + \theta_{n-1,k,5}^{\Delta}) + \frac{2KW_1\ \theta_{n-1,k,6}}{(\Delta\bar{x})^2}\right.$$

$$+ \frac{2K_5}{\Delta\bar{y}_5\Delta\bar{y}_6}(\theta_{n,k-1,5} + \theta_{n,k-1,5}^{\Delta}) + \frac{2KW_3\ \theta_{n,k+1,6}}{(\Delta\bar{y}_6)^2} + \frac{2KW_1^{\Delta}}{(\Delta\bar{x})^2}(\theta_{n-1,k,6}^{\Delta}$$

$$\left. - \theta_{n,k,6}^{\Delta}) + \frac{2KW_3^{\Delta}(\theta_{n,k+1,6}^{\Delta} - \theta_{n,k,6}^{\Delta})}{(\Delta\bar{y}_6)^2} + \frac{2L^2\Delta\bar{y}_5\ B_5K_5}{\alpha_5\ \Delta\bar{y}_6}\theta_{n,k,5}^{\Delta}\right]\}$$

$$H_{n,k,6} \leq H_{sm} \tag{44b}$$

with $\theta_{i,k,6} = H_{i,k,6}/\hat{C}_{ps}\rho_s T_{ref}$ $\quad i = 1, \ldots, n$

For the melting point:

$$H_{i,k,6} = H^{\Delta}_{i,k,6} + \frac{\Delta t T_{ref}}{2L^2}\left\{-\left[\frac{2L^2\Delta\bar{y}_5 K_5}{\alpha_5 A_5 \Delta\bar{y}_6} + \frac{2KW_1}{(\Delta\bar{x})^2} + \frac{2KW_3}{(\Delta\bar{y}_6)^2}\right]\theta_m\right.$$

$$+ (\theta_{i+1,k,5} + \theta_{i-1,k,5} + \theta^{\Delta}_{i+1,k,5} + \theta^{\Delta}_{i-1,k,5})\frac{K_5\,\Delta\bar{y}_5}{\Delta\bar{y}_6(\Delta\bar{x})^2} + \frac{KW_2\,\theta_{i+1,k,6}}{(\Delta\bar{x})^2}$$

$$+ \frac{KW_1\,\theta_{i-1,k,6}}{} + \frac{2K_5}{\Delta\bar{y}_5\Delta\bar{y}_6}(\theta_{i,k-1,5} + \theta^{\Delta}_{i,k-1,5}) + \frac{KW_1^{\Delta}}{(\Delta\bar{x})^2}(\theta^{\Delta}_{i-1,k,6} - \theta^{\Delta}_{i,k,6})$$

$$- \frac{KW_2^{\Delta}}{(\Delta\bar{x})^2}(\theta^{\Delta}_{i,k,6} - \theta^{\Delta}_{i+1,k,6}) + \frac{2KW_3\theta_{i,k+1,6}}{(\Delta\bar{y}_6)} + \frac{2KW_3^{\Delta}}{(\Delta\bar{y}_6)^2}(\theta^{\Delta}_{i,k+1,6} -$$

$$\left.\theta^{\Delta}_{i,k,6}) + \frac{2L^2\Delta\bar{y}_5\,B_5\,K_5}{\alpha_5\,\Delta\bar{y}_6}\,\theta^{\Delta}_{i,k,5}\right\}$$

$$i = 2, \ldots, n-1 \qquad H_{sm} < H_{i,k,6} < H_{lm} \tag{45}$$

Substitution of equation (22) into the above equation yields

At the centerline of the gap:

$$i = 1, \quad H_{1,k,6} = H^{\Delta}_{1,k,6} + \frac{\Delta t T_{ref}}{2L^2}\left\{-\left[\frac{2L^2\Delta\bar{y}_5 K_5}{\alpha_5 A_5\Delta\bar{y}_6} + \frac{2KW_2}{(\Delta\bar{x})^2} + \frac{2KW_3}{(\Delta\bar{y}_6)^2}\right]\theta_m\right.$$

$$+ \frac{2K_5}{\Delta\bar{y}_6}\frac{\Delta\bar{y}_5}{(\Delta\bar{x})^2}(\theta_{2,k,5} + \theta^{\Delta}_{2,k,5}) + \frac{2KW_2\theta_{2,k,6}}{(\Delta\bar{x})^2} + \frac{2K_5}{\Delta\bar{y}_5\,\Delta\bar{y}_6}(\theta_{1,k-1,5} +$$

$$\theta^{\Delta}_{1,k-1,5}) + \frac{2KW_2^{\Delta}}{(\Delta\bar{x})^2}(\theta^{\Delta}_{2,k,6} - \theta^{\Delta}_{1,k,6}) + \frac{2KW_3^{\Delta}}{(\Delta\bar{y}_6)^2}(\theta^{\Delta}_{1,k+1,6} - \theta^{\Delta}_{1,k,6})$$

$$\left. + \frac{2KW_3\,\theta_{1,k+1,6}}{(\Delta\bar{y}_6)^2} + \frac{2L^2\,\Delta\bar{y}_5\,B_5\,K_5}{\alpha_5\,\Delta\bar{y}_6}\,\theta^{\Delta}_{1,k,5}\right\}$$

$$H_{sm} < H_{1,k,6} < H_{lm} \tag{46a}$$

At the centerline of the heater:

$$i = n,\ H_{n,k,6} = H^{\Delta}_{n,k,6} + \frac{\Delta t T_{ref}}{2L^2}\{-[\frac{2L^2\,\Delta\bar{y}_5\,K_5}{\alpha_5\,A_5\,\Delta\bar{y}_6} + \frac{2KW_1}{(\Delta\bar{x})^2} + \frac{2KW_3}{(\Delta\bar{y}_6)^2}]\,\theta_m$$

$$+ \frac{2K_5\,\Delta\bar{y}_5}{\Delta\bar{y}_6\,(\Delta\bar{x})^2}(\theta_{n-1,k,5} + \theta^{\Delta}_{n-1,k,5}) + \frac{2KW_1\,\theta_{n-1,k,6}}{(\Delta\bar{x})^2} + \frac{2\,K_5}{\Delta\bar{y}_5\,\Delta\bar{y}_6}(\theta_{n,k-1,5}$$

$$+ \theta^{\Delta}_{n,k-1,5}) + \frac{2KW_1^{\Delta}}{(\Delta\bar{x})^2}(\theta^{\Delta}_{n-1,k,6} - \theta^{\Delta}_{n,k,6}) + \frac{2KW_3^{\Delta}}{(\Delta\bar{y}_6)^2}(\theta^{\Delta}_{n,k+1,6} - \theta^{\Delta}_{n,k,6})$$

$$+ \frac{2KW_3\,\theta_{n,k+1,6}}{(\Delta\bar{y}_6)^2} + \frac{2L^2\,\Delta\bar{y}_5\,B_5\,K_5}{\alpha_5\,\Delta\bar{y}_6}\theta^{\Delta}_{n,k,5}\}$$

$$H_{sm} < H_{n,k,6} < H_{lm} \qquad (46b)$$

with $\theta_{i,k,6} = \theta_m$, $i = 1, \ldots, n$

For the liquid phase:

$$H_{i,k,6} = \{\frac{\Delta t\,K_5\,\Delta\bar{y}_5}{\hat{C}_{pl}\rho_l\Delta\bar{y}_6\alpha_5A_5} + \frac{\Delta t}{2L^2\hat{C}_{pl}\rho_l}[\frac{KW_1 + KW_2}{(\Delta\bar{x})^2} + \frac{2KW_3}{(\Delta\bar{y}_6)^2}] + 1\}^{-1} x$$

$$\{H^{\Delta}_{i,k,6} + \frac{\Delta t T_{ref}}{2L^2}[(\theta_{i+1,k,5} + \theta_{i-1,k,5} + \theta^{\Delta}_{i+1,k,5} + \theta^{\Delta}_{i-1,k,5})\frac{K_5\Delta\bar{y}_5}{\Delta\bar{y}_6(\Delta\bar{x})^2}$$

$$+ \frac{KW_2\,\theta_{i+1,k,6} + KW_1\,\theta_{i-1,k,6}}{(\Delta\bar{x})^2} + \frac{2K_5}{\Delta\bar{y}_5\Delta\bar{y}_6}(\theta_{i,k-1,5} + \theta^{\Delta}_{i,k-1,5}) +$$

$$\frac{KW_1}{(\Delta\bar{x})^2}(\theta^{\Delta}_{i-1,k,6} - \theta^{\Delta}_{i,k,6}) - \frac{KW_2}{(\Delta\bar{x})^2}(\theta^{\Delta}_{i,k,6} - \theta^{\Delta}_{i+1,k,6}) + \frac{2KW_3^{\Delta}}{(\Delta\bar{y}_6)^2}(\theta^{\Delta}_{i,k+1,6}$$

$$- \theta^{\Delta}_{i,k,6}) + \frac{2KW_3\,\theta_{i,k+1,6}}{(\Delta\bar{y}_6)^2} - [\frac{2L^2\Delta\bar{y}_5\,K_5}{\alpha_5\,A_5\,\Delta\bar{y}_6} + \frac{KW_1 + KW_2}{(\Delta\bar{x})^2} + \frac{2KW_3}{(\Delta\bar{y}_6)^2}]$$

$$[\theta_m - \frac{1}{\hat{C}_{pl}} (\hat{C}_{ps}\ \theta_m + \frac{L_f}{T_{ref}})] + \frac{2L^2\ \Delta\bar{y}_5\ B_5\ K_5}{\alpha_5\ \Delta\bar{y}_6}\ \theta^{\Delta}_{i,k,5}]\}$$

$$i = 2, \ldots, n-1 \qquad H_{i,k,6} \geq H_{lm} \tag{47}$$

Substituting equation (22) into equation (47) gives

At the centerline of the gap:

$$i = 1, \quad H_{1,k,6} = \{\frac{\Delta t\ K_5\ \Delta\bar{y}_5}{\hat{C}_{pl}\rho_1\Delta\bar{y}_6\alpha_5 A_5} + \frac{\Delta t}{2L^2\ \hat{C}_{pl}\ \rho_1}\ [\frac{2KW_2}{(\Delta\bar{x})^2} + \frac{2KW_3}{(\Delta\bar{y}_6)^2}] + 1\ \}^{-1}$$

$$\times \{H^{\Delta}_{1,k,6} + \frac{\Delta t T_{ref}}{2L^2}\ [\frac{2K_5\ \Delta\bar{y}_5}{\Delta\bar{y}_6(\Delta\bar{x})^2}\ (\theta_{2,k,5} + \theta^{\Delta}_{2,k,5}) + \frac{2KW_2\ \theta_{2,k,6}}{(\Delta\bar{x})^2}$$

$$+ \frac{2K_5}{\Delta\bar{y}_5\ \Delta\bar{y}_6}\ (\theta_{1,k-1,5} + \theta^{\Delta}_{1,k-1,5}) + \frac{2KW_3\ \theta_{1,k+1,6}}{(\Delta\bar{y}_6)^2} + \frac{2KW_2}{(\Delta\bar{x})^2}^{\Delta}\ (\theta^{\Delta}_{2,k,6} - \theta^{\Delta}_{1,k,6})$$

$$+ \frac{2KW_3}{(\Delta\bar{y}_6)^2}^{\Delta}\ (\theta^{\Delta}_{1,k+1,6} - \theta^{\Delta}_{1,k,6}) - [\frac{2L^2\ \Delta\bar{y}_5\ K_5}{\alpha_5\ A_5\ \Delta\bar{y}_6} + \frac{2KW_2}{(\Delta\bar{x})^2} + \frac{2KW_3}{(\Delta\bar{y}_6)^2}]$$

$$[\theta_m - \frac{1}{\hat{C}_{pl}}\ (\hat{C}_{ps}\ \theta_m + \frac{L_f}{T_{ref}})] + \frac{2L^2\ \Delta\bar{y}_5\ B_5\ K_5}{\alpha_5\ \Delta\bar{y}_6}\ \theta^{\Delta}_{1,k,5}]\}$$

$$H_{1,k,6} \geq H_{lm} \tag{48a}$$

At the centerline of the heater:

$$i=n, \quad H_{n,k,6} = \{\frac{\Delta t\ \ K_5\ \Delta\bar{y}_5}{\hat{C}_{pl}\rho_1\ \Delta\bar{y}_6\ \alpha_5\ A_5} + \frac{\Delta t}{2L^2\ \hat{C}_{pl}\ \rho_1}\ [\frac{2KW_1}{(\Delta\bar{x})^2} + \frac{2KW_3}{(\Delta\bar{y}_6)^2}] + 1\ \}^{-1}$$

$$\times \{H^{\Delta}_{n,k,6} + \frac{\Delta t T_{ref}}{2L^2}\ [\frac{2K_5\ \Delta\bar{y}_5}{\Delta\bar{y}_6(\Delta\bar{x})^2}\ (\theta_{n-1,k,5} + \theta^{\Delta}_{n-1,k,5}) + \frac{2KW_1\ \theta_{n-1,k,6}}{(\Delta\bar{x})^2}$$

$$+\frac{2K_5}{\Delta\bar{y}_5\Delta\bar{y}_6}\left(\theta_{n,k-1,5}+\theta^{\Delta}_{n,k-1,5}\right)+\frac{2KW_3\,\theta_{n,k+1,6}}{(\Delta\bar{y}_6)^2}+\frac{2KW_1^{\Delta}}{(\Delta\bar{x})^2}$$

$$\left(\theta^{\Delta}_{n-1,k,6}-\theta^{\Delta}_{n,k,6}\right)+\frac{2KW_3^{\Delta}}{(\Delta\bar{y}_6)^2}\left(\theta^{\Delta}_{n,k+1,6}-\theta^{\Delta}_{n,k,6}\right)-\left[\frac{2L^2\Delta\bar{y}_5\,K_5}{\alpha_5 A_5\Delta\bar{y}_6}\right.$$

$$\left.+\frac{2KW_1}{(\Delta\bar{x})^2}+\frac{2KW_3}{(\Delta\bar{y}_6)^2}\right]\left[\theta_m-\frac{1}{\hat{C}_{pl}}\left(\hat{C}_{ps}\,\theta_m+\frac{L_f}{T_{ref}}\right)\right]+\frac{2L^2\Delta\bar{y}_5 B_5 K_5}{\alpha_5\,\Delta\bar{y}_6}\,\theta^{\Delta}_{n,k,5}\Big]\Big\}$$

$$H_{n,k,6}\geq H_{1m} \tag{48b}$$

$$\text{with } \theta_i\theta_{k,6}=\frac{H_{i,k,6}}{\hat{C}_{pl}\rho_l T_{ref}}-\frac{1}{\hat{C}_{pl}}\left(\hat{C}_{ps}\,\theta_m+\frac{L_f}{T_{ref}}\right)+\theta_m,\ i=1,\ \ldots,\ n$$

b. Ice-Ambient Interface

Let (i, m) be one of the ice-ambient interface nodes as shown in Figure 4c. Substitution of analog equation (20) into equation (14b) yields:

$$-K_6\left(\frac{\theta_{i,m+1,6}-\theta_{i,m-1,6}+\theta^{\Delta}_{i,m+1,6}-\theta^{\Delta}_{i,m-1,6}}{4\,\Delta\bar{y}_6}\right)$$

$$=h_{b2}\,L\left(\frac{\theta_{i,m,6}+\theta^{\Delta}_{i,m,6}}{2}-\theta_{g2}\right) \tag{49}$$

Temperatures $\theta_{i,m+1,6}$ and $\theta^{\Delta}_{i,m+1,6}$ are fictitious and are eliminated using equation (35) and employing the average thermal conductivity approach. Combining the resulting equation with equation (12) gives

For the solid phase:

$$H_{i,m,6}=\left\{1+\frac{\Delta t}{2L^2\hat{C}_{ps}\rho_s}\left[\frac{KW_1+KW_2}{(\Delta\bar{x})^2}+\frac{2KW_4}{(\Delta\bar{y}_6)^2}+\frac{2h_{b2}L}{\Delta\bar{y}_6}\right]\right\}^{-1}\times$$

$$\{H^{\Delta}_{i,m,6} + \frac{\Delta t T_{ref}}{2L^2}\left[\frac{KW_2\,\theta_{i+1,m,6} + KW_1\,\theta_{i-1,m,6}}{(\Delta\bar{x})^2} + \frac{2KW_4\,\theta_{i,m-1,6}}{(\Delta\bar{y}_6)^2}\right.$$

$$+ \frac{KW_1^{\Delta}}{(\Delta\bar{x})^2}(\theta^{\Delta}_{i-1,m,6} - \theta^{\Delta}_{i,m,6}) - \frac{KW_2^{\Delta}}{(\Delta\bar{x})^2}(\theta^{\Delta}_{i,m,6} - \theta^{\Delta}_{i+1,m,6}) - \frac{2KW_4^{\Delta}}{(\Delta\bar{y}_6)^2}$$

$$\left.(\theta^{\Delta}_{i,m,6} - \theta^{\Delta}_{i,m-1,6}) + \frac{2h_{b2}L}{\Delta\bar{y}_6}(2\,\theta_{g2} - \theta^{\Delta}_{i,m,6})\right]\}$$

$$i = 2, \ldots, n-1 \quad , \quad H_{i,m,6} \leq H_{sm} \tag{50}$$

Substitution of equation (22) into the above equation yields

At the centerline of the gap:

$$i = 1, \quad H_{1,m,6} = \{1+\frac{\Delta t}{2L^2\hat{C}_{ps}\rho_s}\left[\frac{2KW_2}{(\Delta\bar{x})^2} + \frac{2KW_4}{(\Delta\bar{y}_6)^2} + \frac{2h_{b2}L}{\Delta\bar{y}_6}\right]\}^{-1} x$$

$$\{H^{\Delta}_{1,m,6} + \frac{\Delta t T_{ref}}{2L^2}\left[\frac{2KW_2\,\theta_{2,m,6}}{(\Delta\bar{x})^2} + \frac{2KW_4\,\theta_{1,m-1,6}}{(\Delta\bar{y}_6)^2} + \frac{2KW_2^{\Delta}}{(\Delta\bar{x})^2}\right.$$

$$\left.(\theta^{\Delta}_{2,m,6} - \theta^{\Delta}_{1,m,6}) - \frac{2KW_4^{\Delta}}{(\Delta\bar{y}_6)^2}(\theta^{\Delta}_{1,m,6} - \theta^{\Delta}_{1,m-1,6}) + \frac{2h_{b2}L}{\Delta\bar{y}_6}(2\,\theta_{g2} - \theta^{\Delta}_{1,m,6})\right]\}$$

$$H_{1,m,6} \leq H_{sm} \tag{51a}$$

At the centerline of the heater:

$$i = n, \quad H_{n,m,6} = \{1 + \frac{\Delta t}{2L^2\hat{C}_{ps}\rho_s}\left[\frac{2KW_1}{(\Delta\bar{x})^2} + \frac{2KW_4}{(\Delta\bar{y}_6)^2} + \frac{2h_{b2}L}{\Delta\bar{y}_6}\right]\}^{-1} x$$

$$\{H^{\Delta}_{n,m,6} + \frac{\Delta t T_{ref}}{2L^2}\left[\frac{2KW_1\,\theta_{n-1,m,6}}{(\Delta\bar{x})^2} + \frac{2KW_4\,\theta_{n,m-1,6}}{(\Delta\bar{y}_6)^2} + \right.$$

$$\frac{2KW_1}{(\Delta\bar{x})^2}\overset{\Delta}{(\theta}_{n-1,m,6} - \overset{\Delta}{\theta}_{n,m,6}) - \frac{2KW_4}{(\Delta\bar{y}_6)^2}\overset{\Delta}{(\theta}_{n,m,6} - \overset{\Delta}{\theta}_{n,m-1,6}) +$$

$$\frac{2h_{b2}L}{\Delta\bar{y}_6}(2\,\theta_{g_2} - \overset{\Delta}{\theta}_{n,m,6})]\}$$

$$H_{n,m,6} \leq H_{sm} \tag{51b}$$

For the melting point:

$$H_{i,m,6} = \overset{\Delta}{H}_{i,m,6} - \frac{\Delta tT_{ref}}{2L^2}\{[\frac{KW_1 + KW_2}{(\Delta\bar{x})^2} + \frac{2KW_4}{(\Delta\bar{y}_6)^2} + \frac{2h_{b2}L}{\Delta\bar{y}_6}]\,\theta_m$$

$$- \frac{KW_2\,\theta_{i+1,m,6} + KW_1\,\theta_{i-1,m,6}}{(\Delta\bar{x})^2} - \frac{2KW_4\,\theta_{i,m-1,6}}{(\Delta\bar{y}_6)^2} - \frac{KW_1}{(\Delta\bar{x})^2}\overset{\Delta}{(\theta}_{i-1,m,6}$$

$$- \overset{\Delta}{\theta}_{i,m,6}) + \frac{KW_2}{(\Delta\bar{x})^2}\overset{\Delta}{(\theta}_{i,m,6} - \overset{\Delta}{\theta}_{i+1,m,6}) + \frac{2KW_4}{(\Delta\bar{y}_6)^2}\overset{\Delta}{(\theta}_{i,m,6} - \overset{\Delta}{\theta}_{i,m-1,6})$$

$$- \frac{2h_{b2}L}{\Delta\bar{y}_6}(2\,\theta_{g_2} - \overset{\Delta}{\theta}_{i,m,6})\}$$

$$i = 2, \ldots, n-1 \qquad H_{sm} < H_{i,m,6} \leq H_{lm} \tag{52}$$

Substituting equation (22) into equation (52) gives

At the centerline of the gap:

$$i = 1, \quad H_{1,m,6} = \overset{\Delta}{H}_{1,m,6} - \frac{\Delta tT_{ref}}{2L^2}\{[\frac{2KW_2}{(\Delta\bar{x})^2} + \frac{2KW_4}{(\Delta\bar{y}_6)^2} + \frac{2h_{b2}L}{\Delta\bar{y}_6}]\,\theta_m$$

$$- \frac{2KW_2\,\theta_{2,m,6}}{(\Delta\bar{x})^2} - \frac{2KW_4\,\theta_{1,m-1,6}}{(\Delta\bar{y}_6)^2} - \frac{2KW_2}{(\Delta\bar{x})^2}\overset{\Delta}{(\theta}_{2,m,6} - \overset{\Delta}{\theta}_{1,m,6})$$

$$+ \frac{2KW_4}{(\Delta\bar{y}_6)^2}\left(\theta^{\Delta}_{1,m,6} - \theta^{\Delta}_{1,m-1,6}\right) - \frac{2h_{b2}L}{\Delta\bar{y}_6}\left(2\,\theta_{g_2} - \theta^{\Delta}_{1,m,6}\right)\}$$

$$H_{sm} < H_{1,m,6} < H_{1m} \tag{53a}$$

At the centerline of the heater:

$$i = n,\ H_{n,m,6} = H^{\Delta}_{n,m,6} - \frac{\Delta t T_{ref}}{2L^2}\left\{\left[\frac{2KW_1}{(\Delta\bar{x})^2} + \frac{2KW_4}{(\Delta\bar{y}_6)^2} + \frac{2h_{b2}L}{\Delta\bar{y}_6}\right]\theta_m\right.$$

$$- \frac{2KW_1\,\theta_{n-1,m,6}}{(\Delta\bar{x})^2} - \frac{2KW_4\,\theta_{n,m-1,6}}{(\Delta\bar{y}_6)^2} - \frac{2KW_1^{\Delta}}{(\Delta\bar{x})^2}\left(\theta^{\Delta}_{n-1,m,6} - \theta^{\Delta}_{n,m,6}\right)$$

$$\left. + \frac{2KW_4^{\Delta}}{(\Delta\bar{y}_6)^2}\left(\theta^{\Delta}_{n,m,6} - \theta^{\Delta}_{n,m-1,6}\right) - \frac{2h_{b2}L}{\Delta\bar{y}_6}\left(2\,\theta_{g_2} - \theta^{\Delta}_{n,m,6}\right)\right\}$$

$$H_{sm} < H_{n,m,6} < H_{1m} \tag{53b}$$

<u>For the liquid phase:</u>

$$H_{i,m,6} = \left\{1 + \frac{\Delta t}{2L^2\hat{C}_{pl}\rho_l}\left[\frac{KW_1 + KW_2}{(\Delta\bar{x})^2} + \frac{2KW_4}{(\Delta\bar{y}_6)^2} + \frac{2h_{b2}L}{\Delta\bar{y}_6}\right]\right\}^{-1} x$$

$$\left\{H^{\Delta}_{i,m,6} - \frac{\Delta t T_{ref}}{2L^2}\left[\left(\frac{KW_1 + KW_2}{(\Delta\bar{x})^2} + \frac{2KW_4}{(\Delta\bar{y}_6)^2} + \frac{4h_{b2}L}{\Delta\bar{y}_6}\right)\left[\theta_m - \right.\right.\right.$$

$$\left.\left.\left.\frac{1}{\hat{C}_{pl}}\left(\hat{C}_{ps}\,\theta_m + \frac{L_f}{T_{ref}}\right)\right] - \frac{1}{(\Delta\bar{x})^2}\left(KW_2\,\theta_{i+1,m,6} + KW_1\,\theta_{i-1,m,6}\right) - \right.\right.$$

$$\frac{2KW_4\,\theta_{i,m-1,6}}{(\Delta\bar{y}_6)^2} - \frac{KW_1^{\Delta}}{(\Delta\bar{x})^2}\left(\theta^{\Delta}_{i-1,m,6} - \theta^{\Delta}_{i,m,6}\right) + \frac{KW_2^{\Delta}}{(\Delta\bar{x})^2}\left(\theta^{\Delta}_{i,m,6}\right.$$

$$\left.\left. - \theta^{\Delta}_{i+1,m,6}\right) + \frac{2KW_4^{\Delta}}{(\Delta\bar{y}_6)^2}\left(\theta^{\Delta}_{i,m,6} - \theta^{\Delta}_{i,m-1,6}\right) - \frac{2h_{b2}L}{\Delta\bar{y}_6}\left(2\,\theta_{g_2} - \theta^{\Delta}_{i,m,6}\right)\right]\right\}$$

$$i = 2, \ldots, n-1, \quad H_{i,m,6} \geq H_{1m} \tag{54}$$

Substitution of equation (22) into equation (54) yields,

At the centerline of the gap:

$$i = 1, \quad H_{1,m,6} = \{1 + \frac{\Delta t}{2L^2 \hat{C}_{p1}\rho_1}\left[\frac{2KW_2}{(\Delta\bar{x})^2} + \frac{2KW_4}{(\Delta\bar{y}_6)^2} + \frac{2h_{b2}L}{\Delta\bar{y}_6}\right]\}^{-1} \times$$

$$\{H^{\Delta}_{1,m,6} - \frac{\Delta t T_{ref}}{2L^2}\left[\left(\frac{2KW_2}{(\Delta\bar{x})^2} + \frac{2KW_4}{(\Delta\bar{y}_6)^2} + \frac{4h_{b2}L}{\Delta\bar{y}_6}\right)\left[\theta_m - \frac{1}{\hat{C}_{p1}}\right.\right.$$

$$\left.\left.(\hat{C}_{ps}\,\theta_m + \frac{L_f}{T_{ref}})\right] - \frac{2KW_2\,\theta_{2,m,6}}{(\Delta\bar{x})^2} - \frac{2KW_4\,\theta_{1,m-1,6}}{(\Delta\bar{y}_6)^2} -\right.$$

$$\frac{2KW_2}{(\Delta\bar{x})^2}(\theta^{\Delta}_{2,m,6} - \theta^{\Delta}_{1,m,6}) + \frac{2KW_4}{(\Delta\bar{y}_6)^2}(\theta^{\Delta}_{1,m,6} - \theta^{\Delta}_{1,m-1,6})$$

$$\left. - \frac{2h_{b2}L}{\Delta\bar{y}_6}(2\,\theta_{g_2} - \theta^{\Delta}_{1,m,6})\right]\}$$

$$H_{1,m,6} \geq H_{1m} \tag{55a}$$

At the centerline of the heater:

$$i = n, \quad H_{n,m,6} = \{1 + \frac{\Delta t}{2L^2 \hat{C}_{p1}\rho_1}\left[\frac{2KW_1}{(\Delta\bar{x})^2} + \frac{2KW_4}{(\Delta\bar{y}_6)^2} + \frac{2h_{b2}L}{\Delta\bar{y}_6}\right]\}^{-1} \times$$

$$\{H^{\Delta}_{n,m,6} - \frac{\Delta t T_{ref}}{2L^2}\left[\left(\frac{2KW_1}{(\Delta\bar{x})^2} + \frac{2KW_4}{(\Delta\bar{y}_6)^2} + \frac{4h_{b2}L}{\Delta\bar{y}_6}\right)\left[\theta_m -\right.\right.$$

$$\left.\left.\frac{1}{\hat{C}_{p1}}(\hat{C}_{ps}\,\theta_m + \frac{L_f}{T_{ref}})\right] - \frac{2KW_1\,\theta_{n-1,m,6}}{(\Delta\bar{x})^2} - \frac{2KW_4\,\theta_{n,m-1,6}}{(\Delta\bar{y}_6)^2}\right.$$

$$- \frac{2KW_1^{\Delta}}{(\Delta\bar{x})^2} (\theta^{\Delta}_{n-1,m,6} - \theta^{\Delta}_{n,m,6}) + \frac{2KW_4^{\Delta}}{(\Delta\bar{y}_6)^2} (\theta^{\Delta}_{n,m,6} - \theta^{\Delta}_{n,m-1,6})$$

$$- \frac{2h_{b2}L}{\Delta\bar{y}_6} (2\,\theta_{g_2} - \theta^{\Delta}_{n,m,6})]\}$$

$$H_{n,m,6} \geq H_{1m} \qquad (53b)$$

The above equations are now ready to be solved numerically.

IV. NUMERICAL SOLUTION BY COMPUTER IMPLEMENTATION

A. Gauss-Seidel Point Iterative Method

The Crank-Nicolson finite differencing formulation used in this study results in a set of algebraic equations which have to be solved simultaneously at each time step. The matrix size of the system is usually so large that the inverse by any direct method requires an excessive amount of calculations, quite apart from any considerations of round-off error. Most important, in this study, is the fact that the material phase at any grid point within the ice-water layer must be determined during the calculations. Accordingly, the system of equations has to be solved by an iterative procedure. The Gauss-Seidel method was chosen to perform this iteration because of its desirable convergence properties.

The Gauss-Seidel method is started with an initial approximation which is improved by successive back substitutions. In particular, a first approximation is used to calculate a second approximation, the second approximation is then used to calculate the third, and so on until some convergence cirterion is met. For example, equation (21b) can be rewritten in the following form:

$$\theta^{N+1}_{i,k,j} = A_j \left\{ \frac{\alpha_j}{2(L\Delta\bar{x})^2} \left[\theta^{N}_{i+1,k,j} + \theta^{N+1}_{i-1,k,j} + \theta^{\Delta}_{i+1,k,j} + \theta^{\Delta}_{i-1,k,j} \right] \right.$$

$$+ \frac{\alpha_j}{2(L\Delta\bar{y}_j)^2} [\theta^N_{i,k+1,j} + \theta^{N+1}_{i,k-1,j} + \theta^{\Delta}_{i,k+1,j} + \theta^{\Delta}_{i,k-1,j}] +$$

$$B_j \theta^{\Delta}_{i,k,j} + \frac{q''_j / L\Delta\bar{y}_j}{\rho_j \hat{C}_{pj} T_{ref}}) \qquad (56)$$

If $\theta^N_{i,k,j}$ denotes the last estimate which is known for all values of i and k, and $\theta^{N+1}_{i,k,j}$ denotes the new value, then $\theta^{N+1}_{i-1,k,j}$ and $\theta^{N+1}_{i,k-1,j}$ will both have already been calculated before computing $\theta^{N+1}_{i,k,j}$. All of the other difference equations can be rewritten in the same form as equation (56). These equations are successively solved over the whole grid system during each time step by making a series of passes until the difference between two successive pass values satisfies some specified small value, called the convergence criterion. A convergence criterion of 0.01% was used in this study. A complete discussion of the Gauss-Seidel method is given in References [40] and [41].

B. Numerical Program Algorithm

Figure 5 shows the flow chart of the computer program. The complete program is listed in the Appendix along with a sample input data file. The program can be used for both conventional English units or metric units by modifying the input-output formats. The program can be reduced to describe the one-dimensional thermal de-icer pad by setting the gap width equal to zero. A metric version of the program has been compiled and is available upon request.

Although the following modifications are not presently in the program, they could be easily incorporated: (1) time-varying ambient temperatures; (2) temperature - dependent heat transfer coefficients; (3) initial position - dependent temperature profiles; (4) imperfect interface contact at specified nodes; and (5) temperature dependent properties, although this would require the use of the Kirchhoff temperature.

V. DISCUSSION OF RESULTS

The computer model formulated in this study has been designed to investigate the effects of a number of parameters on one and two-dimensional de-icer performance. De-icer performance is measured by the de-icing time, which is the time required to raise the ice-abrasion shield interface temperature to 32°F, and, if the phase change is considered, to melt a thin layer of ice. The remaining ice can then be shed as a result of the dynamic forces acting on the outer surface of the aircraft blade.

In order to test the resulting program and algorithm, Figure 6 shows the one-dimensional comparison of results between the present study and those of Campbell [11] (an approximate analytical solution), Stallabrass [5] and Baliga [4]. Layer thickness and layer materials correspond to a standard design de-icer pad and are shown in the inset of Figure 6. The temperature rise plotted on the ordinate is the difference between 32°F and the initial temperature. E.g., if the initial temperature of the de-icer pad is -8°F, then a temperature rise of 40°F is necessary to bring the abrasion shield-ice interface temperature to 32°F, which corresponds to a de-icing time of approximately 7 seconds. It can be seen that excellent agreement is achieved between the present program and the approximate analytical solution. The results of Stallabrass [5] and Baliga [4] show a slightly optimistic temperature rise beyond 5 seconds.

A number of parameters were investigated using the present program, and, wherever possible, the results are compared with the results of Stallabrass [5], Baliga [4] and Marano [6] to illustrate de-icer performance. The one-dimensional model is the subject of Sections A through F below. The phase change is not considered in Sections A through H, whereas Sections I through L incorporate the Enthalpy method for the phase change simulation. For all of the following cases, unless otherwise specified, values of $h_{b1} = 1$ Btu/ft^2-hr-°F and $h_{b2} = 10^6$ Btu/ft^2-hr-°F were used. Material property data for this study are presented in Table 1.

A. Effect of Power Density

Figure 7 shows the results of the effect of heater power density on the de-icing time for various ambient temperatures. The power density for the heater ranged from 15 to 40 Watts/in^2. Good agreement is obtained with the results of Stallabrass [5], Baliga [4] and Marano [6]. A slight variation between results occurs because of the more optimistic nature of Stallabrass' and Baliga's results as indicated in Figure 6. Examination of Figure 7 reveals that the practical minimum power density for the de-icer is 25 Watts/in^2, which agrees with the observation made from tests both in the laboratory and on various helicopter blades [5]. For power densities on the order of 15 or 20 Watts/in^2, particularly at low ambient temperatures, de-icing times are quite long.

B. Effect of Heater Element Thickness

The heater element usually is made up either of a woven mat of wires and glass fibers, or of resistance ribbon. Woven mats are an order of magnitude thicker than resistance ribbon. Figure 8 presents a comparison with the results of Marano [6] for different thickness heaters. Curve 1 represents the response of a point (zero thickness) heater, which is an idealization and yields the best possible results. Curve 2 represents the response of a heater composed of resistance ribbon, and Curve 3 represents the response of a heater composed of a woven mat. It can be seen that good agreement between the two studies is obtained. In addition, Figure 8 shows that heater thickness does not drastically affect de-icer performance. The maximum difference between the de-icing times for the various thickness heaters shown is less than two seconds.

C. Effect of Insulation Thickness Ratio and Insulation Material

In order to obtain optimum de-icer performance, it is desired that a maximum amount of energy released from the heater be directed toward the ice layer. This can be accomplished by increasing the insulation thickness beneath the heater. The effect on energy transfer of increasing this thickness relative to the insulation thickness above the heater is shown in Figure 9. An insulation thickness of 0.010 inches was assumed for the outer epoxy/glass insulation layer for the present investigation. Figure 9 presents a comparison of de-icing times with the results of Baliga [4] for the effect of varying the insulation thickness ratio: inner insulation thickness/outer insulation thickness. Again, good agreement between the

studies is obtained. As shown in Figure 9, when the ratio is increased from 1 through 5 (Curve 1, 2, 3), the de-icing time decreases appreciably. It can be seen that increasing the inner insulation from 0.020" to 0.050" reduces the time required for a 45°F temperature rise from nearly 8.7 seconds to just over 6.9 seconds, a 21% improvement. It is also seen that increasing the insulation thickness ratio from 5 to 10 only has an appreciable effect for very low ambient temperatures (Curves 3 and 4).

Figure 10 shows a comparison with Baliga's results for the effect on the de-icing time when the epoxy/glass inner insulation layer having a thermal conductivity of 0.22 Btu/ft-hr-°F is replaced by a layer of Polytrifluorochloroethylene (KEL-F) of the same thickness but having a thermal conductivity of 0.04 Btu/ft-hr-°F. As shown in Figure 10, for a 45°F temperature rise, the de-icing time is reduced by 40% (Curves 1 and 3). Therefore, the use of an inner insulation material of very low thermal conductivity is recommended if it is also a good electrical insulator.

D. Effect of Substrate Material

An interesting result was obtained when a stainless steel substrate was substituted for the aluminum alloy substrate. It might be expected, because of the lower thermal conductivity and lower thermal diffusivity of the stainless steel, that the de-icing time would be reduced. However, the opposite was in fact found to be the case, as shown in Figure 11, which also contains Stallabrass' [5] results. This result is attributed to the higher thermal capacity per unit volume of the stainless steel.

E. Effect of Variable Heater Output

A number of time-dependent heater outputs have been investigated in this study. In this section, a ramp function heater output is presented and the temperature response at all interfacial nodes is determined. Figures 12a and b depict the temperature response for a point heat source with a ramp function output, 5 seconds on, 1 second off. These results are compared to a constant point heat source. In all cases the ambient temperature was -4°F. Both sources have an average power density of 25 Watts/in^2. As expected, the temperature at the various interfacial nodes drops as the heater is switched off, and rises after the heater is switched on. The temperature at the outer surface of the ice remains constant at -4°F. This is due to the large heat transfer coefficient at this surface. As indicated in Figures 12a and b, if heat is applied such that the heater is operated for a period of time until the ice-abrasion shield interface reaches 32°F, and then is switched off until another layer of ice forms on the blade surface, the total energy consumption for de-icing can be reduced. The computer program developed in this study has been tested with constant, ramp and sinusoidal heater outputs; however, it can be easily modified to accommodate any other type of variable heater output.

F. Effect of Initial Ice Layer Thickness

In order to determine what effect the ice layer thickness has on de-icer performance, an investigation was performed in which the initial ice layer thickness was varied from 0.10" to 0.50". Figure 13 shows the

results of this investigation, along with the corresponding results obtained by Marano [6]. It can be seen that the de-icing times for the thicker ice layers did not differ appreciably. However, for a thin ice layer (0.10") with a large convection rate at the ice-ambient interface, the de-icing time increased significantly. The reason for this unexpected result is that any ice layer acts somewhat as an "insulator" and therefore slows the passage of heat, thus allowing the supplied thermal energy to raise the abrasion shield-ice interface temperature. Consequently, for thicker initial layers of ice, this rate of temperature rise is relatively high, which results in shorter de-icing times. Conversely, for the case of very thin initial ice layers with high convection rates at the outer surface, the thermal energy supplied to the abrasion shield-ice interface is conducted through the ice layer and is convected to the ambient at high enough rates that the interface temperature rises more slowly, thus increasing the de-icing time.

G. Effect of Gap Width

Earlier attempts at analyzing transient heat flow in de-icer pads with only one-dimensional mathematical models proved to be inadequate for prediction purposes, as a 3 to 5 times greater energy requirement was needed in actual operation as versus that predicted. This difference has been attributed to the effect of two-dimensional heat flow, i.e., the effect of delayed heating over the gap between heater elements. The two-dimensional model of Figure 2 was programmed to investigate the effect of the width of the gap between legs of the heater elment. Gap

widths of 0.010", 0.030", 0.050" and 0.070" were investigated. Figure 14 employed an insulation thickness ratio of 2, a heater of zero thickness, but having a width of 0.510", and a 0.010" stainless steel abrasion shield and a 0.100" substrate. The heat transfer coefficients used were h_{b1} = 10 Btu/ft^2-hr-°F and h_{b2} = 200 Btu/ft^2-hr-°F. Figure 14 shows how much more time is required to achieve a given temperature rise over the gap than over the heater element. The results of Stallabrass [5] are also shown. It can be seen that to raise the temperature over the centerline of a 0.070" gap by 36°F requires 5.2 seconds more time than to raise the temperature over the centerline of the heater element by the same amount. The two-dimensional results of Stallabrass [5] are seen to be more optimistic than those obtained in the present study. Since Stallabrass used an explicit finite difference formulation which required small time and space increments in order to maintain stability and achieve accuracy, it is possible that excessive computer time prevented sufficient testing to find the increment sizes below which repetitive results were obtained. This would account for the difference in the results of the two studies, particularly at large gap widths. A 0.010" gap is seen to have an almost negligible effect on the abrasion shield-ice interface temperature rise.

H. Effect of Heat Transfer Coefficient

The magnitudes of the heat transfer coefficients, h_{b1} and h_{b2} of Figure 1, have a greater effect on de-icer performance than do any of the parameters previously discussed when the blade has a very thin initial ice layer at low ambient temperature. As shown in Table 2, to raise the

temperature over the centerline of a 0.070" gap by 36°F requires 11.3 seconds with heat transfer coefficient values of h_{b1} = 10 Btu/ft^2-hr-°F and h_{b2} = 200 Btu/ft^2-hr-°F, and 14.2 seconds with h_{b1} = 1 Btu/ft^2-hr-°F and h_{b2} = 10^6 Btu/ft^2-hr-°F. The initial ice layer thickness is 0.15". The reason for this phenomenon is already described in the Section F, i.e., the heat is rapidly conducted away from the abrasion shield-ice interface for very thin ice layers, low ambient temperatures, and high heat transfer coefficients. It can be seen from Table 2 that the de-icing time does not change for a temperature rise of 10.8°F. However, for high temperature increases (lower ambient temperatures) and greater gap widths, the heat transfer coefficient effect is very evident.

I. Effect of Phase Change

In the earlier part of this study, the phase change in the ice layer has been neglected, i.e., no account has yet been made for the latent heat needed to melt the ice. The Enthalpy method is applied to simulate the phase change in the ice layer as described in Chapter III. Figure 15 shows the temperature response for the substrate, heater, abrasion shield-ice interface and ice-ambient interface in the two-dimensional de-icer pad. It can be seen that the abrasion shield-ice interface over the center of the gap requires more time (11 sec.) to achieve a temperature of 32°F than does the same interface over the center of the heater element (4.6 sec.).

Figure 16 shows a more detailed comparison with the results of Stallabrass [5] for the effect of the phase change on the abrasion shield-

ice interface temperature. This de-icer pad had a gap width of 0.050", a power density of 25 Watts/in^2, an initial equilibrium temperature of 23°F, and a stainless steel abrasion shield and substrate 0.010" thick, respectively. Two curves are shown in Figure 16: the interface temperature above the center of the heater element and that above the center of the gap, both plotted as a function of time. Excellent agreement is achieved between the present study and Stallabrass' results. Curves 1, 4 and 6 show the interface temperatures would behave if the latent heat of the ice were not taken into account, i.e., if no phase change took place. These curves show that the interface temperatures increase continuously. Curves 2, 3, 5 and 7 show the temperature response if the latent heat of the ice is taken into account, illustrating that a plateau becomes evident when the abrasion shield-ice interface temperature reaches 32°F. This plateau remains until enough heat has been transferred into the nodal volume to completely melt all of the ice in that volume, after which the interface temperature smoothly increases. However, this plateau is a consequence of the numerical solution technique, and in reality does not occur. As mentioned in Marano [6], the temperature response at the abrasion shield-ice interface and for any point in the ice layer has a very strong nodal dependence. If more than 90 nodes are used in the ice layer, the temperature response curves will not exhibit a plateau. However, such simulations consume a large amount of computer time, and the average temperatures obtained are identical with those resulting when a lesser number of nodes is used [6]. It can be seen from Figure 16 that the phase change does not occur over the center of the

gap until about 4.2 seconds for the present study, as versus 0.9 seconds over the center of the heater.

J. Effect of Abrasion Shield

The abrasion shield has sometimes been called the heat diffuser for it will diffuse or conduct the heat laterally, thus producing greater uniformity of the temperature distribution at the abrasion shield-ice interface. Table 3 employed the same basic de-icer pad as given in Figure 16, with the abrasion shield material being changed each time. Good agreement is shown in Table 3 as compared with the results of Stallabrass [5]. Case 1 is the case presented in Figure 16, i.e., a 0.010" stainless steel abrasion shield. The values tabulated are the de-icing times for the abrasion shield-ice interface to reach 32°F over the center of the heater element and over the center of the gap. Initial equilibrium temperature in all cases was 23°F and the power density was 25 Watts/in^2. Case 2 shows that replacing the thin stainless steel abrasion shield by the same thickness of a more highly conductive material (nickel) has little effect. This is true also of a 0.010" plating of nickel on 0.010" of stainless steel (Case 3). However, as the thickness of the more conductive material is increased, a great improvement is shown (compare Case 3 and Case 4). Case 5 shows that by locating the better thermal conductor beneath the poorer one, more heat flows parallel to the blade surface from the warmer to the colder regions. In Case 6, an additional insulating layer has been inserted between the two metal layers of Case 5. Although the de-icing time has been increased, the uniformity of the

heat distribution has been greatly improved. However, this process of improving lateral heat flow should not be taken too far because the added material will increase the thermal capacity of the system which in turn will increase the de-icing time.

Table 3 depicts the effect of increasing the thickness of a good conductor (nickel) from zero (Case 1) to 0.020" (Case 4). Further increase in the thickness of the nickel will yield further improvement in de-icing time over the gap before passing through a minimum; then the de-icing time will start to increase. Clearly, narrow heater gaps require a thinner abrasion shield as a heat diffuser to produce greater uniformity of surface temperature, while wider heater gaps require a thicker abrasion shield.

K. Effect of Ice Shedding

As soon as a thin layer of ice is melted, the ice layer plus any water which has formed is shed from the de-icer pad due to the aerodynamic and/or centrifugal forces acting on the outer surface of the composite blade. Once the heater has been turned off, a new ice layer may form. Figure 17 shows the temperature response of the de-icer pad for ice shedding for the first 20 second cycle. The heater was turned on for 10 seconds and then off for 10 seconds, and the ice was replaced every 20 seconds. The ice was shed when the interface over the heater gap reached 32°F and melted. Sharp decreases in the heater element temperatures are shown to occur at 6.8 seconds and at 10.0 seconds. The former decrease is from the ice being shed, and the latter is from the

heater being turned off. The abrasion shield surface temperature drops immediately from 32°F to -4°F when the ice is shed. Only the substrate temperature remains warm after 20 seconds. During ice shedding, the program time step had to be drastically reduced in order to accurately follow the abrupt changes in temperature which occur.

Figure 18 shows the temperature response for the second cycle, from 20 to 40 seconds. The temperature profiles are quite similar to those in Figure 17. The only difference is that, since the substrate temperature is initially hotter because of residual heat, the de-icing time is deereased to 6.2 seconds.

L. Effect of Refreezing

From the results of Section K, it would be interesting to see the composite blade temperature response if the ice layer could not be shed and refreezing occurs. As shown in Figure 19, the heater was turned on for 10 seconds and then was turned off. In this case, the water at the abrasion shield-ice interface begins to refreeze after 12.0 seconds, and has completely solidified after 19.2 seconds.

VI. CONCLUSIONS AND RECOMMENDATIONS

The two-dimensional numerical simulation model developed in this study for the electrothermal de-icer pad has been shown to predict accurate temperature profiles for several boundary conditions and thermal heat sources. Parametric studies using the simulation to investigate such practical composite blade design aspects as the effect due to different heating functions on the rate and depth of ice melting, the effect of the abrasion shield on lateral heat transfer, the effect of the phase change on de-icer performance, etc., have been completed. The results were found to agree comparatively well with previous numerical calculations by Stallabrass [5], Baliga [4] and Marano [6]. The simulation contains the following improvements over Stallabrass' [5] two-dimensional numerical technique for the electrothermal de-icer pad:

(1) The Crank-Nicolson implicit finite difference scheme was used instead of the explicit forward finite difference method. This decreased the total number of calculations and promoted accuracy and stability;

(2) The Enthalpy method was used to simulate the phase change in the ice layer;

(3) The simulation can apply to shedding and refreezing of the ice layer.

(4) In addition, the program can be easily modified to handle time and position-varying ambient temperatures, temperature-dependent heat transfer coefficients, and imperfect contact between layers at specified nodes.

The computer program was run on the University of Toledo IBM 4341 computer. A 20 x 29 mesh was used to represent the 6 layers of the composite body. Typical computing times for a total simulation time of 20 seconds were 11 minutes without the phase change and 18 minutes with the phase change.

Based on the progress thus far, it is recommended that the following additional work be carried out:

(1) A complete experimental study should be conducted on de-icer pads in order to provide an exhaustive examination of the assumptions used in the simulation model and on model accuracy. It was originally anticipated that such experimental data would be available from tests conducted in the NASA Lewis Icing Tunnel. Unfortunately, the experimental study, originally scheduled for Summer, 1982, has been delayed until summer, 1983. At that time time important analysis should be carried out;

(2) In order to assess the effect of blade geometry on de-icer design, an analysis should be conducted using the true blade shape. This work is already underway at The University of Toledo, where a free-surface coordinate transformation technique is being investigated.

(3) Available model simulations which predict the rate of ice deposition on blade surfaces should be coupled with the internal blade heat transfer programs in order to simulate the total process of ice formation and removal.

APPENDIX

COMPLETE PROGRAM LISTING

AND

SAMPLE INPUT DATA FILE

```
//UOFT1575 JOB (UT,
// 06200016,19)
// EXEC   FORTXCLG,PARM='BCD'
//FORT.SYSIN  DD *
C       NUMERICAL SIMULATION OF TWO-DIMENSIONAL HEAT TRANSFER
C          IN COMPOSITE BODIES WITH PHASE CHANGE.
C
C       THIS PROGRAM CAN CALCULATE THE TEMPERATURE PROFILE IN
C       A COMPOSITE SLAB WHICH HAS CONVECTIVE,CONSTANT TEMP-
C       ERATURE OR MIXED BOUNDARY CONDITIONS.
C
C       THE PROGRAM CAN ALSO BE USED FOR COMPOSITE BODY PROBLEMS
C             WITH CONSTANT OR VARIABLE HEAT SOURCES.
C
C
C       AK              = THERMAL CONDUCTIVITIES OF LAYERS.
C       ALP             = THERMAL DIFFUSIVITIES OF LAYERS.
C       AKL             = THERMAL CONDUCTIVITY OF WATER.
C       ALPL            = THERMAL DIFFUSIVITY OF WATER.
C       CA              = CONSTANT.
C       CHANGE          = FUNCTION PROGRAM TO CORRECTING THERMAL
C                         CONDUCTIVITIES OF EACH NODE IN THE ICE LAYER
C                         FOR PHASE CHANGE
C       CPS,CPL         = SPECIFIC HEAT OF ICE AND WATER PER UNIT VOLUME.
C       DES,DEL         = DENSITY OF ICE AND WATER.
C       DTAUI           = INITIAL TIME STEP.
C       DTAUM           = INTERMEDIATE TIME STEP.
C       DTAUF           = FINAL TIME STEP.
C       DX              = SPACING BETWEEN NODES IN THE X-DIRECTION OF THE
C                         GRID.
C       DY              = SPACING BETWEEN NODES IN THE Y-DIRECTION OF THE
C                         GRID.
C       EL              = LENGTH OF EACH LAYER.
C       HEAD            = HEADINGS.
C       H1              = HEAT TRANSFER COEFF. AT LOWER BOUNDARY.
C       H2              = HEAT TRANSFER COEFF. AT UPPER BOUNDARY.
C       HLAM            = LATENT HEAT OF ICE.
C       IBC1            = 1, IMPLIES TEMPERATURE IS CONSTANT AT X=1.
C       IBC1            = 2, IMPLIES CONVECTIVE HEAT TRANSFER AT X=1.
C       IBC2            = 1, IMPLIES TEMPERATURE IS CONSTANT AT X=2.
C       IBC2            = 2, IMPLIES CONVECTIVE HEAT TRANSFER  AT X=2.
C       ICL             = NUMBER OF CYCLE FOR SHEDDING ICE.
C       ICOUNT          = COUNTER ON TIME STEP.
C       IFREQ           = NUMBER OF TIME STEPS BETWEEN SUCCESSIVE
C                                 PRINTING OF THE TEMPERATURE PROFILE.
C       IG              = 1, IMPLIES PHASE CHANGE IN ICE LAYER IS NOT
C                                                          CONSIDERED.
C       IG              = 2, IMPLIES PHASE CHANGE IN ICE LAYER IS
C                                                          . CONSIDERED.
C       IH              = 1, IMPLIES NO HEAT SOURCE.
C       IH              = 2, IMPLIES POINT HEAT SOURCE.
C       IH              = 3, IMPLIES HEAT GENERATION WITHIN SLAB.
C       IHQ             = 1, IMPLIES CONSTANT HEAT SOURCE.
C       IHQ             = 2, IMPLIES STEP FUNCTION HEAT SOURCE.
```

```
C       IHQ          = 3,  IMPLIES RAMP FUNCTION HEAT SOURCE.
C       IHQ          = 4,  IMPLIES SINE FUNCTION HEAT SOURCE.
C       IJ           = SLAB WITHIN WHICH HEAT GENERATION OCCURS.
C       IRF          = 1, IMPLIES REFREEZING ICE LAYER IS NOT
C                                                    CONSIDERED.
C       IRF          = 2, IMPLIES REFREEZING ICE LAYER IS CONSIDERED.
C       ISH          = 1, IMPLIES SHEDDING ICE LAYER IS NOT CONSIDERED.
C       ISH          = 2, IMPLIES SHEDDING ICE LAYER IS CONSIDERED.
C       L            = NUMBER OF LAYERS IN SLAB
C       L1           = LOWER SLAB NUMBER FOR POINT HEAT SOURCE.
C       L2           = UPPER SLAB NUMBER FOR POINT HEAT SOURCE.
C       M            = NUMBER OF NODES IN THE Y-DIRECTION OF THE GRID
C       MM           = INTERFACE NODE NUMBERS.
C       N            = NUMBER OF NODES IN THE X-DIRECTION OF THE GRID
C       NISP         = NUMBER OF TIME STEPS FOR WHICH INTIAL TIME
C                                                    STEP IS USED.
C       NMSP         = NUMBER OF TIME STEPS FOR WHICH INTERMIDIATE
C                                                    TIME STEP IS USED.
C       NFSP         = NUMBER OF TIME STEPS FOR REFREEZING ICE LAYER.
C       NHSP         = NUMBER OF TIME STEPS FOR SHEDDING AT 2ND CYCLE.
C       NTSP         = NUMBER OF TIME STEPS FOR STOPPING THE PROGRAM.
C       NO           = NUMBER OF NODES IN EACH LAYER IN THE Y-DIRECTION
C                      OF THE GRID
C       NO1          = LOWER NODE NUMBER FOR FINITE THICKNESS HEATER.
C       NO2          = UPPER NODE NUMBER FOR FINITE THICKNESS HEATER.
C       NODE         = NODE AT WHICH POINT HEAT SOURCE IS APPLIED.
C       Q            = POINT HEAT SOURCE  WATTS/IN*IN.
C       Q2           = VOLUMETRIC HEAT SOURCE WATTS/IN*IN*IN.
C       QHEAT2       = FUNCTION PROGRAM FOR STEP FUNCTION HEAT INPUT.
C       QHEAT3       = FUNCTION PROGRAM FOR RAMP FUNCTION HEAT INPUT.
C       QHEAT4       = FUNCTION PROGRAM FOR SINE FUNCTION HEAT INPUT.
C       QV           = INPUT FOR VARIABLE HEAT SOURCE.
C       T            = NON-DIMENSIONAL TEMPERATURE.
C       TE           = TEMPERATURE.
C       TG1          = AMBIENT TEMPERATURE AT LOWER BOUNDARY OF SLAB.
C       TG2          = AMBIENT TEMPERATURE AT UPPER BOUNDARY OF SLAB.
C       TIN          = INITIAL TEMPERATURE IN SLAB.
C       TLEN1        = TOTAL LENGTH OF THE SLAB IN THE Y-DIRECTION
C                      OF THE GRID
C       TLEN2        = WIDTH OF THE HEATER
C       TLEN3        = GAP WIDTH
C       TMP          = ICE MELTING TEMPERATURE.
C       TOFF         = OFF TIME OF STEP HEAT INPUT.
C       TON          = ON TIME OF STEP HEAT INPUT.
C       TR           = NON-DIMENSIONAL TEMPERATURE AT PREVIOUS
C                      TIME STEP
C       TREF         = REFERENCE TEMPERATURE.
C       TX1          = CONSTANT TEMPERATURE AT LOWER SLAB BOUNDARY.
C       TX2          = CONSTANT TEMPERATURE AT UPPER SLAB BOUNDARY.
C
C
      DATA IN/5/,IO/6/
      DIMENSION HEAD(42,80),DIF(30,95),THOLD(30,95),CONST(30,95)
      DIMENSION PHOLD(30,95),TOLD(30,95),H(30,95),HO(30,95)
```

```
      DIMENSION T(30,95),TR(30,95),TO(30,95),TEO(30,95),FDIST(30,95)
      DIMENSION ALP(7),CPD(7),NO(7),MM(7),DY(7),AK(7),EL(7),TE(30,95)
      DOUBLE PRECISION E1,F1,G1,P1,P2
      DOUBLE PRECISION A(7),B(7),C(7),D(7),E(7)
      COMMON /BLA1/HSMP,HLMP,AKS,AKL
C
C     INPUT  DATA
C
      DO 5 I=1,20
      READ(IN,700)(HEAD(I,J),J=1,80)
    5 CONTINUE
      READ(IN,701)L,N,M,TLEN1,TLEN2,TLEN3
C
      DO 10 I=1,N
      DO 10 J=1,M
      PHOLD(I,J)=0.
      TOLD(I,J)=0.
      THOLD(I,J)=0.
      CONST(I,J)=0.
      FDIST(I,J)=0.
      H(I,J)=0.
      HO(I,J)=0.
      T(I,J)=0.
      TE(I,J)=0.
      TO(I,J)=0.
      TEO(I,J)=0.
      TR(I,J)=0.
      DIF(I,J)=0.
   10 CONTINUE
      DO 15 K=1,L
      A(K)=0.
      B(K)=0.
      C(K)=0.
      D(K)=0.
      DY(K)=0.
      E(K)=0.
      CPD(K)=0.
      ALP(K)=0.
      AK(K)=0.
      EL(K)=0.
      DY(K)=0.
      NO(K)=0
      MM(K)=0
   15 CONTINUE
C
C     INPUT DATA
C
      DO 20 I=21,24
   20 READ(IN,700)(HEAD(I,J),J=1,80)
      DO 25 K=1,L
      READ(IN,702) NO(K),EL(K),AK(K),ALP(K)
   25 CONTINUE
      DO 30 I=25,27
   30 READ(IN,700)(HEAD(I,J),J=1,80)
```

```
      READ(IN,703)IH,NODE,L1,L2
      READ(IN,704)IJ,NO1,NO2,IHQ
      READ(IN,705)Q,TON,TOFF,QV
      DO 35 I=28,30
   35 READ(IN,700)(HEAD(I,J),J=1,80)
      READ(IN,706)IBC1,IBC2
      READ(IN,716)TX1,TX2
      READ(IN,707)TG1,H1,TG2,H2
      READ(IN,708)TIN,TREF
      DO 40 I=31,33
   40 READ(IN,700)(HEAD(I,J),J=1,80)
      READ(IN,709)IG,HLAM,ALPL,AKL,DEL,CPL,DES,CPS
      READ(IN,710)TMP
      DO 45 I=34,36
   45 READ(IN,700)(HEAD(I,J),J=1,80)
      READ(IN,711)DTAUI,NISP,DTAUM,NMSP,DTAUF
      READ(IN,712)IFREQ
      READ(IN,713)ISH,IRF,NFSP,ICL,NHSP,NTSP
C
C      PRINT THE DATA
C
      DO 50 I=1,20
   50 WRITE(IO,775)(HEAD(I,J),J=1,80)
      WRITE(IO,717)L,N,M,TLEN1,TLEN2,TLEN3
      DO 55 I=21,24
   55 WRITE(IO,775)(HEAD(I,J),J=1,80)
      DO 60 K=1,L
      WRITE(IO,702)NO(K),EL(K),AK(K),ALP(K)
   60 CONTINUE
      DO 65 I=25,27
   65 WRITE(IO,775)(HEAD(I,J),J=1,80)
      IF(IH.EQ.1) GO TO 70
      IF(IH.EQ.2) GO TO 75
      WRITE(IO,718)IJ,NO1,NO2
      GO TO 80
   70 WRITE(IO,719)
      GO TO 90
   75 WRITE(IO,720)NODE,L1,L2
   80 IF(IHQ.NE.1) GO TO 85
      WRITE(IO,721)Q
   85 IF(IHQ.NE.1)WRITE(IO,722)TON,TOFF
      IF(IHQ.EQ.2)WRITE(IO,724)QV
      IF(IHQ.EQ.3)WRITE(IO,726)QV
      IF(IHQ.EQ.4)WRITE(IO,727)QV
   90 CONTINUE
      DO 95 I=28,30
   95 WRITE(IO,775)(HEAD(I,J),J=1,80)
      IF(IBC1.EQ.2) GO TO 100
      WRITE(IO,729)TX1
      GO TO 105
  100 WRITE(IO,730)TG1,H1
  105 IF(IBC2.EQ.2) GO TO 110
      WRITE(IO,732)TX2
      GO TO 115
```

```
  110 WRITE(IO,734)TG2,H2
  115 WRITE(IO,736)TIN,TREF
      WRITE(IO,775)(HEAD(28,J),J=1,80)
      IF(IG.EQ.1)GO TO 120
      WRITE(IO,738)
      WRITE(IO,775)(HEAD(31,J),J=1,80)
      WRITE(IO,775)(HEAD(30,J),J=1,80)
      WRITE(IO,775)(HEAD(32,J),J=1,80)
      WRITE(IO,775)(HEAD(33,J),J=1,80)
      WRITE(IO,740)HLAM,AKL,ALPL,DEL,CPL,DES
      WRITE(IO,750)CPS
      WRITE(IO,752)TMP
      GO TO 125
  120 WRITE(IO,753)
  125 WRITE(IO,775)(HEAD(28,J),J=1,80)
      DO 130 I=34,36
  130 WRITE(IO,775)(HEAD(I,J),J=1,80)
      WRITE(IO,754)DTAUI,NISP,DTAUM,NMSP,DTAUF
      IF(ISH.EQ.1) GO TO 135
      WRITE(IO,756)
      IF(IRF.EQ.1) GO TO 135
      WRITE(IO,758)NFSP,ICL,NHSP
  135 WRITE(IO,760)IFREQ,NTSP
      WRITE(IO,775)(HEAD(1,J),J=1,80)
      WRITE(IO,762)
      WRITE(IO,775)(HEAD(18,J),J=1,80)
      WRITE(IO,775)(HEAD(1,J),J=1,80)
C
C       INITIAL CONDITIONS
C
      MJ=M
      IRP=0
      INCL=1
      NIP=0
      JSH=1
      G2TIME=TG2/TREF
      G1TIME=TG1/TREF
      TMP=TMP/TREF
      X2TIME=TX2/TREF
      X1TIME=TX1/TREF
      TLEN1=TLEN1/12.
      TLEN2=TLEN2/12.
      TLEN3=TLEN3/12.
      DO 140 J=1,L
  140 EL(J)=EL(J)/12.
      TIN=TIN/TREF
      TON=TON/3600.
      TOFF=TOFF/3600.
      DTAUI=DTAUI/3600.
      DTAUM=DTAUM/3600.
      DTAUF=DTAUF/3600.
      TAUI=TAUI/3600.
      TAUF=TAUF/3600.
      TAFI=TAFI/3600.
```

```
      DO 150 I=1,N
      DO 150 J=1,M
      FDIST(I,J)=TIN
      IF(TIN.LT.TMP) GO TO 145
      H(I,J)=CPL*TREF*FDIST(I,J)+DEL*(CPS*TMP*TREF/DES+HLAM)-TMP*TREF*
     1CPL
  145 H(I,J)=CPS*FDIST(I,J)*TREF
  150 CONTINUE
C
C     INTERFACE  NODE  NUMBERING
C
      MM(1)=NO(1)
      DO 160 I=2,L
      MM(I)=MM(I-1)+NO(I)-1
  160 CONTINUE
C
      AKS=AK(L)
      INC=MM(L-1)
      DX=(TLEN2+TLEN3)/(N*TLEN1)
C
C       SET UP GAP NODE
C
      NODEH=IFIX(TLEN3/(DX*TLEN1))+1
      NODEG=NODEH+1
      IF(TLEN3.EQ.0.) GO TO 165
      WRITE(IO,764)NODEG
      GO TO 170
  165 WRITE(IO,764)NODEH
C
C       PRINT THE INITIAL TEMPERATURE PROFILE AND ENTHALPYS
C
  170 DO 175 I=1,N
      DO 175 J=1,M
  175 T(I,J)=FDIST(I,J)
      DTAU=0.
      TAU=0.
      WRITE(IO,766) TAU
      DO 180 I=1,N
      DO 180 J=1,M
  180 TEO(I,J)=T(I,J)*TREF
      WRITE(IO,768)((TEO(I,J),J=1,M),I=1,N)
      HSMP=CPS*TMP*TREF
      HLMP=DEL*(CPS*TMP*TREF/DES+HLAM)
      HAFP=(HSMP+HLMP)/2.
C
C     CALCULATION OF CONSTANTS
C
      LA=0
      DTAU=DTAUI
  200 ICOUNT=1
      MOW=MJ-1
      NIP=NIP+1
C
C     DETERMINE THE TIME STEP
```

```
C
      IF(NIP.EQ.NISP+1) DTAU=DTAUM
      IF(JSH.EQ.3) GO TO 210
      IF(NIP.EQ.NMSP+1) DTAU=DTAUF
  210 IF(NIP.EQ.NHSP+1) DTAU=DTAUI
      LA=LA+1
      A1=1./DTAU
      IF(IRF.EQ.1) GO TO 215
      IF(NIP.EQ.NFSP) GO TO 687
C
C     CONVERGENCE CRITERIA
C
  215 EPSI=0.0001
C
C     CALCULATION OF CONSTANTS
C
      NOW=N-1
      DO 220 K=1,L
      DY(K)=EL(K)/(TLEN1*(NO(K)-1))
      C(K)=ALP(K)/(2.*TLEN1*TLEN1*DX*DX)
      D(K)=ALP(K)/(2.*TLEN1*TLEN1*DY(K)*DY(K))
      A(K)=1./(A1+2.*(C(K)+D(K)))
      B(K)=A1-2.*(C(K)+D(K))
      CPD(K)=AK(K)/ALP(K)
  220 CONTINUE
      NEW=L-1
      IF(L.EQ.1) GO TO 230
      DO 225 K=1,NEW
      E(K)=1./(1./(D(K)*A(K))+(AK(K+1)*DY(K))/(AK(K)*DY(K+1)*A(K+1)*
     1D(K+1)))
  225 CONTINUE
  230 DO 240 I=1,N
      DO 240 J=1,MJ
      TO(I,J)=T(I,J)
  240 CONTINUE
      DO 250 I=1,N
      DO 250 J=INC,MJ
      HO(I,J)=H(I,J)
  250 CONTINUE
      TI=TLEN1*TLEN1
      X1=1./(DX*DX)
      YL1=DY(L)*DY(L)
      YL2=DY(L-1)*DY(L-1)
      E1=2.*TLEN1*TLEN1*DY(1)*DY(1)/(A(1)*ALP(1))
      F1=4.*H1*TLEN1*DY(1)/AK(1)
      G1=1./(E1+F1/2.)
      P1=4.*H2*TLEN1*DY(L)/AK(L)
      P2=1./(1./(D(L)*A(L))+P1/2.)
      VAS=DTAU/(2.*TL*CPS)
      VAL=DTAU/(2.*TL*CPL)
      VA1=DTAU*AK(L-1)/(2.*CPS*TL*DY(L)*DY(L-1))
      VA2=DTAU*AK(L-1)/(2.*CPL*TL*DY(L)*DY(L-1))
      VA3=DTAU*TREF/(2.*TL)
      VA4=AK(L-1)*DY(L-1)*X1/DY(L)
```

```
      VA5=AK(L-1)/(DY(L-1)*DY(L))
      VA9=2.*H2*TLEN1/DY(L)
C
C     HEAT TERM INCLUSION
C
      IF(IHQ.EQ.1)Q1=Q
      IF(IHQ.EQ.2)Q1=QHEAT2(TAU,DTAU,TON,TOFF,QV)
      IF(IHQ.EQ.3)Q1=QHEAT3(TAU,DTAU,TON,TOFF,QV)
      IF(IHQ.EQ.4)Q1=QHEAT4(TAU,DTAU,TON,TOFF,QV)
      Q2=2.*3.4121*144.*Q1
C
C     CALCULATION OF CONSTANTS OF FINITE THICKNESS HEATER
C
      HEAT=Q2*DY(IJ)*TLEN1*DY(IJ)*TLEN1/(TREF*AK(IJ)*EL(IJ))
      FACT1=AK(IJ)*DY(IJ-1)/(AK(IJ-1)*DY(IJ))
      FACT2=AK(IJ+1)*DY(IJ)/(AK(IJ)*DY(IJ+1))
C
C     CALCULATION OF NEW TIME
C
      TAU=TAU+DTAU
C
      IF(L.NE.1) GO TO 295
  260 DO 270 I=1,N
      DO 270 J=2,MOW
      THOLD(I,J)=T(I,J)
  270 CONTINUE
C
C     CONSTANT AMBIENT TEMPERATURE BOUNDARY CONDITIONS FOR
C     ONE LAYER CASE ONLY
C
      DO 275 I=1,N
      T(I,1)=X1TIME
      T(I,M)=X2TIME
  275 CONTINUE
C
C     CALCULATION OF TEMPERATURES IN THE INTERIOR OF ONE LAYER
C     CASE ONLY
C
      DO 285 J=2,MOW
      T(1,J)=A(1)*(C(1)*2.*(T(2,J)+TO(2,J))+D(1)*(T(1,J+1)+T(1,J-1)+
     1TO(1,J+1)+TO(1,J-1))+B(1)*TO(1,J))
      DO 280 I=2,NOW
      T(I,J)=A(1)*(C(1)*(T(I+1,J)+T(I-1,J)+TO(I+1,J)+TO(I-1,J))+
     1D(1)*(T(I,J+1)+T(I,J-1)+TO(I,J+1)+TO(I,J-1))+B(1)*TO(I,J))
  280 CONTINUE
      T(N,J)=A(1)*(C(1)*2.*(T(N-1,J)+TO(N-1,J))+D(1)*(T(N,J+1)+
     1T(N,J-1)+TO(N,J+1)+TO(N,J-1))+B(1)*TO(N,J))
  285 CONTINUE
C
      DUMAX=0.
C
C     CHECK CONVERGENCE FOR CONSTANT TEMPERATURE BOUNDARY CONDITIONS
C     OF ONE LAYER CASE ONLY
C
```

```
      DO 290 I=1,N
      DO 290 J=2,MOW
      DIF(I,J)=ABS(T(I,J)-THOLD(I,J))
  290 DUMAX=AMAX1(DIF(I,J),DUMAX)
      GO TO 680
  295 IF((IBC1.EQ.1).AND.(IBC2.EQ.1))GO TO 315
C
C     GAUSS-SEIDEL REITERATION
C
  300 DO 305 I=1,N
      DO 305 J=1,MJ
      TOLD(I,J)=T(I,J)
  305 CONTINUE
C
C     CALCULATION OF TEMPERATURES AT THE INNER-AMBIENT INTERFACE
C
      T(1,1)=G1*(DY(1)*DY(1)*2.*(T(2,1)+TO(2,1))*X1+2.*(T(1,2)+
     1TO(1,2))+(B(1)/D(1)-F1/2.)*TO(1,1)+F1*G1TIME)
      DO 310 I=2,NOW
      T(I,1)=G1*(DY(1)*DY(1)*(T(I+1,1)+T(I-1,1)+TO(I+1,1)+TO(I-1,1))
     1*X1+2.*(T(I,2)+TO(I,2))+(B(1)/D(1)-F1/2.)*TO(I,1)+F1*G1TIME)
  310 CONTINUE
      T(N,1)=G1*(DY(1)*DY(1)*2.*(T(N-1,1)+TO(N-1,1))*X1+2.*(T(N,2)+
     1TO(N,2))+(B(1)/D(1)-F1/2.)*TO(N,1)+F1*G1TIME)
      GO TO 330
C
  315 DO 320 I=1,N
      DO 320 J=2,MOW
      PHOLD(I,J)=T(I,J)
  320 CONTINUE
C
C     CONVECTION BOUNDARY CONDITIONS FOR ONE LAYER CASE ONLY
C
      DO 325 I=1,N
      T(I,1)=X1TIME
      T(I,M)=X2TIME
  325 CONTINUE
C
  330 LIST=2
C
C
C     CALCULATION OF TEMPERATURES IN THE INTERIOR OF THE LAYER
C     AND AT THE INTERFACE BETWEEN LAYERS
C
C
      DO 600 K=1,L
      NN=MM(K)
      NNEW=NN-1
      INC1=INC+1
      IF(IH.EQ.3) GO TO 335
      GO TO 340
  335 IF(NN.EQ.NO2) GO TO 445
  340 IF(LIST.GT.NNEW) GO TO 360
      DO 355 J=LIST,NNEW
```

```
      IF(IG.EQ.1) GO TO 345
      IF(J.EQ.INC1) GO TO 530
  345 T(1,J)=A(K)*(C(K)*2.*(T(2,J)+TO(2,J))+D(K)*(T(1,J+1)+
     1T(1,J-1)+TO(1,J+1)+TO(1,J-1))+B(K)*TO(1,J))
      DO 350 I=2,NOW
      T(I,J)=A(K)*(C(K)*(T(I+1,J)+T(I-1,J)+TO(I+1,J)+TO(I-1,J))+
     1D(K)*(T(I,J+1)+T(I,J-1)+TO(I,J+1)+TO(I,J-1))+B(K)*TO(I,J))
  350 CONTINUE
      T(N,J)=A(K)*(C(K)*2.*(T(N-1,J)+TO(N-1,J))+D(K)*(T(N,J+1)+
     1T(N,J-1)+TO(N,J+1)+TO(N,J-1))+B(K)*TO(N,J))
  355 CONTINUE
  360 LIST=NN+1
      IF(IG.EQ.1) GO TO 375
      IF(ISH.EQ.1) GO TO 370
      IF(IRF.EQ.1) GO TO 370
      IF(IRP.EQ.1) GO TO 365
      IF(NIP.GE.NFSP) GO TO 370
      IF((JSH.EQ.2).AND.(NN.EQ.INC)) GO TO 610
      GO TO 370
  365 IF((JSH.EQ.3).AND.(NN.EQ.INC)) GO TO 610
  370 IF(NN.EQ.INC) GO TO 475
  375 IF(NN.EQ.MJ) GO TO 605
      IF(IH.EQ.3) GO TO 380
      IF(IH.EQ.2) GO TO 385
      IF(IH.EQ.1) GO TO 395
  380 IF(NN.EQ.NO1) GO TO 430
      GO TO 395
  385 IF(NN.EQ.NODE) GO TO 390
      GO TO 395
  390 IF(TLEN3.EQ.0.) GO TO 415
  395 T(1,NN)=E(K)*((DY(K)*DY(K)/(DX*DX)+DY(K+1)*DY(K)*AK(K+1)/
     1(DX*DX*AK(K)))*2.*(T(2,NN)+TO(2,NN))+2.*(T(1,NN-1)+TO(1,NN-1))+
     22.*AK(K+1)*DY(K)*(T(1,NN+1)+TO(1,NN+1))/(AK(K)*DY(K+1))+(B(K)/
     3D(K)+AK(K+1)*DY(K)*B(K+1)/(AK(K)*D(K+1)*DY(K+1)))*TO(1,NN))
      DO 410 I=2,NOW
      IF(IH.EQ.2) GO TO 400
      IF(IH.EQ.1) GO TO 405
      IF(IH.EQ.3) GO TO 405
  400 IF((NN.EQ.NODE).AND.(I.EQ.NODEG)) GO TO 420
  405 T(I,NN)=E(K)*((DY(K)*DY(K)/(DX*DX)+DY(K+1)*DY(K)*AK(K+1)/
     1(DX*DX*AK(K)))*(T(I+1,NN)+T(I-1,NN)+TO(I+1,NN)+TO(I-1,NN))+2.*
     2(T(I,NN-1)+TO(I,NN-1))+2.*AK(K+1)*DY(K)*(T(I,NN+1)+TO(I,NN+1))/
     3(AK(K)*DY(K+1))+(B(K)/D(K)+AK(K+1)*DY(K)*B(K+1)/(AK(K)*
     4D(K+1)*DY(K+1)))*TO(I,NN))
  410 CONTINUE
      T(N,NN)=E(K)*((DY(K)*DY(K)/(DX*DX)+DY(K+1)*DY(K)*AK(K+1)/
     1(DX*DX*AK(K)))*2.*(T(N-1,NN)+TO(N-1,NN))+2.*(T(N,NN-1)+
     2TO(N,NN-1))+2.*AK(K+1)*DY(K)*(T(N,NN+1)+TO(N,NN+1))/(AK(K)*
     3DY(K+1))+(B(K)/D(K)+AK(K+1)*DY(K)*B(K+1)/(AK(K)*D(K+1)*
     4DY(K+1)))*TO(N,NN))
      GO TO 600
C
C     POINT HEATER
C
```

```
  415 T(1,NODE)=E(L1)*((DY(L1)*DY(L1)/(DX*DX)+DY(L2)*DY(L1)*AK(L2)/
     1(DX*DX*AK(L1)))*2.*(T(2,NODE)+TO(2,NODE))+2.*(T(1,NODE-1)+
     2TO(1,NODE-1))+2.*AK(L2)*DY(L1)*(T(1,NODE+1)+TO(1,NODE+1))/
     3(AK(L1)*DY(L2))+(B(L1)/D(L1)+AK(L2)*DY(L1)*B(L2)/(AK(L1)*
     4D(L2)*DY(L2)))*TO(1,NODE)+4.*TLEN1*DY(L1)*Q1*3.4121*144./
     5(TREF*AK(L1)))
  420 DO 425 I=NODEG,NOW
      T(I,NODE)=E(L1)*((DY(L1)*DY(L1)/(DX*DX)+DY(L2)*DY(L1)*AK(L2)/
     1(DX*DX*AK(L1)))*(T(I+1,NODE)+T(I-1,NODE)+TO(I+1,NODE)+
     2TO(I-1,NODE))+2.*(T(I,NODE-1)+TO(I,NODE-1))+2.*AK(L2)*DY(L1)*
     3(T(I,NODE+1)+TO(I,NODE+1))/(AK(L1)*DY(L2))+(B(L1)/D(L1)+
     4AK(L2)*DY(L1)*B(L2)/(AK(L1)*D(L2)*DY(L2)))*TO(I,NODE)+4.*
     5TLEN1*DY(L1)*Q1*3.4121*144./(TREF*AK(L1)))
  425 CONTINUE
      T(N,NODE)=E(L1)*((DY(L1)*DY(L1)/(DX*DX)+DY(L2)*DY(L1)*AK(L2)/
     1(DX*DX*AK(L1)))*2.*(T(N-1,NODE)+TO(N-1,NODE))+2.*(T(N,NODE-1)+
     2TO(N,NODE-1))+2.*AK(L2)*DY(L1)*(T(N,NODE+1)+TO(N,NODE+1))/
     3(AK(L1)*DY(L2))+(B(L1)/D(L1)+AK(L2)*DY(L1)*B(L2)/(AK(L1)*
     4D(L2)*DY(L2)))*TO(N,NODE)+4.*TLEN1*DY(L1)*Q1*3.4121*144./
     5(TREF*AK(L1)))
      GO TO 600
C
C     FINITE THICKNESS HEATER
C
  430 IF(TLEN3.NE.0.) Q7=0.
      IF(TLEN3.EQ.0.) Q7=HEAT
      T(1,NO1)=E(IJ-1)*((DY(IJ-1)*DY(IJ-1)/(DX*DX)+DY(IJ)*DY(IJ)*
     1FACT1/(DX*DX))*2.*(T(2,NO1)+TO(2,NO1))+2.*(T(1,NO1-1)+
     2TO(1,NO1-1))+2.*FACT1*(T(1,NO1+1)+TO(1,NO1+1))+(B(IJ-1)/D(IJ-1)+
     3B(IJ)*FACT1/D(IJ))*TO(1,NO1)+Q7*FACT1)
      DO 435 I=2,NOW
      IF(I.LT.NODEG) Q8=0.
      IF(I.GE.NODEG) Q8=HEAT
      T(I,NO1)=E(IJ-1)*((DY(IJ-1)*DY(IJ-1)/(DX*DX)+DY(IJ)*DY(IJ)*
     1FACT1/(DX*DX))*(T(I+1,NO1)+T(I-1,NO1)+TO(I+1,NO1)+TO(I-1,NO1))+
     22.*(T(I,NO1-1)+TO(I,NO1-1))+2.*FACT1*(T(I,NO1+1)+TO(I,NO1+1))+
     3(B(IJ-1)/D(IJ-1)+B(IJ)*FACT1/D(IJ))*TO(I,NO1)+Q8*FACT1)
  435 CONTINUE
      T(N,NO1)=E(IJ-1)*((DY(IJ-1)*DY(IJ-1)/(DX*DX)+DY(IJ)*DY(IJ)*
     1FACT1/(DX*DX))*2.*(T(N-1,NO1)+TO(N-1,NO1))+2.*(T(N,NO1-1)+
     2TO(N,NO1-1))+2.*FACT1*(T(N,NO1+1)+TO(N,NO1+1))+(B(IJ-1)/D(IJ-1)+
     3B(IJ)*FACT1/D(IJ))*TO(N,NO1)+HEAT*FACT1)
      GO TO 600
  445 IF((NO2-NO1).EQ.1) GO TO 465
C
C     MORE THAN TWO NODES IN THE HEATER
C
  450 NFW=NO1+1
      NNFW=NO2-1
      DO 460 IL=NFW,NNFW
      IF(TLEN3.EQ.0.) Q3=Q2
      IF(TLEN3.NE.0.) Q3=0.
      T(1,IL)=A(IJ)*C(IJ)*2.*(T(2,IL)+TO(2,IL))+D(IJ)*(T(1,IL+1)+
     1T(1,IL-1)+TO(1,IL+1)+TO(1,IL-1))+B(IJ)*TO(1,IL)+Q3/(EL(IJ)*TREF*
```

```
     22.*CPD(IJ)))
      DO 455 I=2,NOW
      IF(I.LT.NODEG) Q4=0.
      IF(I.GE.NODEG) Q4=Q2
      T(I,IL)=A(IJ)*(C(IJ)*(T(I+1,IL)+T(I-1,IL)+TO(I+1,IL)+TO(I-1,IL))+
     1D(IJ)*(T(I,IL+1)+T(I,IL-1)+TO(I,IL+1)+TO(I,IL-1))+B(IJ)*TO(I,IL)+
     2Q4/(EL(IJ)*TREF*2.*CPD(IJ)))
  455 CONTINUE
      T(N,IL)=A(IJ)*(C(IJ)*2.*(T(N-1,IL)+TO(N-1,IL))+D(IJ)*(T(N,IL+1)+
     1T(N,IL-1)+TO(N,IL+1)+TO(N,IL-1))+B(IJ)*TO(N,IL)+Q2/(TREF*EL(IJ)*
     22.*CPD(IJ)))
  460 CONTINUE
  465 IF(TLEN3.EQ.0.) Q5=HEAT
      IF(TLEN3.NE.0.) Q5=0.
      T(1,NO2)=E(IJ)*((DY(IJ)*DY(IJ)/(DX*DX)+DY(IJ+1)*DY(IJ+1)*FACT2/
     1(DX*DX))*2.*(T(2,NO2)+TO(2,NO2))+2.*(T(1,NO2-1)+TO(1,NO2-1))+2.*
     2FACT2*(T(1,NO2+1)+TO(1,NO2+1))+(B(IJ)/D(IJ)+B(IJ+1)*FACT2/
     3D(IJ+1))*TO(1,NO2)+Q5)
      DO 470 I=2,NOW
      IF(I.LT.NODEG) Q6=0.
      IF(I.GE.NODEG) Q6=HEAT
      T(I,NO2)=E(IJ)*((DY(IJ)*DY(IJ)/(DX*DX)+DY(IJ+1)*DY(IJ+1)*FACT2/
     1(DX*DX))*(T(I+1,NO2)+T(I-1,NO2)+TO(I+1,NO2)+TO(I-1,NO2))+2.*
     2(T(I,NO2-1)+TO(I,NO2-1))+2.*FACT2*(T(I,NO2+1)+TO(I,NO2+1))+(B(IJ)
     3/D(IJ)+B(IJ+1)*FACT2/D(IJ+1))*TO(I,NO2)+Q6)
  470 CONTINUE
      T(N,NO2)=E(IJ)*((DY(IJ)*DY(IJ)/(DX*DX)+DY(IJ+1)*DY(IJ+1)*FACT2/
     1(DX*DX))*2.*(T(N-1,NO2)+TO(N-1,NO2))+2.*(T(N,NO2-1)+TO(N,NO2-1))+
     22.*FACT2*(T(N,NO2+1)+TO(N,NO2+1))+(B(IJ)/D(IJ)+B(IJ+1)*FACT2/
     3D(IJ+1))*TO(N,NO2)+HEAT)
      LIST=NN+1
      GO TO 600
C
C     CALCULATION OF ENTHALPYS AND TEMPERATURES AT THE SHIELD-
C     WATER INTERFACE
C
  475 IF(ICOUNT.NE.1) GO TO 480
      CALL CHANGE(HO(2,INC),HO(1,INC),HO(2,INC),HO(1,INC1),HO(1,INC),
     1IPO,AKO1,AKO2,AKO3,AKO4)
      CONST(1,INC)=AKO2*X1*2.*(TO(2,INC)-TO(1,INC))+2.*AKO3*(TO(1,INC+1)
     1-TO(1,INC))/YL1
  480 CALL CHANGE(H(2,INC),H(1,INC),H(2,INC),H(1,INC1),H(1,INC),IP,
     1AK1,AK2,AK3,AK4)
      VA6=(TMP*TREF-(DEL*(CPS*TMP*TREF/DES+HLAM)/CPL))/TREF
      VK1=(AK1+AK2)*X1
      VK2=(AK3+AK4)/YL1
      VK3=2.*AK3/YL1
      VK4=2.*AK4/YL1
      GO TO(483,485,487),IP
C     ICE
  483 H(1,INC)=1./(VA1/(D(L-1)*A(L-1))+VA5*(VK1+VK3)+1.)*(HO(1,INC)+
     1VA3*((T(2,INC)+TO(2,INC))*2.*VA4+X1*2.*AK2*T(2,INC)+2.*VA5*(
     2T(1,INC-1)+TO(1,INC-1))+VK3*T(1,INC+1)+CONST(1,INC)+B(L-1)*VA5*
     3TO(1,INC)/D(L-1)))
```

```
      T(1,INC)=H(1,INC)/(CPS*TREF)
      IF(H(1,INC).LE.HSMP) GO TO 490
      IP=1
C     MELTING POINT
  485 H(1,INC)=HO(1,INC)+VA3*(-(VA5/(D(L-1)*A(L-1))+VK1+VK3)*TMP+(
     1T(2,INC)+TO(2,INC))*2.*VA4+X1*AK2*2.*T(2,INC)+2.*VA5*(T(1,INC-1)+
     2TO(1,INC-1))+VK3*T(1,INC+1)+CONST(1,INC)+B(L-1)*VA5*TO(1,INC)/
     3D(L-1))
      T(1,INC)=TMP
      IF(H(1,INC).GT.HSMP.AND.H(1,INC).LT.HLMP) GO TO 490
      IF(IP.EQ.1.OR.IP.EQ.3) GO TO 490
C     LIQUID WATER
  487 H(1,INC)=1./(VA2/(D(L-1)*A(L-1))+VAL*(VK1+VK3)+1.)*(HO(1,INC)+
     1VA3*((T(2,INC)+TO(2,INC))*2.*VA4+X1*2.*AK2*T(2,INC)+2.*VA5*(
     2T(1,INC-1)+TO(1,INC-1))+VK3*T(1,INC+1)+CONST(1,INC)-(VA5/(D(L-1)*
     3A(L-1))+VK1+VK3)*VA6+B(L-1)*VA5*TO(1,INC)/D(L-1)))
      T(1,INC)=H(1,INC)/(TREF*CPL)-DEL*(CPS*TMP*TREF/DES+HLAM)/(CPL*TREF
     1)+TMP
      IF(H(1,INC).GE.HLMP) GO TO 490
      IP=3
      GO TO 483
  490 DO 510 I=2,NOW
      IF(ICOUNT.NE.1) GO TO 495
      CALL CHANGE(HO(I-1,INC),HO(I,INC),HO(I+1,INC),HO(I,INC1),
     1HO(I,INC),IPO,AKO1,AKO2,AKO3,AKO4)
      CONST(I,INC)=AKO1*X1*(TO(I-1,INC)-TO(I,INC))-AKO2*X1*(TO(I,INC)-
     1TO(I+1,INC))+2.*AKO3*(TO(I,INC+1)-TO(I,INC))/YL1
  495 CALL CHANGE(H(I-1,INC),H(I,INC),H(I+1,INC),H(I,INC1),H(I,INC),IP
     1AK1,AK2,AK3,AK4)
      VK1=(AK1+AK2)*X1
      VK2=(AK3+AK4)/YL1
      VK3=2.*AK3/YL1
      VK4=2.*AK4/YL1
      GO TO(503,505,507),IP
C     ICE
  503 H(I,INC)=1./(VA1/(D(L-1)*A(L-1))+VAS*(VK1+VK3)+1.)*(HO(I,INC)+
     1VA3*((T(I+1,INC)+T(I-1,INC)+TO(I+1,INC)+TO(I-1,INC))*VA4+X1*(AK2*
     2T(I+1,INC)+AK1*T(I-1,INC))+2.*VA5*(T(I,INC-1)+TO(I,INC-1))+VK3*
     3T(I,INC+1)+CONST(I,INC)+B(L-1)*VA5*TO(I,INC)/D(L-1)))
      T(I,INC)=H(I,INC)/(CPS*TREF)
      IF(H(I,INC).LE.HSMP) GO TO 510
      IP=1
C     MELTING POINT
  505 H(I,INC)=HO(I,INC)+VA3*(-(VA5/(D(L-1)*A(L-1))+VK1+VK3)*TMP+(
     1T(I+1,INC)+T(I-1,INC)+TO(I+1,INC)+TO(I-1,INC))*VA4+X1*(AK2*
     2T(I+1,INC)+AK1*T(I-1,INC))+2.*VA5*(T(I,INC-1)+TO(I,INC-1))+VK3*
     3T(I,INC+1)+CONST(I,INC)+B(L-1)*VA5*TO(I,INC)/D(L-1))
      T(I,INC)=TMP
      IF(H(I,INC).GT.HSMP.AND.H(I,INC).LT.HLMP) GO TO 510
      IF(IP.EQ.1.OR.IP.EQ.3) GO TO 510
C     LIQUID WATER
  507 H(I,INC)=1./(VA2/(D(L-1)*A(L-1))+VAL*(VK1+VK3)+1.)*(HO(I,INC)+VA3*
     1((T(I+1,INC)+T(I-1,INC)+TO(I+1,INC)+TO(I-1,INC))*VA4+X1*(AK2*
     2T(I+1,INC)+AK1*T(I-1,INC))+2.*VA5*(T(I,INC-1)+TO(I,INC-1))+VK3*
```

```
     3T(I,INC+1)+CONST(I,INC)-(VA5/(D(L-1)*A(L-1))+VK1+VK3)*VA6+B(L-1)*
     4VA5*TO(I,INC)/D(L-1)))
      T(I,INC)=H(I,INC)/(TREF*CPL)-DEL*(CPS*TMP*TREF/DES+HLAM)/(CPL*TREF
     1)+TMP
      IF(H(I,INC).GE.HLMP) GO TO 510
      IP=3
      GO TO 503
  510 CONTINUE
      IF(ICOUNT.NE.1) GO TO 520
      CALL CHANGE(HO(N-1,INC),HO(N,INC),HO(N-1,INC),HO(N,INC1),HO(N,INC)
     1,IPO,AKO1,AKO2,AKO3,AKO4)
      CONST(N,INC)=AKO1*X1*2.*(TO(N-1,INC)-TO(N,INC))+2.*AKO3*(
     1TO(N,INC+1)-TO(N,INC))/YL1
  520 CALL CHANGE(H(N-1,INC),H(N,INC),H(N-1,INC),H(N,INC1),H(N,INC),IP,
     2AK1,AK2,AK3,AK4)
      VK1=(AK1+AK2)*X1
      VK2=(AK3+AK4)/YL1
      VK3=2.*AK3/YL1
      VK4=2.*AK4/YL1
      GO TO(523,525,527),IP
C     ICE
  523 H(N,INC)=1./(VA1/(D(L-1)*A(L-1))+VAS*(VK1+VK3)+1.)*(HO(N,INC)+
     1VA3*((T(N-1,INC)+TO(N-1,INC))*2.*VA4+X1*2.*AK1*T(N-1,INC)+2.*VA5*
     2(T(N,INC-1)+TO(I,INC-1))+VK3*T(N,INC+1)+CONST(N,INC)+B(L-1)*VA5*
     4TO(N,INC)/D(L-1)))
      T(N,INC)=H(N,INC)/(TREF*CPS)
      IF(H(N,INC).LE.HSMP) GO TO 600
      IP=1
C     MELTING POINT
  525 H(N,INC)=HO(N,INC)+VA3*(-(VA5/(D(L-1)*A(L-1))+VK1+VK3)*TMP+(
     1T(N-1,INC)+TO(N-1,INC))*2.*VA4+X1*AK1*2.*T(N-1,INC)+2.*VA5*(
     2T(N,INC-1)+TO(N,INC-1))+VK3*T(N,INC+1)+CONST(N,INC)+B(L-1)*VA5*
     3TO(N,INC)/D(L-1))
      T(N,INC)=TMP
      IF(H(N,INC).GT.HSMP.AND.H(N,INC).LT.HLMP) GO TO 600
      IF(IP.EQ.1.OR.IP.EQ.3) GO TO 600
C     LIQUID WATER
  527 H(N,INC)=1./(VA2/(D(L-1)*A(L-1))+VAL*(VK1+VK3)+1.)*(HO(N,INC)+VA3*
     1((T(N-1,INC)+TO(N-1,INC))*2.*VA4+X1*2.*AK1*T(N-1,INC)+2.*VA5*(
     2T(N,INC-1)+TO(N,INC-1))+VK3*T(N,INC+1)+CONST(N,INC)-(VA5/(D(L-1)*
     3A(L-1))+VK1+VK3)*VA6+B(L-1)*VA5*TO(N,INC)/D(L-1)))
      T(N,INC)=H(N,INC)/(TREF*CPL)-DEL*(CPS*TMP*TREF/DES+HLAM)/(CPL*TREF
     1)+TMP
      IF(H(N,INC).GE.HLMP) GO TO 600
      IP=3
      GO TO 523
C
C     CALCULATION OF ENTHALPYS AND TEMPERATURES IN THE INTERIOR OF
C     THE ICE-WATER LAYER
C
  530 DO 590 J=INC1,MOW
      IF(ICOUNT.NE.1) GO TO 535
      CALL CHANGE(HO(2,J),HO(1,J),HO(2,J),HO(1,J+1),HO(1,J-1),IPO,
     1AKO1,AKO2,AKO3,AKO4)
```

```
      CONST(1,J)=AKO2*X1*2.*(TO(2,J)-TO(1,J))+(AKO3*(TO(1,J+1)-TO(1,J)
     1-AKO4*(TO(1,J)-TO(1,J-1)))/YL1
  535 CALL CHANGE(H(2,J),H(1,J),H(2,J),H(1,J+1),H(1,J-1),IP,AK1,AK2,
     1AK3,AK4)
      VK1=(AK1+AK2)*X1
      VK2=(AK3+AK4)/YL1
      VK3=2.*AK3/YL1
      VK4=2.*AK4/YL1
      GO TO(543,545,547),IP
C     ICE
  543 H(1,J)=1./(1.+VAS*(VK1+VK2))*(HO(1,J)+VA3*(X1*2.*AK2*T(2,J)+(
     1AK3*T(1,J+1)+AK4*T(1,J-1))/YL1+CONST(1,J)))
      T(1,J)=H(1,J)/(CPS*TREF)
      IF(H(1,J).LE.HSMP) GO TO 550
      IP=1
C     MELTING POINT
  545 H(1,J)=HO(1,J)+VA3*(-(VK1+VK2)*TMP+X1*2.*AK2*T(2,J)+(AK3*T(1,J+1)+
     1AK4*T(1,J-1))/YL1+CONST(1,J))
      T(1,J)=TMP
      IF(H(1,J).GT.HSMP.AND.H(1,J).LT.HLMP) GO TO 550
      IF(IP.EQ.1.OR.IP.EQ.3) GO TO 550
C     LIQUID WATER
  547 H(1,J)=1./(1.+VAL*(VK1+VK2))*(HO(1,J)+VA3*(-(VK1+VK2)*VA6+X1*
     12.*AK2*T(2,J)+(AK3*T(1,J+1)+AK4*T(1,J-1))/YL1+CONST(1,J)))
      T(1,J)=H(1,J)/(CPL*TREF)-DEL*(CPS*TMP*TREF/DES+HLAM)/(CPL*TREF)+
     1TMP
      IF(H(1,J).GE.HLMP) GO TO 550
      IP=3
      GO TO 543
  550 DO 570 I=2,NOW
      IF(ICOUNT.NE.1) GO TO 555
      CALL CHANGE(HO(I-1,J),HO(I,J),HO(I+1,J),HO(I,J+1),HO(I,J-1),
     1IPO,AKO1,AKO2,AKO3,AKO4)
      CONST(I,J)=AKO1*X1*(TO(I-1,J)-TO(I,J))-AKO2*X1*(TO(I,J)-TO(I+1,J))
     1+(AKO3*(TO(I,J+1)-TO(I,J))-AKO4*(TO(I,J)-TO(I,J-1)))/YL1
  555 CALL CHANGE(H(I-1,J),H(I,J),H(I+1,J),H(I,J+1),H(I,J-1),IP,
     1AK1,AK2,AK3,AK4)
      VK1=(AK1+AK2)*X1
      VK2=(AK3+AK4)/YL1
      VK3=2.*AK3/YL1
      VK4=2.*AK4/YL1
      GO TO(563,565,567),IP
C     ICE
  563 H(I,J)=1./(1.+VAS*(VK1+VK2))*(HO(I,J)+VA3*(X1*(AK2*T(I+1,J)+AK1*
     1T(I-1,J))+(AK3*T(I,J+1)+AK4*T(I,J-1))/YL1+CONST(I,J)))
      T(I,J)=H(I,J)/(CPS*TREF)
      IF(H(I,J).LE.HSMP) GO TO 570
      IP=1
C     MELTING POINT
  565 H(I,J)=HO(I,J)+VA3*(-(VK1+VK2)*TMP+X1*(AK2*T(I+1,J)+AK1*T(I-1,J))+
     1(AK3*T(I,J+1)+AK4*T(I,J-1))/YL1+CONST(I,J))
      T(I,J)=TMP
      IF(H(I,J).GT.HSMP.AND.H(I,J).LT.HLMP) GO TO 570
      IF(IP.EQ.1.OR.IP.EQ.3) GO TO 570
```

```
C     LIQUID WATER
  567 H(I,J)=1./(1.+VAL*(VK1+VK2))*(HO(I,J)+VA3*(-(VK1+VK2)*VA6+X1*(AK2*
     1T(I+1,J)+AK1*T(I-1,J))+(AK3*T(I,J+1)+AK4*T(I,J-1))/YL1+CONST(I,J))
     2)
      T(I,J)=H(I,J)/(TREF*CPL)-DEL*(CPS*TMP*TREF/DES+HLAM)/(CPL*TREF)+
     1TMP
      IF(H(I,J).GE.HLMP) GO TO 570
      IP=3
      GO TO 563
  570 CONTINUE
      IF(ICOUNT.NE.1) GO TO 575
      CALL CHANGE(HO(N-1,J),HO(N,J),HO(N-1,J),HO(N,J+1),HO(N,J-1),
     1IPO,AKO1,AKO2,AKO3,AKO4)
      CONST(N,J)=AKO1*X1*2.*(TO(N-1,J)-TO(N,J))+(AKO3*(TO(N,J+1)-TO(N,J)
     1)-AKO4*(TO(N,J)-TO(N,J-1)))/YL1
  575 CALL CHANGE(H(N-1,J),H(N,J),H(N-1,J),H(N,J+1),H(N,J-1),IP,AK1,
     1AK2,AK3,AK4)
      VK1=(AK1+AK2)*X1
      VK2=(AK3+AK4)/YL1
      VK3=2.*AK3/YL1
      VK4=2.*AK4/YL1
      GO TO(583,585,587),IP
C     ICE
  583 H(N,J)=1./(1.+VAS*(VK1+VK2))*(HO(N,J)+VA3*(X1*AK1*2.*T(N-1,J)+
     1(AK3*T(N,J+1)+AK4*T(N,J-1))/YL1+CONST(N,J)))
      T(N,J)=H(N,J)/(CPS*TREF)
      IF(H(N,J).LE.HSMP) GO TO 590
      IP=1
C     MELTING POINT
  585 H(N,J)=HO(N,J)+VA3*(-(VK1+VK2)*TMP+X1*2.*AK1*T(N-1,J)+(AK3*
     1T(N,J+1)+AK4*T(N,J-1))/YL1+CONST(N,J))
      T(N,J)=TMP
      IF(H(N,J).GT.HSMP.AND.H(N,J).LT.HLMP) GO TO 590
      IF(IP.EQ.1.OR.IP.EQ.3) GO TO 590
C     LIQUID WATER
  587 H(N,J)=1./(1.+VAL*(VK1+VK2))*(HO(N,J)+VA3*(-(VK1+VK2)*VA6+X1*2.*
     1AK1*T(N-1,J)+(AK3*T(N,J+1)+AK4*T(N,J-1))/YL1+CONST(N,J)))
      T(N,J)=H(N,J)/(TREF*CPL)-DEL*(CPS*TMP*TREF/DES+HLAM)/(CPL*TREF)+
     1TMP
      IF(H(N,J).GE.HLMP) GO TO 590
      IP=3
      GO TO 583
  590 CONTINUE
  600 CONTINUE
  605 IF((IBC1.EQ.1).AND.(IBC2.EQ.1))GO TO 672
      IF(IG.EQ.2) GO TO 615
C
C     CALCULATION OF TEMPERATURES AT THE OUTER-AMBIENT INTERFACE
C     WITHOUT PHASE CHANGE
C
  610 T(1,MJ)=P2*(YL1*2.*(T(2,MJ)+TO(2,MJ))*X1+2.*(T(1,MJ-1)+
     1TO(1,MJ-1))+(B(L)/D(L)-PI/2.)*TO(1,MJ)+P1*G2TIME)
      DO 612 I=2,NOW
      T(I,MJ)=P2*(YL1*(T(I+1,MJ)+T(I-1,MJ)+TO(I+1,MJ)+TO(I-1,MJ))*X1
```

```
     1+2.*(T(I,MJ-1)+TO(I,MJ-1))+(B(L)/D(L)-P1/2.)*TO(I,MJ)+P1*G2TIME)
  612 CONTINUE
      T(N,MJ)=P2*(YL1*2.*(T(N-1,MJ)+TO(N-1,MJ))*X1+2.
     1*(T(N,MJ-1)+TO(N,MJ-1))+(B(L)/D(L)-P1/2.)*TO(N,MJ)+P1*G2TIME)
      GO TO 677
C
C     CALCULATION OF TEMPERATURES AND ENTHALPYS AT THE OUTER-
C     AMBIENT INTERFACE
C
  615 IF(ICOUNT.NE.1) GO TO 617
      CALL CHANGE(HO(2,M),HO(1,M),HO(2,M),HO(1,M),HO(1,M-1),IPO,
     1AKO1,AKO2,AKO3,AKO4)
      CONST(1,M)=-AKO2*X1*2.*(TO(2,M)-TO(1,M))+2.*AKO4*(TO(1,M)-
     1TO(1,M-1))/YL1
  617 CALL CHANGE(H(2,M),H(1,M),H(2,M),H(1,M),H(1,M-1),IP,AK1,
     1AK2,AK3,AK4)
      VK1=(AK1+AK2)*X1
      VK2=(AK3+AK4)/YL1
      VK3=2.*AK3/YL1
      VK4=2.*AK4/YL1
      GO TO(623,625,627),IP
C     ICE
  623 H(1,M)=1./(1.+VAS*(VK1+VK4+VA9))*(HO(1,M)-VA3*(-X1*2.*AK2*T(2,M)-
     1VK4*T(1,M-1)+CONST(1,M)-VA9*(G?TIME*2.-TO(1,M))))
      T(1,M)=H(1,M)/(CPS*TREF)
      IF(H(1,M).LE.HSMP) GO TO 630
      IP=1
C     MELTING POINT
  625 H(1,M)=HO(1,M)-VA3*((VK1+VK4+VA9)*TMP-X1*2.*AK2*T(2,M)-VK4*
     1T(1,M-1)+CONST(1,M)-VA9*(G2TIME*2.-TO(1,M)))
      T(1,M)=TMP
      IF(H(1,M).GT.HSMP.AND.H(1,M).LT.HLMP) GO TO 630
      IF(IP.EQ.1.OR.IP.EQ.3) GO TO 630
C     LIQUID WATER
  627 H(1,M)=1./(1.+VAL*(VK1+VK4+VA9))*(HO(1,M)-VA3*((VK1+VK4+VA9)*
     1VA6-X1*AK2*2.*T(2,M)-VK4*T(1,M-1)+CONST(1,M)-VA9*(G2TIME*2.-
     1TO(1,M))))
      T(1,M)=H(1,M)/(TREF*CPL)-DEL*(CPS*TMP*TREF/DES+HLAM)/(CPL*TREF)+
     1TMP
      IF(H(1,M).GE.HLMP) GO TO 630
      IP=3
      GO TO 623
  630 DO 650 I=2,NOW
      IF(ICOUNT.NE.1) GO TO 635
      CALL CHANGE(HO(I-1,M),HO(I,M),HO(I+1,M),HO(I,M),HO(I,M-1),IPO,
     1AKO1,AKO2,AKO3,AKO4)
      CONST(I,M)=-AKO1*X1*(TO(I-1,M)-TO(I,M))+AKO2*X1*(TO(I,M)-TO(I+1,M)
     1)+2.*AKO4*(TO(I,M)-TO(I,M-1))/YL1
  635 CALL CHANGE(H(I-1,M),H(I,M),H(I+1,M),H(I,M),H(I,M-1),IP,AK1,
     1AK2,AK3,AK4)
      VK1=(AK1+AK2)*X1
      VK2=(AK3+AK4)/YL1
      VK3=2.*AK3/YL1
      VK4=2.*AK4/YL1
```

```
      GO TO(643,645,647),IP
C     ICE
  643 H(I,M)=1./(1.+VAS*(VK1+VK4+VA9))*(HO(I,M)-VA3*(-X1*(AK2*T(I+1,M)+
     1AK1*T(I-1,M))-VK4*T(I,M-1)+CONST(I,M)-VA9*(G2TIME*2.-TO(I,M))))
      T(I,M)=H(I,M)/(TREF*CPS)
      IF(H(I,M).LE.HSMP) GO TO 650
      IP=1
C     MELTING POINT
  645 H(I,M)=HO(I,M)-VA3*((VK1+VK4+VA9)*TMP-X1*(AK2*T(I+1,M)+AK1*
     1T(I-1,M))-VK4*T(I,M-1)+CONST(I,M)-VA9*(G2TIME*2.-TO(I,M)))
      T(I,M)=TMP
      IF(H(I,M).GT.HSMP.AND.H(I,M).LT.HLMP) GO TO 650
      IF(IP.EQ.1.OR.IP.EQ.3) GO TO 650
C     LIQUID WATER
  647 H(I,M)=1./(1.+VAL*(VK1+VK4+VA9))*(HO(I,M)-VA3*((VK1+VK4+VA9)*VA6-
     1X1*(AK2*T(I+1,M)+AK1*T(I-1,M))-VK4*T(I,M-1)+CONST(I,M)-VA9*
     2(G2TIME*2.-TO(I,M))))
      T(I,M)=H(I,M)/(TREF*CPL)-DEL*(CPS*TMP*TREF/DES+HLAM)/(CPL*TREF)+
     1TMP
      IF(H(I,M).GE.HLMP) GO TO 650
      IP=3
      GO TO 643
  650 CONTINUE
      IF(ICOUNT.NE.1) GO TO 655
      CALL CHANGE(HO(N-1,M),HO(N,M),HO(N-1,M),HO(N,M),HO(N,M-1),IPO,
     1AKO1,AKO2,AKO3,AKO4)
      CONST(N,M)=-AKO1*2.*X1*(TO(N-1,M)-TO(N,M))+2.*AKO4*(TO(N,M)-
     1TO(N,M-1))/YL1
  655 CALL CHANGE(H(N-1,M),H(N,M),H(N-1,M),H(N,M),H(N,M-1),IP,AK1,AK2,
     1AK3,AK4)
      VK1=(AK1+AK2)*X1
      VK2=(AK3+AK4)/YL1
      VK3=2.*AK3/YL1
      VK4=2.*AK4/YL1
      GO TO(663,665,667),IP
C     ICE
  663 H(N,M)=1./(1.+VAS*(VK1+VK4+VA9))*(HO(N,M)-VA3*(-X1*AK1*2.*T(N-1,M)
     1-VK4*T(N,M-1)+CONST(N,M)-VA9*(G2TIME*2.-TO(N,M))))
      T(N,M)=H(N,M)/(CPS*TREF)
      IF(H(N,M).LE.HSMP) GO TO 670
      IP=1
C     MELTING POINT
  665 H(N,M)=HO(N,M)-VA3*((VK1+VK4+VA9)*TMP-X1*AK1*2.*T(N-1,M)-VK4*
     1T(N,M-1)+CONST(N,M)-VA9*(G2TIME*2.-TO(N,M)))
      T(N,M)=TMP
      IF(H(N,M).GT.HSMP.AND.H(N,M).LT.HLMP) GO TO 670
      IF(IP.EQ.1.OR.IP.EQ.3) GO TO 670
C     LIQUID WATER
  667 H(N,M)=1./(1.+VAL*(VK1+VK4+VA9))*(HO(N,M)-VA3*((VK1+VK4+VA9)*VA6-
     1X1*2.*AK1*T(N-1,M)-VK4*T(N,M-1)+CONST(N,M)-VA9*(G2TIME*2.-
     2TO(N,M))))
      T(N,M)=H(N,M)/(TREF*CPL)-DEL*(CPS*TMP*TREF/DES+HLAM)/(CPL*TREF)+
     1TMP
      IF(H(N,M).GE.HLMP) GO TO 670
```

```
      IP=3
      GO TO 663
  670 GO TO 677
  672 DUMAX=0.
C
C     CHECK THE CONVERGENCE FOR CONVECTION BOUNDARY CONDITIONS
C     OF ONE LAYER CASE ONLY
C
      DO 675 I=1,N
      DO 675 J=2,MOW
      DIF(I,J)=ABS(T(I,J)-PHOLD(I,J))
      DUMAX=AMAX1(DIF(I,J),DUMAX)
  675 CONTINUE
      GO TO 680
C
C     CHECK CONVERGENCE OF THE GAUSS-SEIDEL ITERATION
C
  677 DUMAX=0.
      DO 678 I=1,N
      DO 678 J=1,MJ
      DIF(I,J)=ABS(T(I,J)-TOLD(I,J))
      DUMAX=AMAX1(DIF(I,J),DUMAX)
  678 CONTINUE
C
C     CHECK SEE IF NEED ANY MORE ITERATION
C
  680 IF(DUMAX.LE.EPSI) GO TO 682
      ICOUNT=ICOUNT+1
      IF(L.EQ.1) GO TO 260
      IF((IBC1.EQ.1).AND.(IBC2.EQ.1))GO TO 315
      IF((IBC1.EQ.2).AND.(IBC2.EQ.2))GO TO 300
C
C
  682 TITAU=TAU*3600.
C
C     DETERMINATION OF WHETHER ICE LAYER SHOULD BE SHED
C
      IF(ISH.EQ.1) GO TO 685
      IF(JSH.EQ.3) GO TO 685
      IF((JSH.EQ.2).AND.(NIP.LT.NFSP)) GO TO 685
      HINC=H(1,INC)
      HINC=HAFP+(HINC-HSMP)/2.
      IF(HINC.LT.HAFP) GO TO 685
      JSH=2
      IF(IRP.EQ.1) JSH=3
      NISP=NIP
C
C     DETERMINATION OF WHETHER THE PROGRAM SHOULD BE TERMINATED
C     BY PHYSICAL TIME
C
  685 TCOUNT=0.015
      IF(TAU.GE.TCOUNT) GO TO 999
C
C     DETERMINATION OF WHETHER THE PROGRAM SHOULD BE TERMINATED
```

```
C     BY INPUT DATA OF TIME STEPS
C
      IF(NIP.GT.NTSP) GO TO 999
C
C     DETERMINATION OF WHETHER TEMPERATURES AND ENTHALPYS
C     FOR THE ICE LAYER SHOULD BE STORED FOR THE PURPOSE OF
C     RECREATING ICE AND SHEDDING THE ICE
C
      IF(IRF.EQ.1) GO TO 694
      IF(NIP.LT.NFSP) GO TO 694
      IF(IRP.EQ.1) GO TO 694
      IF((ISH.EQ.1).AND.(JSH.EQ.1)) GO TO 694
  687 DO 692 I=1,N
      DO 692 J=INC,M
      T(I,J)=TIN
      IF(TIN.LT.TMP) GO TO 690
      H(I,J)=CPL*TREF*T(I,J)+DEL*(CPS*TMP*TREF/DES+HLAM)-TMP*TREF*
     1CPL
  690 H(I,J)=CPS*T(I,J)*TREF
  692 CONTINUE
      IRP=1
  694 IF(ISH.EQ.1) GO TO 695
      IF((JSH.EQ.2).AND.(NIP.LT.NFSP))MJ=INC
      IF((JSH.EQ.2).AND.(NIP.GE.NFSP))MJ=M
      IF((JSH.EQ.3).AND.(NIP.GE.NFSP))MJ=INC
      IF(JSH.EQ.1)MJ=M
  695 IF(LA.NE.IFREQ) GO TO 200
      TITAU=TAU*3600.
C
C     PRINT OUT OF PROGRAM
C
      WRITE(IO,766)TITAU
      DO 697 I=1,N
      DO 697 J=1,MJ
      TR(I,J)=T(I,J)
      TE(I,J)=TR(I,J)*TREF
  697 CONTINUE
      WRITE(IO,768)((TE(I,J),I=1,N),J=1,MJ)
      IF(IRF.EQ.2.AND.NIP.EQ.NFSP) GO TO 699
      WRITE(IO,770)ICOUNT
  699 LA=0
      GO TO 200
  700 FORMAT(80A1)
  701 FORMAT(56X,I3/56X,I3/56X,I3/56X,F10.6/56X,F10.6/56X,F10.6)
  702 FORMAT(7X,I2,7X,F10.5,9X,F13.6,14X,F13.6)
  703 FORMAT(53X,I3/53X,I3/53X,I3/53X,I3)
  704 FORMAT(53X,I3/53X,I3/53X,I3/53X,I3)
  705 FORMAT(53X,F11.5/53X,F11.5/53X,F11.5/53X,F11.5)
  706 FORMAT(53X,I3/53X,I3)
  707 FORMAT(46X,F13.6/46X,F15.6/46X,F13.6/46X,F15.6)
  708 FORMAT(46X,F13.6/46X,F13.6)
  709 FORMAT(61X,I3/47X,F13.6/47X,F13.6/47X,F13.6/47X,F13.6/47X,F13.6
     1/47X,F13.6/47X,F13.6)
  710 FORMAT(47X,F13.6)
```

```
711 FORMAT(50X,F13.6/50X,I3/50X,F13.6/50X,I3/50X,F13.6)
712 FORMAT(50X,I3)
713 FORMAT(68X,I2/68X,I2/58X,I3/50X,I3/50X,I3/50X,I3)
716 FORMAT(46X,F13.6/46X,F13.6)
717 FORMAT(/ ' TOTAL NUMBER OF SLABS',38X,'L=',I3/ ' TOTAL NUMBER
   1OF NODES IN THE X-DIRECTION OF THE GRID',3X,'N=',I3/ ' TOTAL
   2 NUMBER OF NODES IN THE Y-DIRECTION OF THE GRID',1X,'M=',
   3 I3/ ' TOTAL LENGTH OF COMPOSITE SLAB IN THE Y-DIRECTION',
   4 6X,'TLEN1=',F13.6,'INCHS'/ ' TOTAL LENGTH OF THE HEATER IN THE
   5X-DIRECTION',8X,'TLEN2=',F13.6,'INCHS'/ ' GAP WIDTH',46X,
   6'TLEN3=',F13.6,'INCHS')
718 FORMAT(' INTERNAL HEAT GENERATION IN SLAB NUMBER',9X,' IJ=',
   1I3/33X,'BETWEEN NODE    NO1=',I3/36X,'AND NODE     NO2=',I3)
719 FORMAT(//10X,'THERE  IS  NO  HEAT  SOURCE  PRESENT  ')
720 FORMAT(/ ' POINT HEAT SOURCE IS PRESENT AT',17X,'NODE=',I3/
   133X,'BETWEEN SLAB     L1=',I3/36X,'AND  SLAB     L2=',I3)
721 FORMAT(/ ' CONSTANT HEAT INPUT OF',28X,'Q =',F13.6,'WATTS/IN*IN')
722 FORMAT(/ ' ON-TIME FOR HEAT INPUT',27X,'TON=',F13.6,'SECS'/
   1' OFF-TIME FOR HEAT INPUT',25X,'TOFF=',F13.6,' SECS')
724 FORMAT(/ ' STEP FUNCTION HEAT INPUT OF',28X,'QV=',F13.6,
   1' WATTS/IN*IN')
726 FORMAT(/ ' RAMP FUNCTION HEAT INPUT OF',28X,'QV=',F13.6,
   1' WATTS/IN*IN')
727 FORMAT(/ ' SINE FUNCTION HEAT INPUT OF',28X,'QV=',F13.6,
   1' WATTS/IN*IN')
729 FORMAT(// ' CONSTANT TEMPERATURE   AT  X=1',17X,' TX1=',F13.6,
   1' DEG.F')
730 FORMAT(// ' CONVECTION OCCURS      AT  X=1'/11X,'AMBIENT TEMPERAT
   1URE',5X,'TG1=',F13.6,'DEG.F'/11X,'HEAT TRANSFER COEFF.',5X,'H1 =',
   2F15.6,'B.T.U/HR.FT.FT.DEG.F')
732 FORMAT(// ' CONSTANT TEMPERATURE   AT  X=2',17X,'TX2=',F13.6,
   1'DEG.F')
734 FORMAT(// ' CONVECTION OCCURS      AT  X=2'/11X,'AMBIENT TEMPERAT
   1URE',5X,'TG2=',F13.6,'DEG.F'/11X,'HEAT TRANSFER COEFF.',5X,'H2 =',
   2F15.6,'B.T.U/HR.FT.FT.DEG.F')
736 FORMAT(/ ' THE INITIAL TEMPERATURE IN THE COMPOSITE SLAB  TIN =',
   1F13.6,'DEG.F'// ' THE REFERENCE TEMPERATURE',20X,' TREF =',F13.6,
   2'DEG.F')
738 FORMAT(// ' THE PHASE CHANGE IN THE ICE LAYER IS CONSIDERED ')
740 FORMAT(/ ' LATENT HEAT OF ICE ',21X,' HLAM =',F13.6,'B.T.U./LB'/
   1' THERMAL CONDUCTIVITY OF WATER',12X,'AKL  =',F13.6,'B.T.U./HR.
   2FT.DEG.F'/ ' THERMAL DIFFUSIVITY OF WATER ',12X,'ALPL =',F13.6,
   3' FT.FT/HR.'/ ' DENSITY OF WATER ',24X,'DEL  =',F13.6,'LB/CU.FT'/
   4 ' SPECIFIC HEAT * DENSITY OF WATER ',8X,'CPL  =',F13.6,'B.T.U./
   5CU.FT.DEG.F'/ ' DENSITY OF ICE ',26X,'DES  =',F13.6,'LB/CU.FT.')
750 FORMAT(/ ' SPECIFIC HEAT * DENSITY OF ICE ',10X,'CPS  =',F13.6,
   1' B.T.U./CU.FT.DEG.F')
752 FORMAT(/ ' ICE MELTING TEMPERATURE',18X,'TMP  =',F13.6,'DEG.F')
753 FORMAT(// ' THE PHASE CHANGE IN THE ICE LAYER IS NOT CONSIDERED')
754 FORMAT(/ ' INITIAL TIME STEP',26X,'DTAUI =',F13.6,'SECS'/28X,
   1'FOR TIME STEPS NISP   =',I3/ ' INTERMIDIATE TIME STEP',21X,
   2'DTAUM =',F13.6,'SECS'/28X,' FOR TIME STEPS NMSP  =',I3/
   3' FINAL TIME STEP',28X,'DTAUF =',F13.6,'SECS')
756 FORMAT(/// ' SHEDDING ICE LAYER IS CONSIDERED')
```

```
  758 FORMAT(/ ' INITIAL TEMPERATURE IS CHANGED FOR TIME STEPS NFSP =',
     1I3/ ' THE CYCLE FOR SHEDDING',24X,'ICL  =',I3/ ' FOR SHEDDING
     2 AT 2ND CYCLE FOR TIME STEPS  NHSP=',I3)
  760 FORMAT(' FREQUENCY OF TIME STEP/PRINT OF OUTPUT',6X,
     1'IFREQ=',I3/ ' FOR TIME STEPS STOP THE PROGRAM',13X,'NTSP =',I3)
  762 FORMAT(///28X,' TEMPERATURE PROFILE  IN  DEGREES F  ')
  764 FORMAT(/2X,'HEATER START AT NODE IN X-DIRECTION',5X,'NODEG=',I3)
  766 FORMAT(///35X,' TIME  TAU =',F15.6,' SECS')
  768 FORMAT(/5X,20F6.2)
  770 FORMAT(/2X,'PASS=',I3)
  775 FORMAT(' ',80A1)
  999 STOP
      END
C
C
C     SUBROUTINE FOR CONSTANT STEP FUNCTION HEAT SOURCE
C
C
      FUNCTION QHEAT2(TAU,DTAU,TON,TOFF,QV)
      TAUR=TAU
      TAUR=TAUR+0.5*DTAU
      IN=IFIX(TAUR/(TON+TOFF))
      IP=IN+1
      B =IN*TOFF+IP*TON
      C =IP*(TON+TOFF)
      QHEAT2=QV
      IF((B.LT.TAU).AND.(TAU.LT.C))QHEAT2=0.
      RETURN
      END
C
C
C     SUBROUTINE FOR RAMP FUNCTION HEAT SOURCE
C
C
      FUNCTION QHEAT3(TAU,DTAU,TON,TOFF,QV)
      TAUR=TAU
      TAUR=TAUR+0.5*DTAU
      IN=IFIX(TAUR/(TON+TOFF))
      YP=TAUR-IN*(TON+TOFF)
      A=QV/TON
      IF(YP.EQ.0) GO TO 20
      IF(YP-TON)10,10,20
   10 QHEAT3=YP*A
      GO TO 50
   20 QHEAT3=0.
   50 RETURN
      END
C
C
C     SUBROUTINE FOR SINE FUNCTION HEAT SOURCE
C
C
      FUNCTION QHEAT4(TAU,DTAU,TON,TOFF,QV)
      TAUR=TAU
```

```
      TAUR=TAUR+0.5*DTAU
      IN=IFIX(TAUR/(TON+TOFF))
      YP=TAUR-IN*(TON+TOFF)
      XP=YP*2.*3.14159/(TON+TOFF)
      QHEAT4=5.*SIN(XP)+QV
      RETURN
      END
C
C
C     SUBROUTINE FOR CORRECTING THERMAL CONDUCTIVITIES FOR PHASE CHANGE
C
C
      SUBROUTINE CHANGE(HL1,HL2,HL3,HL4,HL5,IPP,AK1,AK2,AK3,AK4)
      COMMON /SEA1/HSMP,HLMP,AKS,AKL
      DIMENSION HL(5),IP(5),CK(5)
      HL(1)=HL1
      HL(2)=HL2
      HL(3)=HL3
      HL(4)=HL4
      HL(5)=HL5
      DO 50 I=1,5
      IF(HL(I).LE.HSMP) GO TO 10
      IF(HL(I).GT.HSMP.AND.HL(I).LT.HLMP) GO TO 20
      IF(HL(I).GE.HLMP) GO TO 30
   10 IP(I)=1
      CK(I)=AKS
      GO TO 50
   20 IP(I)=2
      X=(HLMP-HL(I))/(HLMP-HSMP)
      CK(I)=X*AKS+(1.-X)*AKL
      GO TO 50
   30 IP(I)=3
      CK(I)=AKL
   50 CONTINUE
      IPP=IP(2)
      AK1=(CK(1)+CK(2))/2.
      AK2=(CK(3)+CK(2))/2.
      AK3=(CK(4)+CK(2))/2.
      AK4=(CK(5)+CK(2))/2.
      RETURN
      END
/*
//GO.FT06F001 DD SYSOUT=A,OUTLIM=9990
//GO.SYSIN  DD *
```

DATA FOR THE PROBLEM

```
COMMENTS:
        IF PHASE CHANGE IS CONSIDERED IG=2
        IF PHASE CHANGE IS NOT CONSIDERED IG=1
        FOR CONSTANT TEMPERATURE BOUNDARY CONDITIONS AT X=1 IBC1=1
         "      "           "          "          "     AT X=2 IBC2=1
         "  CONVECTION BOUNDARY CONDITIONS             AT X=1 IBC1=2
         "       "          "          "               AT X=2 IBC2=2
```

```
        IF NO HEAT SOURCE IS PRESENT                    IH  = 1
        IF POINT HEAT SOURCE IS PRESENT                 IH  = 2
        IF INTERNAL HEAT GENERATION IN A SLAB OCCURS    IH  = 3
        IF CONSTANT HEAT INPUT IS USED                  IHQ = 1
        IF STEP FUNCTION HEAT INPUT IS USED             IHQ = 2
        IF RAMP FUNCTION HEAT INPUT IS USED             IHQ = 3
        IF SINE FUNCTION HEAT INPUT IS USED             IHQ = 4
-------------------------------------------------------------------------
DATA FOR THE COMPOSITE BODY
**************************
TOTAL NUMBER OF SLABS                                    L= 6
TOTAL NUMBER OF NODES IN THE X-DIRECTION OF THE GRID     N= 20
TOTAL NUMBER OF NODES IN THE Y-DIRECTION OF THE GRID     M= 29
TOTAL LENGTH OF COMPOSITE SLAB IN THE Y-DIRECTION  TLEN1=  0.413000 INCHS
TOTAL LENGTH OF THE HEATER OF THE GRID             TLEN2=  0.255000 INCHS
GAP WIDTH                                          TLEN3=  0.015000 INCHS
DATA FOR EACH SLAB:
-------------------
NUMBER OF NODES    LENGTH          THERMAL CONDUCTIVITY        THERMAL DIFFUSIVITY
                 IN INCHS.      IN B.T.U./HR..FT.'F.          IN FT*FT/HR.
        5          0.08700          66.500000                    1.650000
        5          0.05000           0.220000                    0.008700
        2          0.00400           7.600000                    0.138000
        3          0.01000           0.220000                    0.008700
        3          0.01200           8.700000                    0.150000
       16          0.25000           1.416000                    0.049200
-----------------------------------
DATA FOR THE HEATER:
--------------------
TYPE OF HEAT SOURCE                                IH=  3
FOR IH=2  POINT HEAT SOURCE  AT                  NODE=  9
                                BETWEEN SLAB      L1=  2
                                  AND  SLAB       L2=  3
FOR IH=3  INTERNAL HEAT GENERATION IN SLAB        IJ=  3
                                BETWEEN NODE      NO1=  9
                                  AND  NODE       NO2= 10
TYPE OF HEAT SOURCE USED                          IHQ=  2
CONSTANT HEAT INPUT OF                             Q =   25.00000WATTS/IN*IN
ON-TIME FOR THE VARIABLE HEAT INPUT              TON  =   10.00000SEC.
OFF-TIME FOR THE VARIABLE HEAT INPUT             TOFF =   10.0000 SECS.
VARIABLE HEAT INPUT OF                            QV =   25.00000WATTS/IN*IN
:::::::::::::::::::::::::::::::::::::::::::::::::::::::::::::::::::::::::
BOUNDARY AND INITIAL CONDITIONS:
--------------------------------
TYPE OF BOUNDARY CONDITION                 AT X=1  IBC1=  2
                                           AT X=2  IBC2=  2
IF IBC1=1, CONSTANT TEMPERATURE  AT X=1   TX1 =    20.000000 DEG.F
IF IBC2=1,      "                AT X=2   TX2 =    20.000000 DEG.F
IF IBC1=2, AMBIENT       "       AT X=1   TG1 =    -4.00000 DEG.F
           HEAT TRANSFER COEFF   AT X=1    H1 =       1.000000
B.T.U./HR.FT*FT*'F
IF IBC2=2, AMBIENT  TEMPERATURE  AT X=2   TG2 =    -4.00000 DEG.F
           HEAT TRANSFER COEFF.  AT X=2    H2 = 1000000.000000
B.T.U/HR.FT.*FT*'F
THE INITIAL TEMPERATURE IN THE SLAB          TIN =    -4.000000 DEG.F
THE REFERENCE TEMPERATURE                    TREF =   32.000000 DEG.F
```

```
PROPERTIES OF WATER:

IS THE PHASE CHANGE CONSIDERED IF YES IG=2 IF NO IG=1      IG=  2
LATENT HEAT OF ICE                          HLAM =   143.40000 B.T.U./LB
THERMAL DIFFUSIVITY OF WATER                ALPL =     0.0051  FT*FT/HR.
   "    CONDUCTIVITY "   "                  AKL  =     0.32    B.T.U./HR.FT.'F.
DENSITY OF WATER                            DEL  =    62.40000 LB./CU.FT
SPECIFIC HEAT*DENSITY OF WATER              CPL  =    62.21280 B.T.U./CU.FT.'F.
DENSITY OF ICE                              DES  =    57.40000 LB./CU.FT
SPECIFIC HEAT*DENSITY OF ICE                CPS  =    28.81480 B.T.U./CU.FT.'F.
ICE MELTING TEMPERATURE                     TMP  =    32.00    DEG.'F.
.ADDITIONAL DATA:
.:::::::::::::::::
 INITIAL TIME STEP                          DTAUI =      0.100000 SECS.
                    FOR TIME STEPS          NISP  = 75
 INTERMIDIATE TIME STEP                     DTAUM =      0.001000 SECS.
                    FOR TIME STEPS          NMSP  =168
 FINAL TIME STEP                            DTAUF =      0.100000 SECS.
FREQUENCY OF TIME STEP PER PRINT OF OUTPUT IFREQ =  3
IS THE SHEDDING ICE LAYER CONSIDERED IF YES ISH=2 IF NO ISH=1    ISH= 2
DOES THE INITIAL TEMPERATURE CHANGE IF YES IRF=2 IF NO IRF=1     IRF= 2
INITIAL TEMPERATURE IS CHANGED FOR EACH TIME STEPS  NFSP =300
THE CYCLE FOR SHEDDING                      ICL   =  2
 FOR SHEDDING AT 2ND CYCLE FOR TIME STEPS   NHSP  =463
 FOR TIME STEPS STOP THE PROGRAM            NTSP  =600
/*
//
```

REFERENCES

1. Sparrow, E. M., S. V. Patankar and S. Ramadhyani, "Analysis of Melting in the Presence of Natural Convection in the Melt Region," Transactions of the ASME 99, 520, November, 1977.
2. Orr, J. L., J. H. Milsum and C. K. Rush, "Electro-Thermal De-Icing Systems: Their Design and Control," National Aeronautical Establishment Canada Commonwealth Advisory Aeronautical Research Council Laboratory Report LR-70, March, 1953.
3. Werner, J. B., "Ice Protection Investigation for Advanced Rotary-Wing Aircraft," Lockheed-California Report IR 25327-10, 1973.
4. Baliga, G., "Numerical Simulation of One-Dimensional Heat Transfer in Composite Bodies with Phase Change," M. Sc. Thesis, The University of Toledo, Toledo, Ohio, 1980.
5. Stallabrass, J. R., "Thermal Aspects of De-Icer Design," presented at the International Helicopter Icing Conference, Ottawa, Canada, 1972.
6. Marano, J. J., "Numerical Simulation of an Electrothermal De-Icer Pad," M. Sc. Thesis, The University of Toledo, Toledo, Ohio, May, 1982.
7. Carslaw, H. S. and J. C. Jaeger, Conduction of Heat in Solids, Clarendon Press, Oxford, 1959.

8. Scott, C., "Temperature Distribution in a Symmetrical Composite Body Placed in a New Environment," Part II of TDR No. ASD-TR-61-436, Part II Contract AF33(616)-7347, November, 1962.

9. Goodman, T. R., "The Adjoint Heat Conduction Problem for Solids," ASTIA-AD-254-769 (AFOSR-520), April, 1961.

10. Bouchillon, C. W., "Unsteady Heat Conduction in Composite Slabs," ASME Paper 64-WA/HT-13, 1964.

11. Campbell, W. F., "A Rapid Analytical Method for Calculating the Early Transient Temperature in a Composite Slab," NRC Lab Report MT-32, 1956.

12. Tittle, C. W., "Boundary Value Problems in Composite Media: Quasi-Orthogonal Functions," J. Appl. Phys. 36, 1486, 1965.

13. Tittle, C. W. and V. L. Robinson, "Analytical Solution of Conduction Problems in Composite Media," ASME Paper 65-WA/HT-52, 1965.

14. Peaceman, D. W. and H. H. Rachford, Jr., "The Numerical Solution of Parabolic and Elliptic Differential Equations," J. Soc. Indust. Appl. Math. 3, No. 1, March, 1955.

15 Von Rosenberg, D. V., Methods for the Numerical Solution of Partial Differential Equations, American Elsevier, 1969.

16. Nogotov, E. F., Applications of Numerical Heat Transfer, McGraw-Hill, New York, 1978.

17. Gent, R. W., and J. T. Cansdale, "One-Dimensional Treatment of Thermal Transients in Electrically De-Iced Helicopter Rotor Blades," RAE Technical Report 80159, 1980.

18. Goodman, T. R., "The Heat Balance Integral and Its Applications to Problems Involving a Change of Phase," Trans. ASME 80, 335, 1958.

19. Citron, S. J., "Heat Conduction in a Melting Slab," J. Aero/Space Sciences 27, 219, 1960.

20. Westphal, K. O., "Series Solution of Freezing Problems with the Fixed Surface Radiating into a Medium of Arbitrary Varying Temperature," Int. J. Heat & Mass Trans. 10, 195, 1967.

21. Chuang, Y. K. and J. Szekely, "On the Use of Green's Functions for Solving Melting and Solidification Problems," Int. J. Heat & Mass Transfer 14, 1285, 1971.

22. Imber, M. and P. B. S. Huang, "Phase Change in a Semi-Infinite Solid with Temperature Dependent Thermal Properties," Int. J. Heat & Mass Transfer 16, 1951, 1973.

23. Ockendon, J. R. and W. R. Hodgkins (editors), Moving Boundary Value Problems in Heat Flow and Diffusion, Oxford Univ. Press, Oxford, 1975.

24. Muehlbauer, J. C. and J. E. Sunderland, "Heat Conduction with Freezing or Melting," App. Mech. Rev. 18, 951, 1965.

25. Rubinstein, K. I., "The Stefan Problem," Trans. Math. Monog., No. 27, American Mathematical Society, 1972.

26. Özişik, M. N., Heat Conduction, Wiley-Interscience, 1980.

27. Heitz, W. I. and J. W. Westwater, "Extension of the Numerical Method for Melting and Freezing Problems," Int. J. Heat & Mass Transfer 13, 1371, 1970.

28. Murray, W. D. and F. Landis, "Numerical and Machine Solutions of Transient Heat Conduction Problems Involving Melting and Freezing. Part 1 - Method of Analysis and Sample Solutions," J. Heat Transfer 81, 106, 1959.

29. Crank, J., "Two Methods for the Numerical Solution of Moving Boundary Problems in Diffusion and Heat Flow," Q. J. Mech. Appl. Math. 10, 220, 1957.

30. Ehrlich, L. W., "A Numerical Method of Solving a Heat Flow Problem with a Moving Boundary," J. Assoc. Comput. Mach. 5, 161, 1958.

31. Voller, V. R., M. Cross and P. G. Walton, "Assessment of Weak Solution Numerical Techniques for Solving Stefan Problems," 172, Department of Mathematics & Computer Studies, Sunderland Polytechnic, U.K., 1979.

32. Atthey, D. R., "A Finite Difference Scheme for Melting Problems," J. Inst. Math. Appl. 13, 353, 1974.

33. Shamsunder, N. and E. M. Sparrow, "Analysis of Multidimensional Conduction Phase Change Via the Enthalpy Model," J. Heat Transfer 75, 333, 1975.

34. Fox, L., in Reference 8, p. 210.

35. Kamenomostskaja, S. L., "On the Stefan Problem," Mat. Sb. 53 (95), 489, 1961.

36. Crowley, A. B., "Numerical Solution of Stefan Problems," Int. J. Heat & Mass Transfer 21, 215, 1978.

37. Bonacina, C., G. Comini, A. Fasano and M. Primicerio, "Numerical Solution of Phase Change Problems," Int. J. Heat & Mass Transfer 16, 581, 1973.

38. Goodrich, L. E., "Efficient Numerical Technique for One-Dimensional Thermal Problems with Phase Change," Int. J. Heat & Mass Transfer 21, 615, 1978.

39. Meyer, G. H., "Multidimensional Stefan Problems," SIAM J. Num. Anal. 10, 522, 1973.

40. Ames, W. F., Nonlinear Partial Differential Equations in Engineering, Academic Press, New York, 1965.

41. Roach, P. J., Computational Fluid Dynamics, Hermosa Publishers, Albuquerque, NM, 1976.

TABLE 1. THERMAL PROPERTIES OF SELECTED MATERIALS

Material	Thermal Conductivity		Spec. Heat		Diffusivity		Density	
	$\frac{Btu}{ft\text{-}hr\text{-}^\circ F}$	$\frac{W}{m\text{-}^\circ C}$	$\frac{Btu}{lb\text{-}^\circ F}$	$\frac{J}{Kg\text{-}^\circ C}$	$\frac{ft^2}{hr}$	$10^5 \frac{m^2}{S}$	$\frac{lb}{ft^3}$	$\frac{Kg}{m^3}$
Aluminum (soft)	124	215	0.23	963	3.20	8.26	169	2705
Aluminum Alloy 75S-T6	66.5	115	0.23	963	1.65	4.26	175	2800
Beryllium Copper	60.5	105	0.10	419	1.17	3.02	515	8250
Copper	220	381	0.092	385	4.29	11.1	557	8900
Nickel	36	62.3	0.105	440	0.62	1.59	556	8900
Nichrome 80/20	7.6	13.2	0.107	448	0.138	0.356	515	8250
Stainless Steel 304	8.7	15.1	0.118	494	0.15	0.387	495	7930
Glass ("E" Glass)	0.6	1.0	0.19	796	0.020	0.052	159	2550
Epoxy Resin	0.10	0.173	0.25	1050	0.0053	0.0137	75	1200
Epoxy/ Glass filled 32%	0.22	0.38	0.23	963	0.0087	0.0225	110	1760
Neoprene	0.108	0.187	0.295	1235	0.0041	0.0105	90	1440
Nylon	0.14	0.24	0.4	1675	0.0050	0.013	70	1120
Polytetra-fluoroethylene (Teflon)	0.15	0.26	0.25	1047	0.0043	0.011	138	2210

TABLE 1. (CONTINUED)

Material	Thermal Conductivity		Spec. Heat		Diffusivity		Density	
	$\frac{Btu}{ft-hr-°F}$	$\frac{W}{m-°C}$	$\frac{Btu}{lb-°F}$	$\frac{J}{Kg-°C}$	$\frac{ft^2}{hr}$	$10^5 \frac{m^2}{s}$	$\frac{lb}{ft^3}$	$\frac{Kg}{m^3}$
Poly-trifluoro-chloro-ethylene (KEL-F)	0.04	0.07	0.216	904	0.0014	0.0036	130	2080
Water 32°F	0.320	0.554	0.997	4174	0.0051	0.0132	62.4	999.6
Ice (Pure) 32°F	1.293	2.238	0.5057	2117	0.0445	0.115	57.2	916.3
14°F	1.356	2.347	0.5038	2109	0.0469	0.121	57.3	917.9
-4°F	1.416	2.451	0.5020	2102	0.0492	0.127	57.4	919.5

Latent Heat of Fusion = 143.4 Btu/lb (333.6 KJ/Kg)

TABLE 2. HEATING TIMES REQUIRED TO PRODUCE GIVEN TEMPERATURE RISES OVER THE CENTERLINES OF THE HEATER ELEMENT AND THE GAP BETWEEN ELEMENTS FOR FOUR GAP WIDTHS.

De-Icer Construction:

Substrate	0.100" 304 Stainless Steel
Inner Insulation	0.020" Epoxy/Glass Laminate
Heater Element	Zero Thickness, 0.510" Wide
Outer Insulation	0.010" Epoxy/Glass Laminate
Abrasion Shield	0.010" 304 Stainless Steel
Ice Layer	0.150"
Power Density	25 Watts/in^2

Temp. Rise	10.8°F		21.6°F		36°F	
Gap Width (in.)	Heater	Gap	Heater	Gap	Heater	Gap
0.010	1.0	1.2	2.5	2.8	5.8	6.4
	(1.0)	(1.2)	(2.5)	(2.8)	(6.1)	(6.8)
0.030	1.0	1.5	2.5	3.6	6.0	7.8
	(1.0)	(1.5)	(2.5)	(3.6)	(6.3)	(8.7)
0.050	1.0	1.9	2.5	4.5	6.1	9.4
	(1.0)	(1.9)	(2.5)	(4.6)	(6.4)	(11.0)
0.070	1.0	2.5	2.5	5.6	6.1	11.3
	(1.0)	(2.5)	(2.5)	(5.8)	(6.5)	(14.2)

$h_{b1} = 10$, $h_{b2} = 200$ ( ) $h_{b1} = 1$, $h_{b2} = 10^6$

TABLE 3. EFFECT OF VARIOUS ABRASION SHIELD MATERIALS ON ABRASION SHIELD-ICE INTERFACE TEMPERATURE

Case	Abrasion Shield	Time to Reach 32°F Over Center of Heater (Sec.)		Time to Reach 32°F Over Center of Gap (Sec.)	
		[5]	Present	[5]	Present
1	0.010" S.S.	0.81	0.9	3.73	4.2
2	0.010" nickel	0.80	0.9	3.37	3.8
3	0.010" nickel over 0.010" S.S.	1.10	1.2	3.36	3.7
4	0.020" nickel over 0.010" S.S.	1.35	1.5	1.97	2.2
5	0.010" S.S. over 0.010" nickel	1.12	1.2	1.59	1.9
6	0.010" S.S. over 0.010" Epoxy/Glass over 0.010" nickel	2.12	2.2	2.34	2.6

Other Data as Follows:

Substrate:	0.100" thick, 304 Stainless Steel
Inner Insulation:	0.020" thick, Epoxy/Glass Laminate
Heater Element:	Zero thickness, 0.510" wide
Other Insulation:	0.010" thick, Epoxy/Glass Laminate
Gap between Elements:	0.050" wide

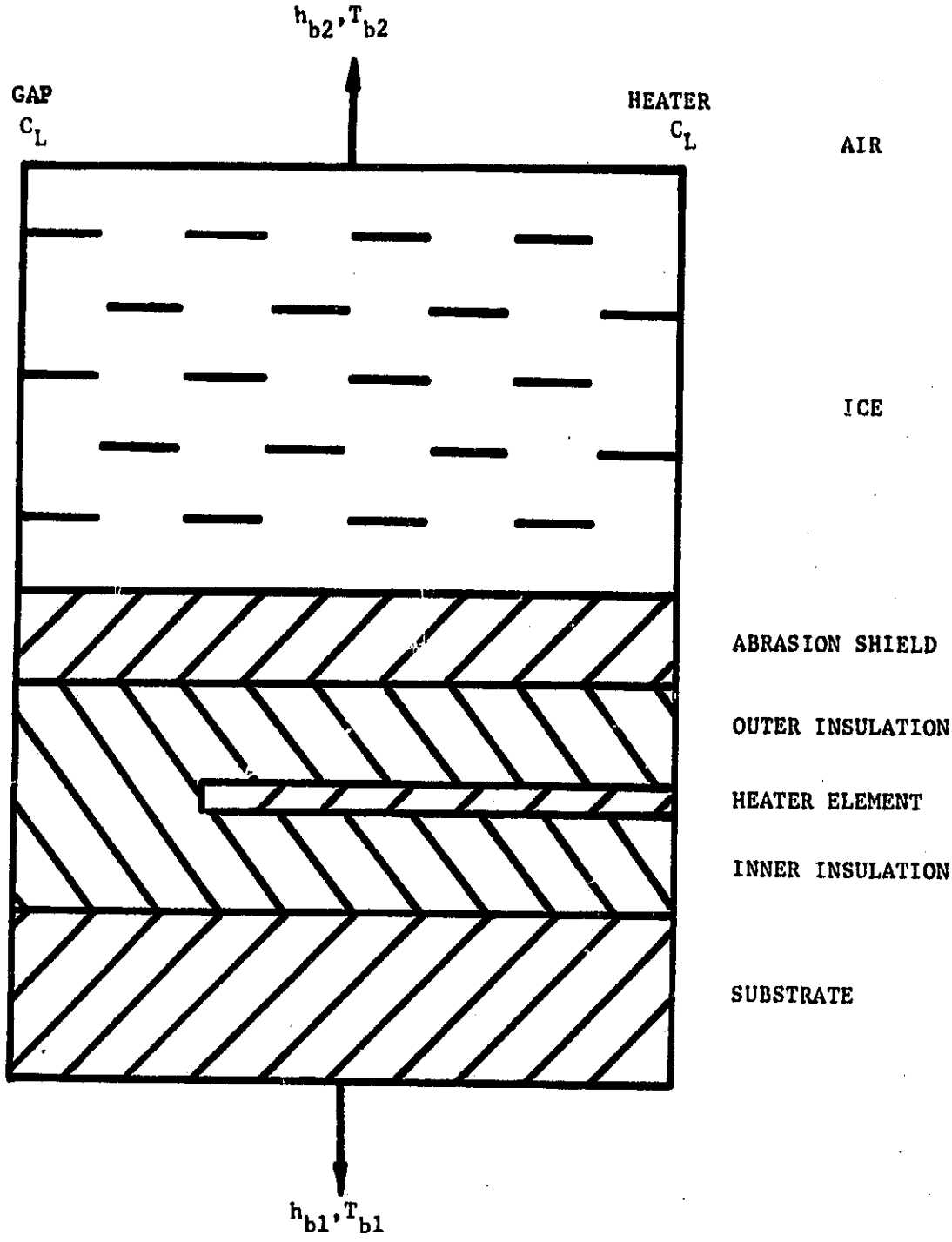

FIGURE 1. TWO-DIMENSIONAL DE-ICER PAD MODEL

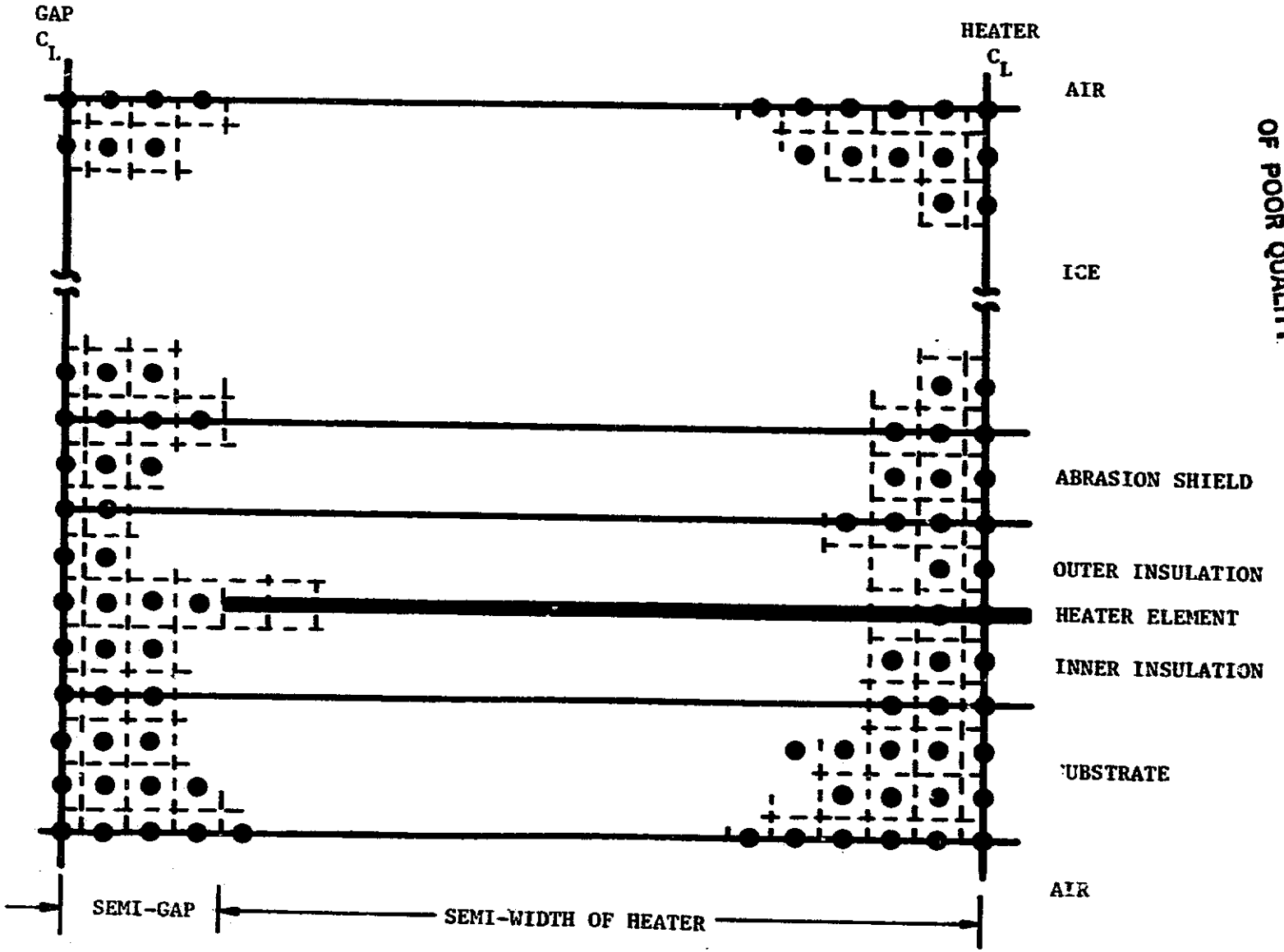

FIGURE 2. TWO-DIMENSIONAL FINITE DIFFERENCE REPRESENTATION

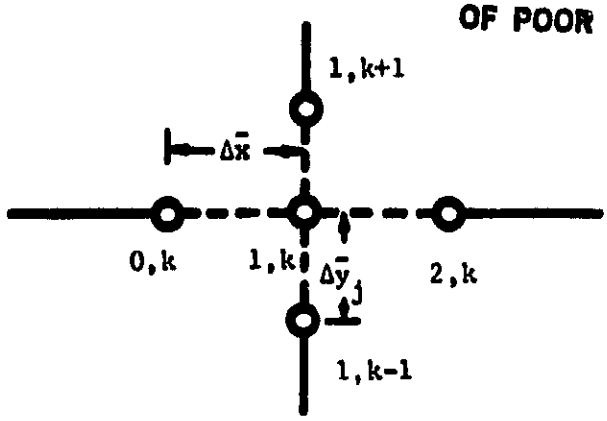

a. Interior Mesh Point at the Center of the Gap

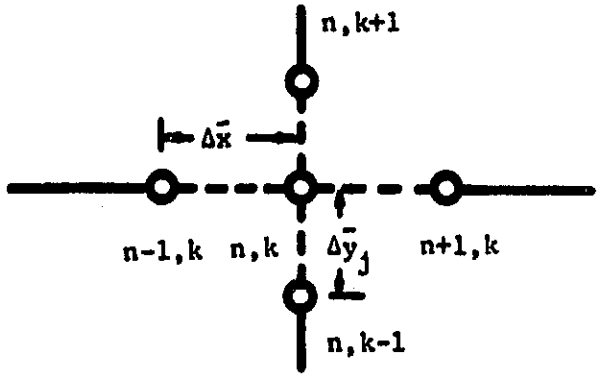

b. Interior Mesh Point at the Center of the Heater

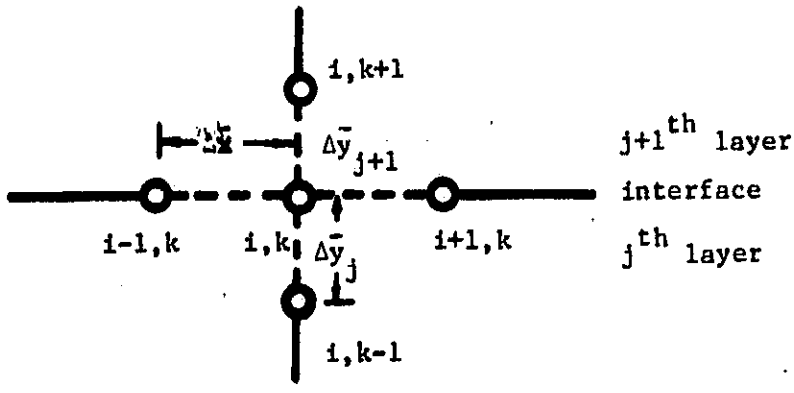

c. Interfacial Point

FIGURE 3. FINITE DIFFERENCE GRID AT SELECTED POINTS

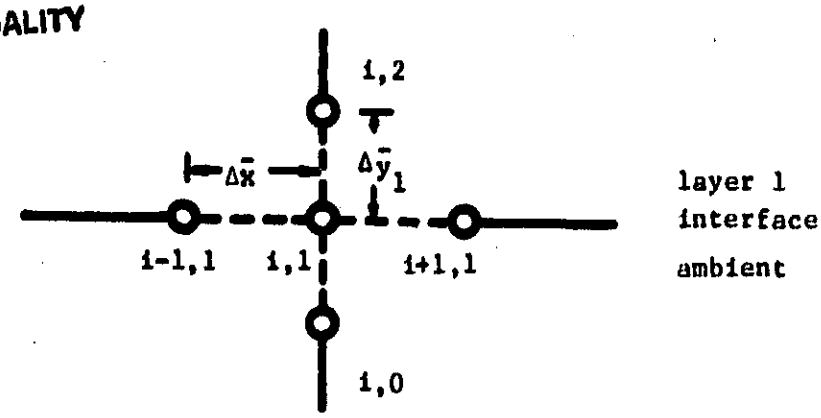

a. Substrate - Ambient Interface

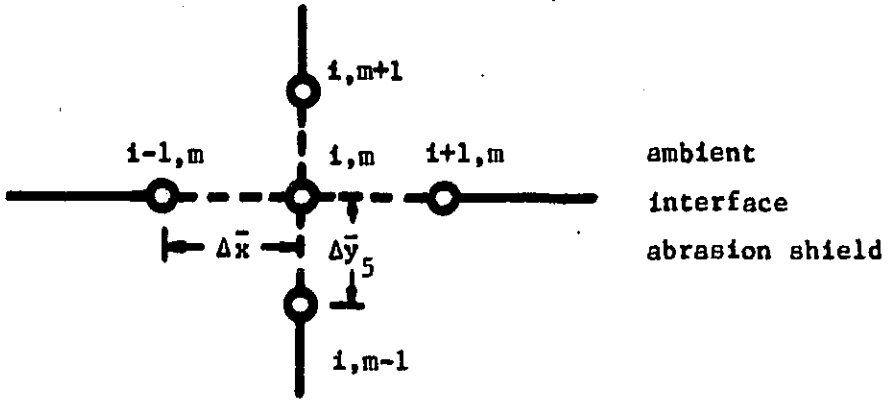

b. Abrasion Shield - Ambient Interface

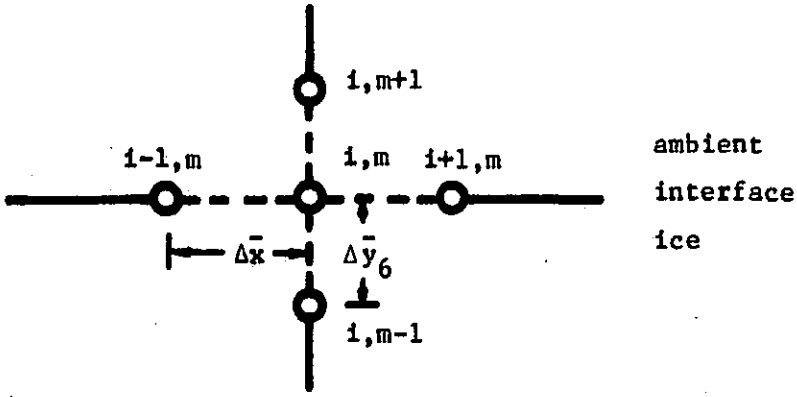

c. Ice-Ambient Interface

FIGURE 4. FINITE DIFFERENCE GRID AT SELECTED POINTS

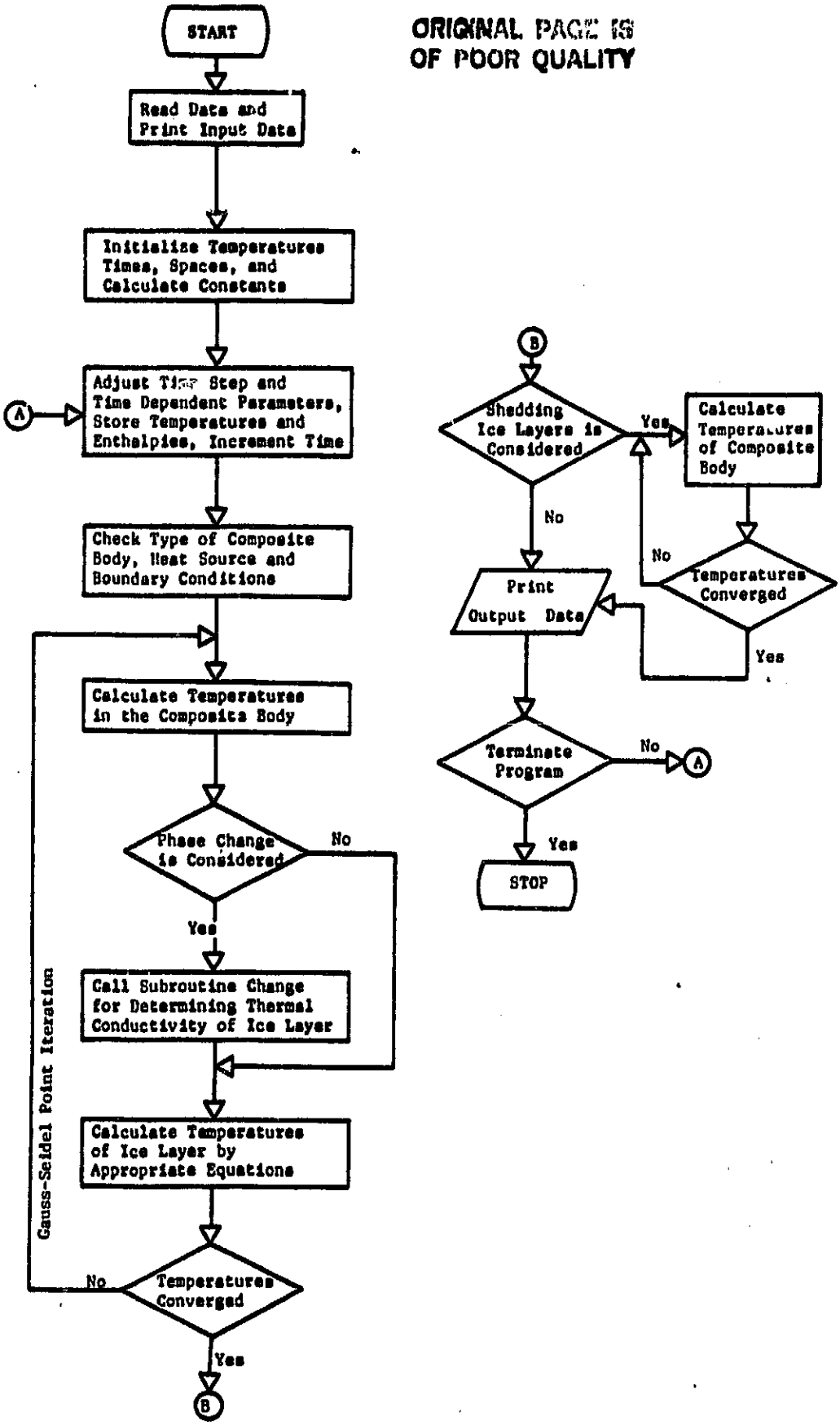

FIGURE 5. FLOW CHART OF COMPUTER PROGRAM

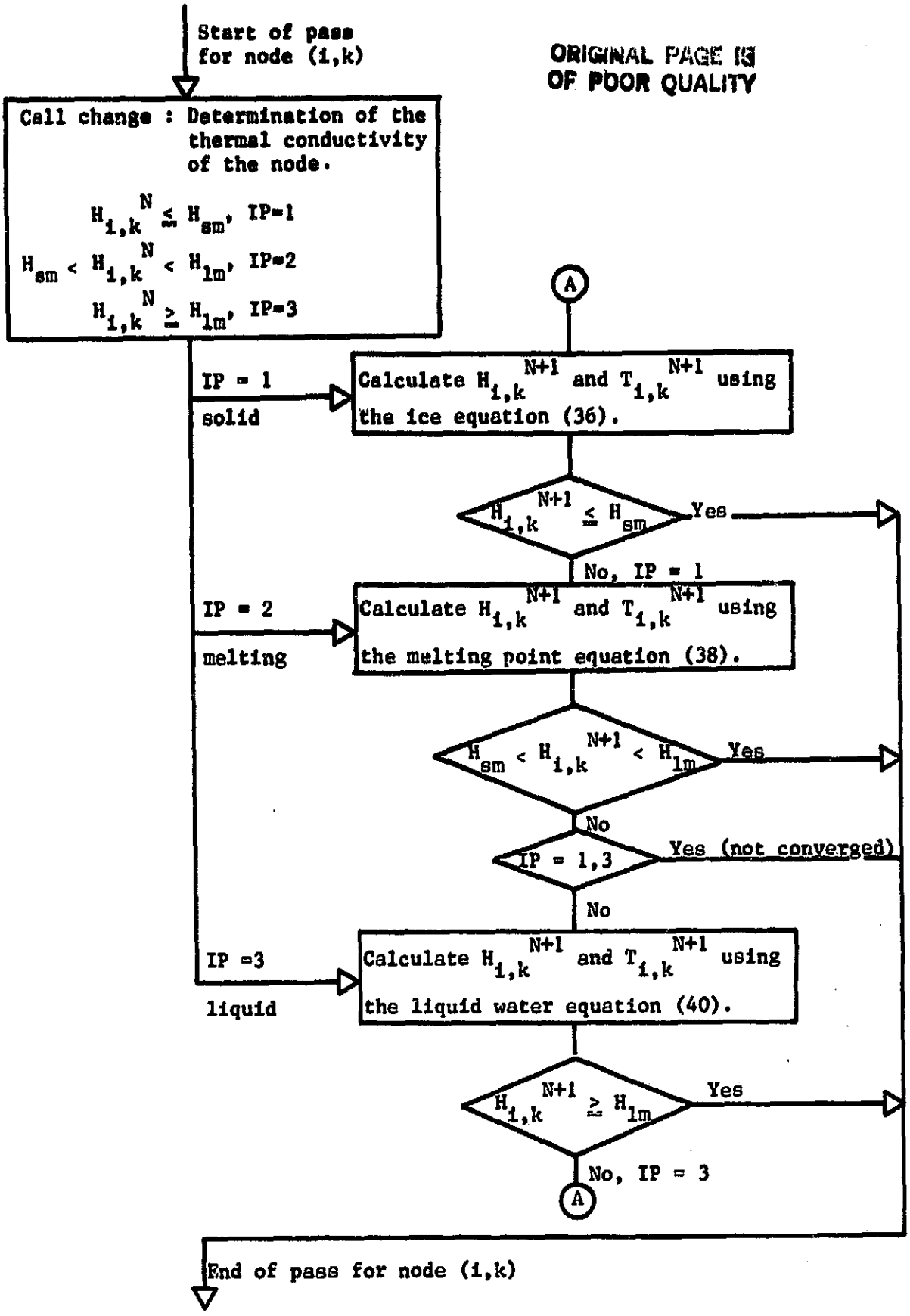

FIGURE 5. FLOW CHART OF COMPUTER PROGRAM (CONTINUED)--- SOLID LIQUID DETERMINATION PROCEDURE FOR ICE-WATER LAYER BY APPLYING ENTHALPY METHOD

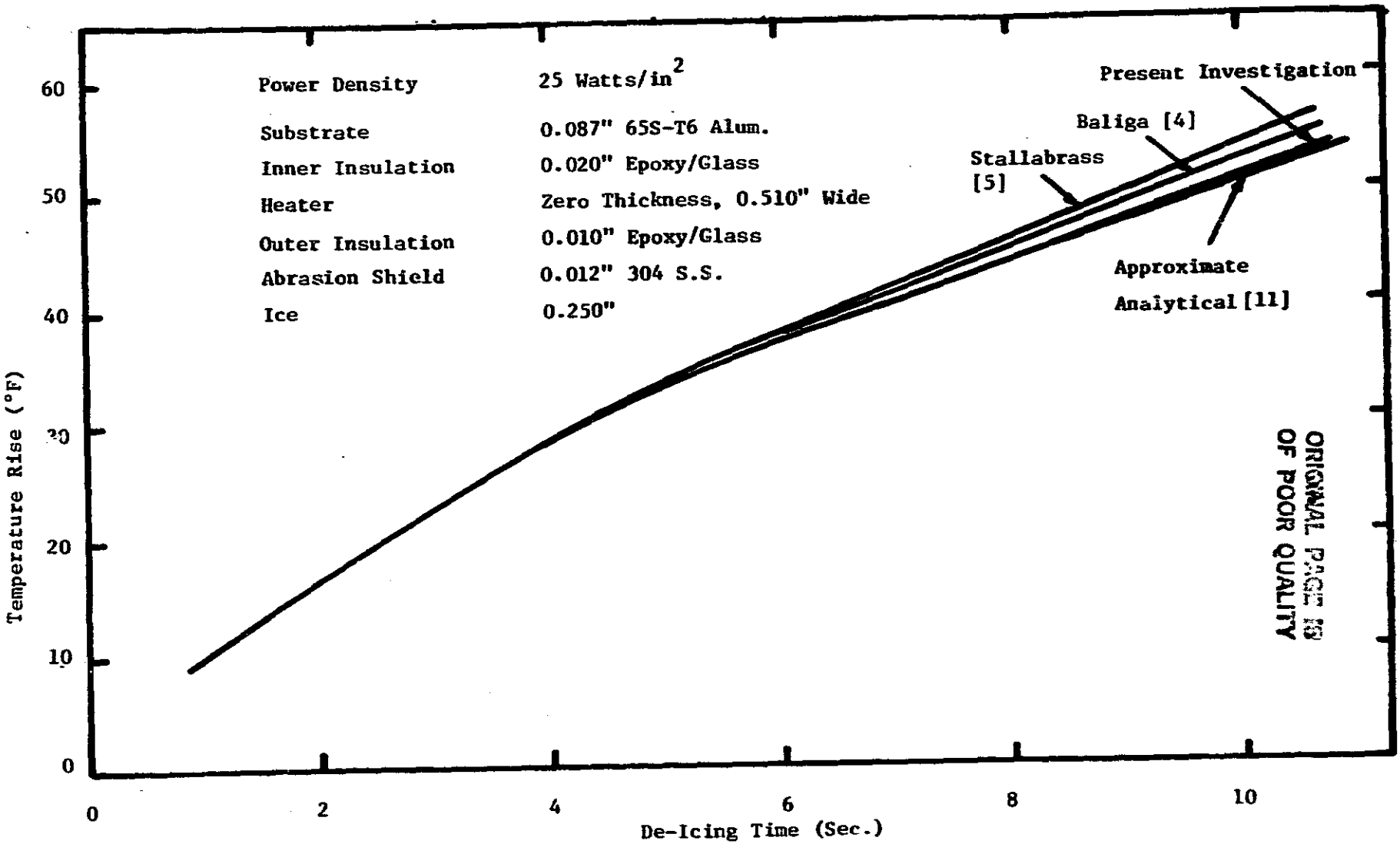

FIGURE 6. COMPARISON OF FINITE DIFFERENCE AND APPROXIMATE ANALYTICAL RESULTS FOR A ONE-DIMENSIONAL DE-ICER PAD

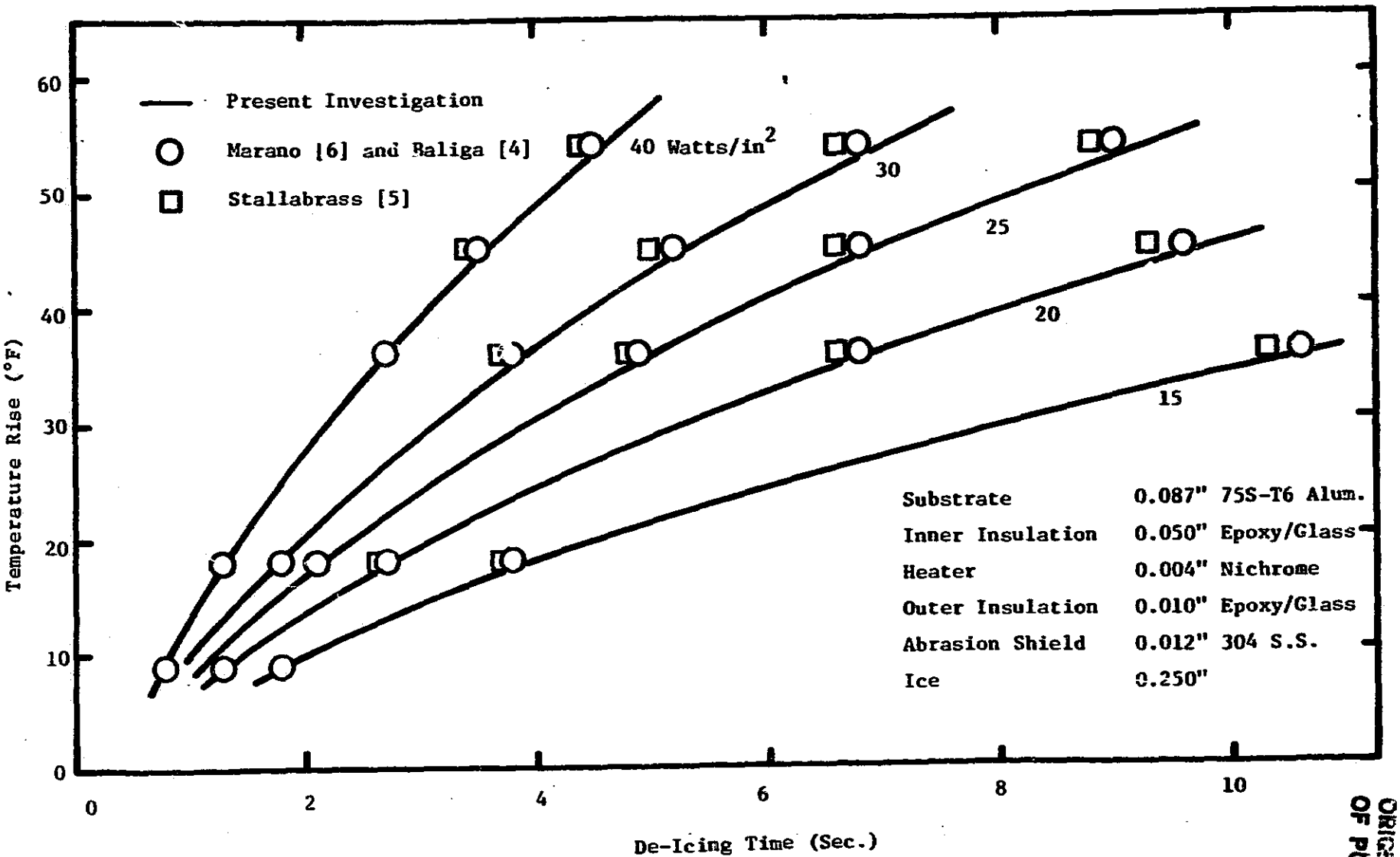

FIGURE 7. EFFECT OF POWER DENSITY ON DE-ICER PERFORMANCE

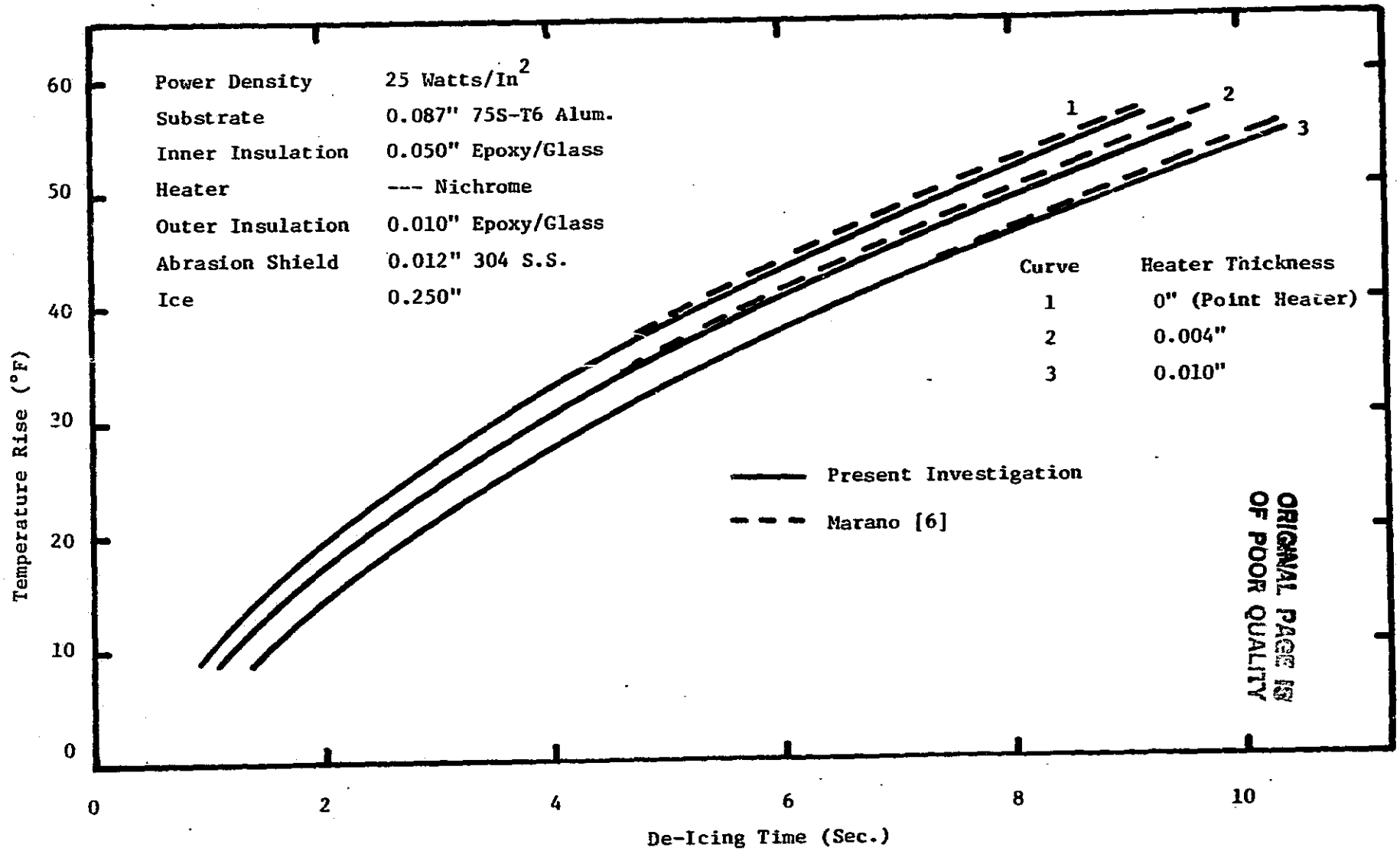

FIGURE 8. COMPARISON OF RESPONSE OF POINT AND FINITE THICKNESS HEATERS

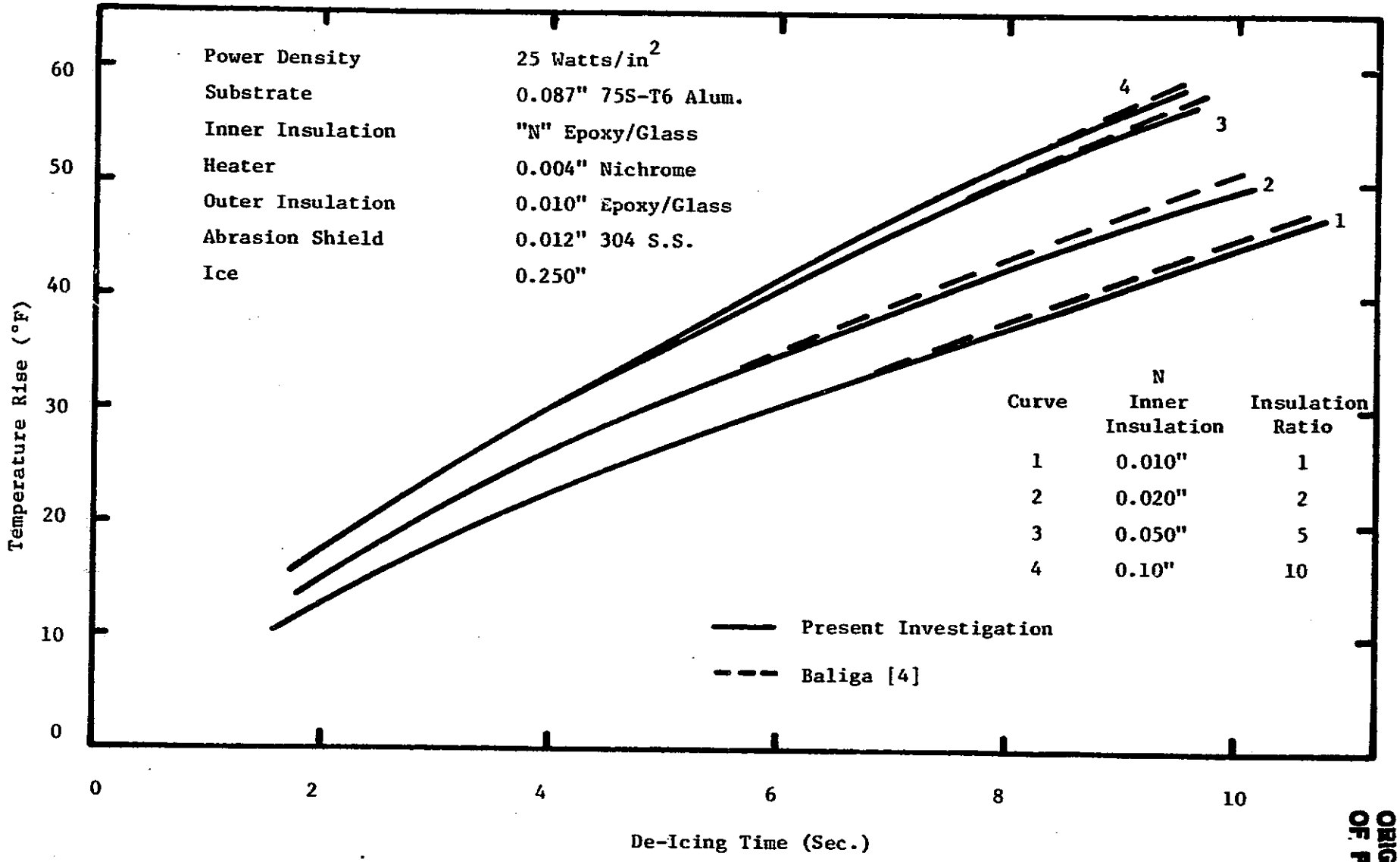

FIGURE 9. COMPARISON OF DE-ICING TIME FOR VARIOUS RATIOS OF INNER TO OUTER INSULATION THICKNESS

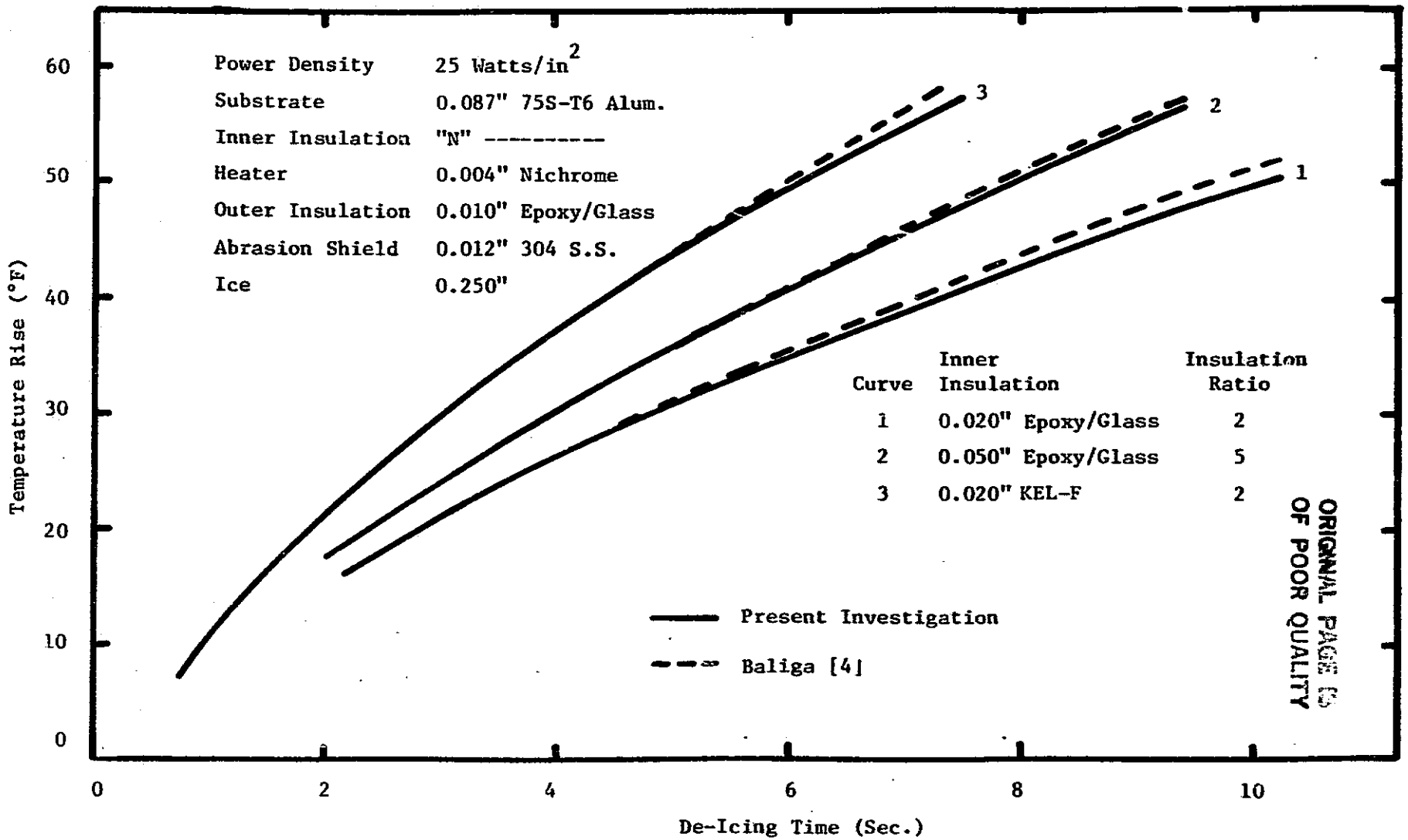

FIGURE 10. EFFECT OF INSULATION THICKNESS RATIO AND THERMAL MATERIAL ON DE-ICING TIME

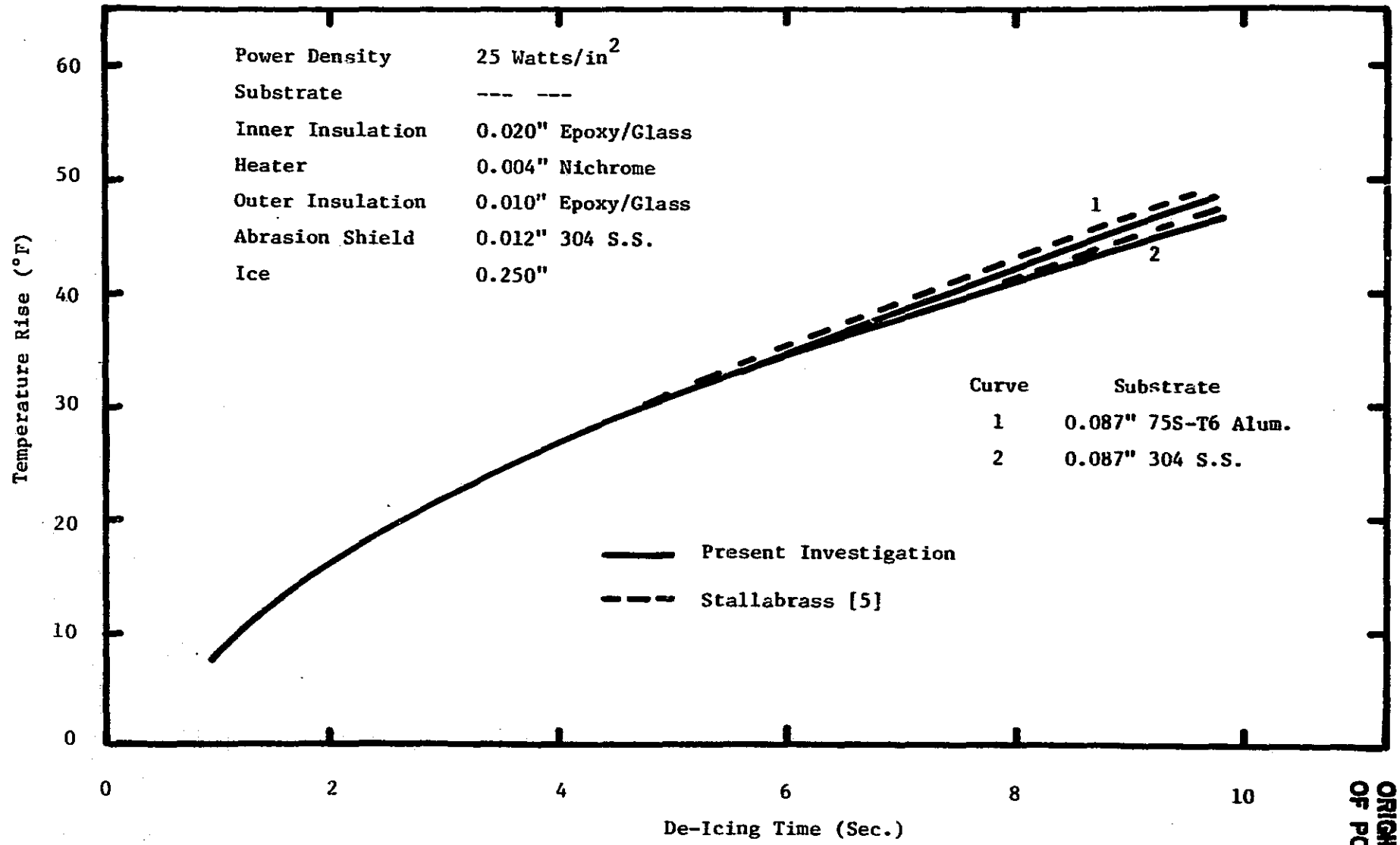

FIGURE 11. COMPARISON OF DE-ICING TIME FOR VARIOUS SUBSTRATE MATERIALS

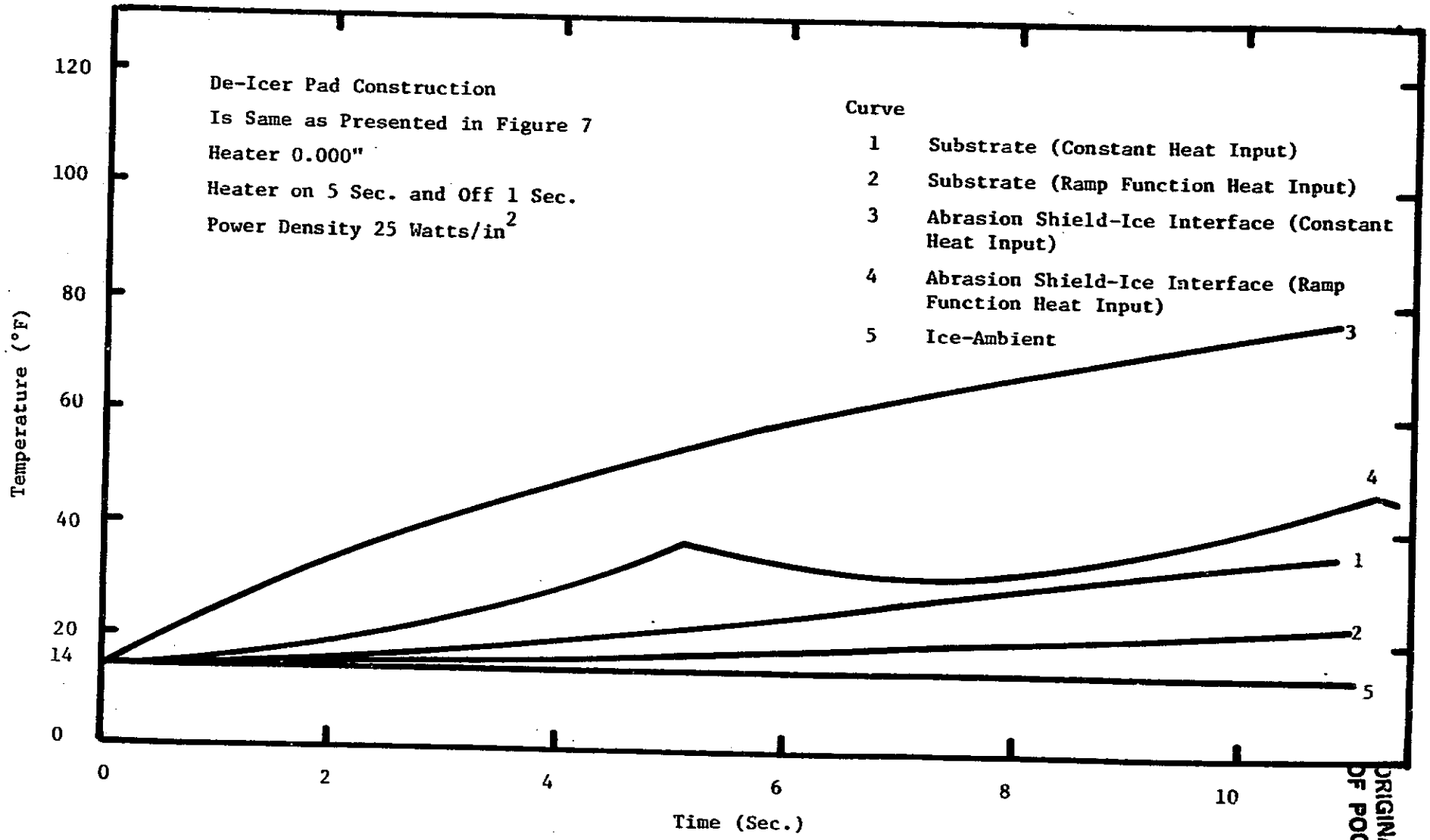

FIGURE 12a. COMPARISON OF INTERFACIAL TEMPERATURE RESPONSE FOR RAMP FUNCTION AND CONSTANT POINT HEAT SOURCE

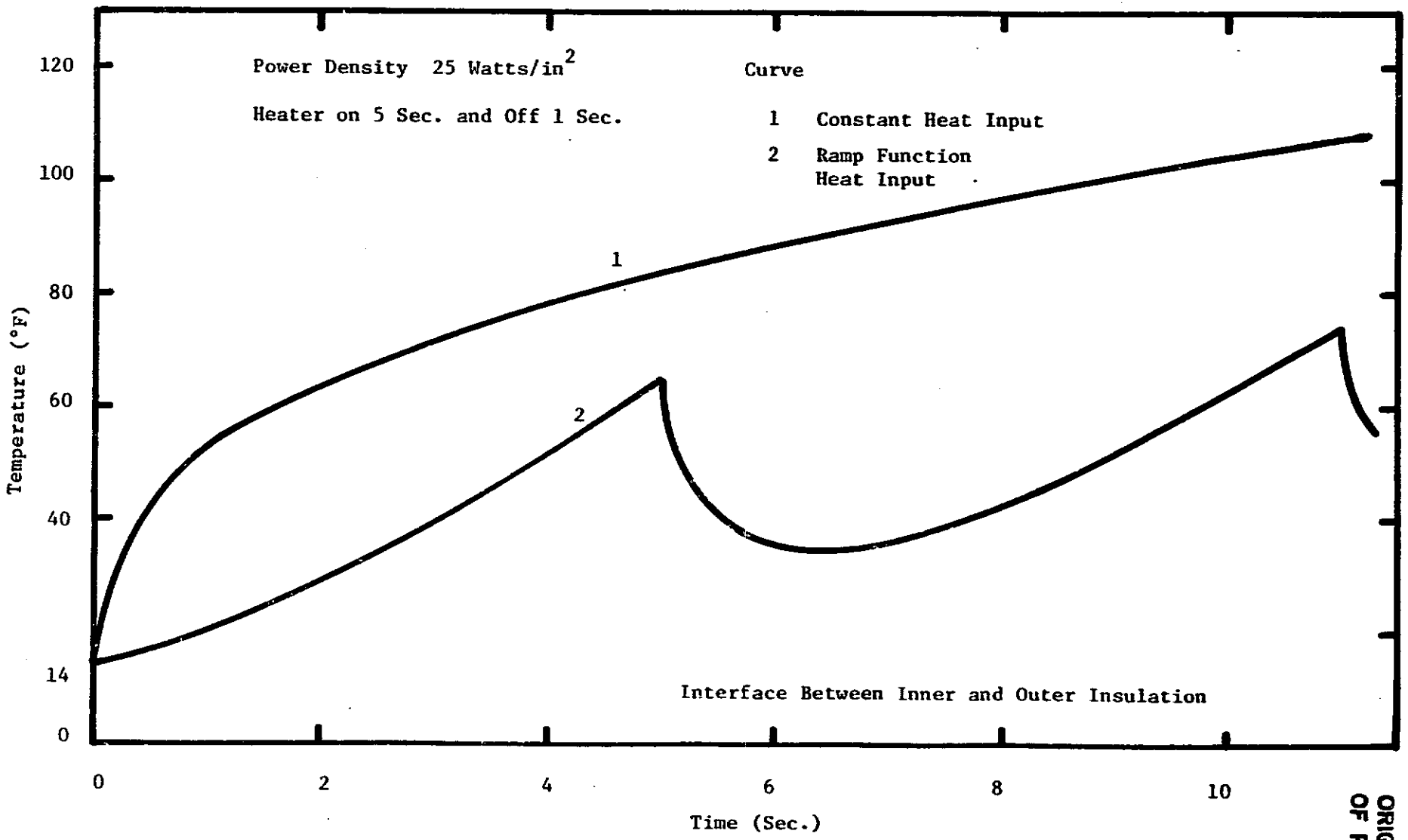

FIGURE 12b. COMPARISON OF INTERFACIAL TEMPERATURE RESPONSE FOR RAMP FUNCTION AND CONSTANT POINT HEAT SOURCE

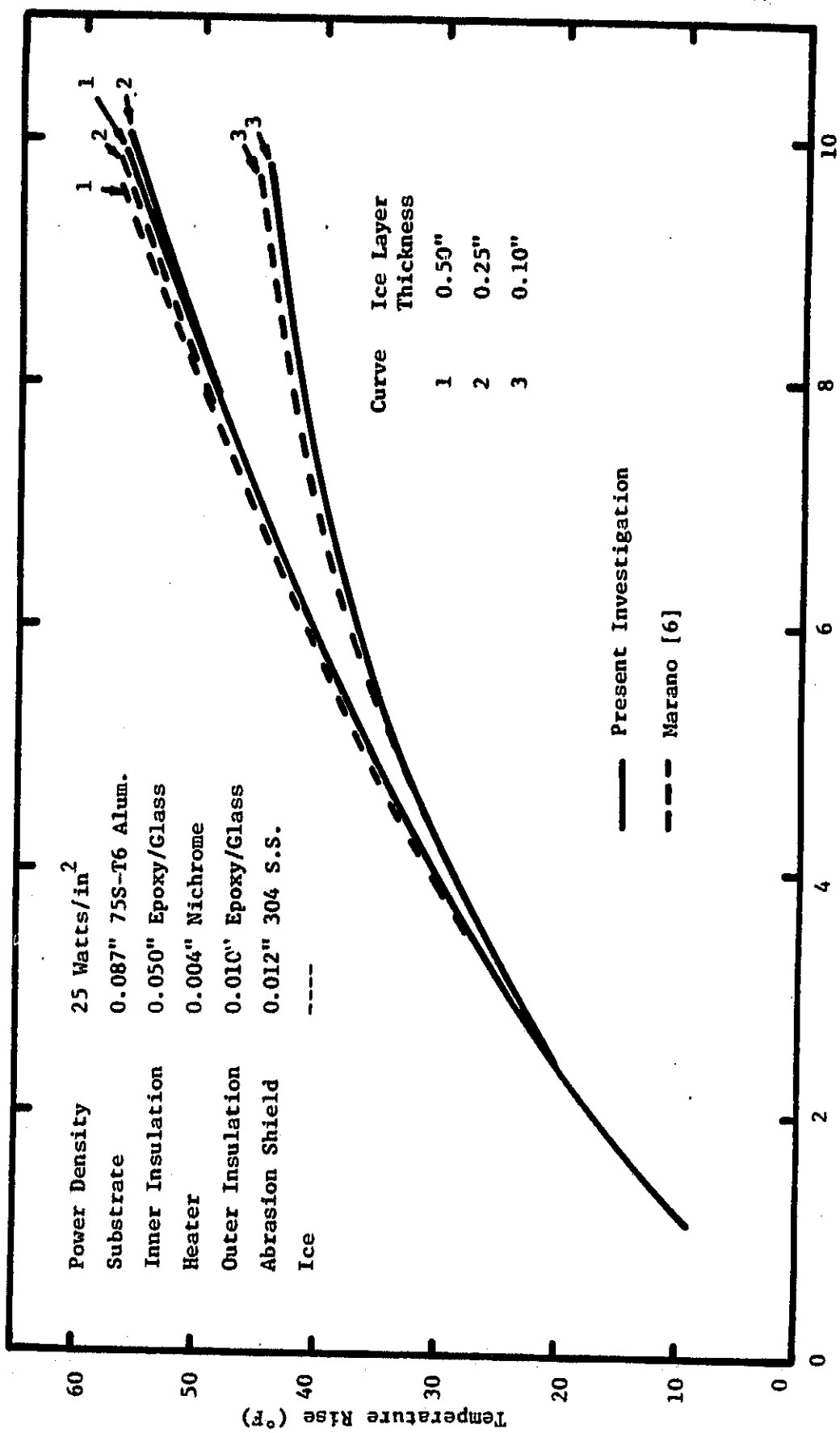

FIGURE 13. EFFECT OF INITIAL ICE LAYER THICKNESS ON DE-ICER PERFORMANCE

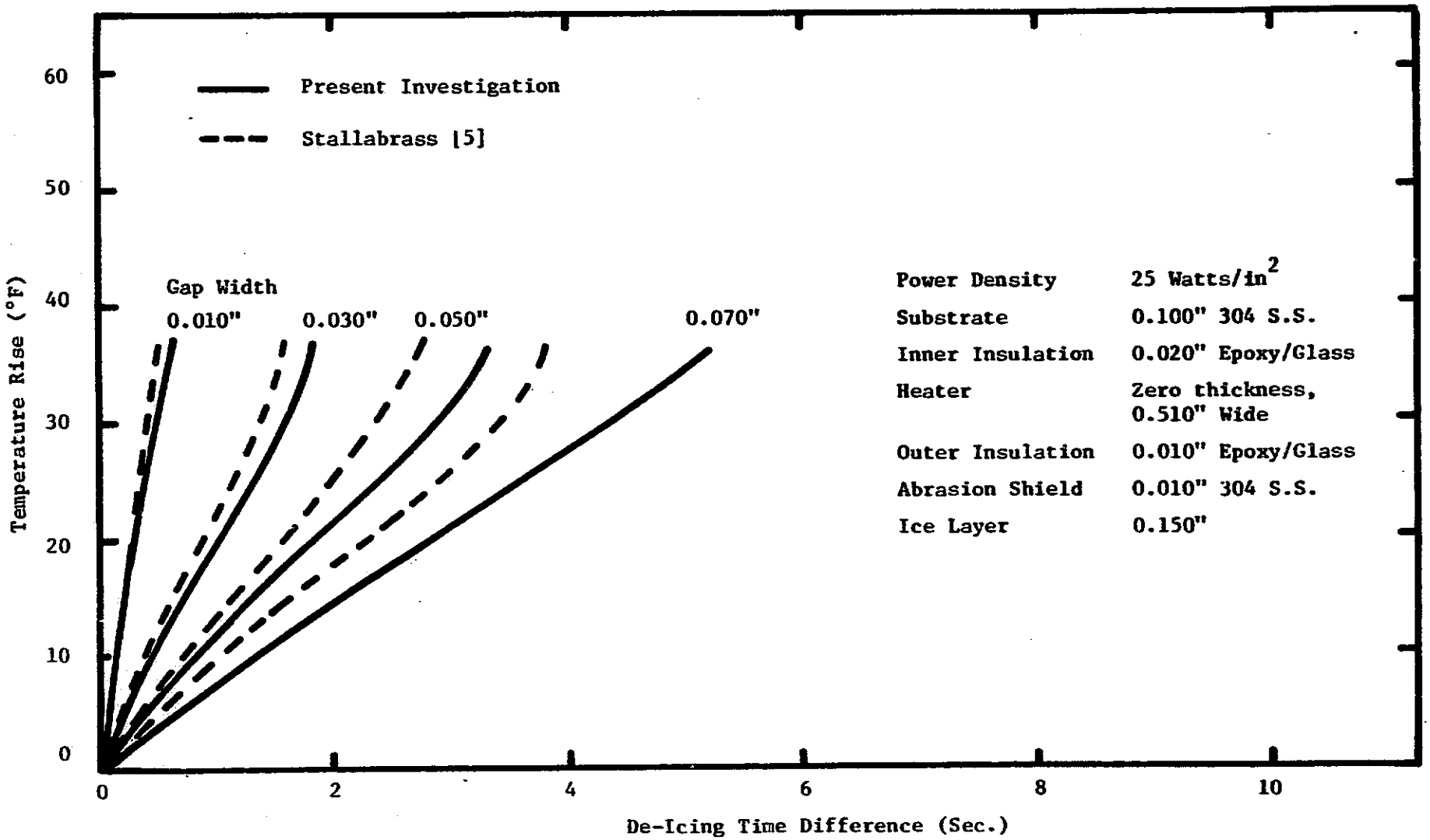

FIGURE 14. TIME DIFFERENCE BETWEEN INTERFACE ABOVE CENTER OF HEATER AND INTERFACE ABOVE CENTER OF GAP TO ACHIEVE A GIVEN TEMPERATURE RISE

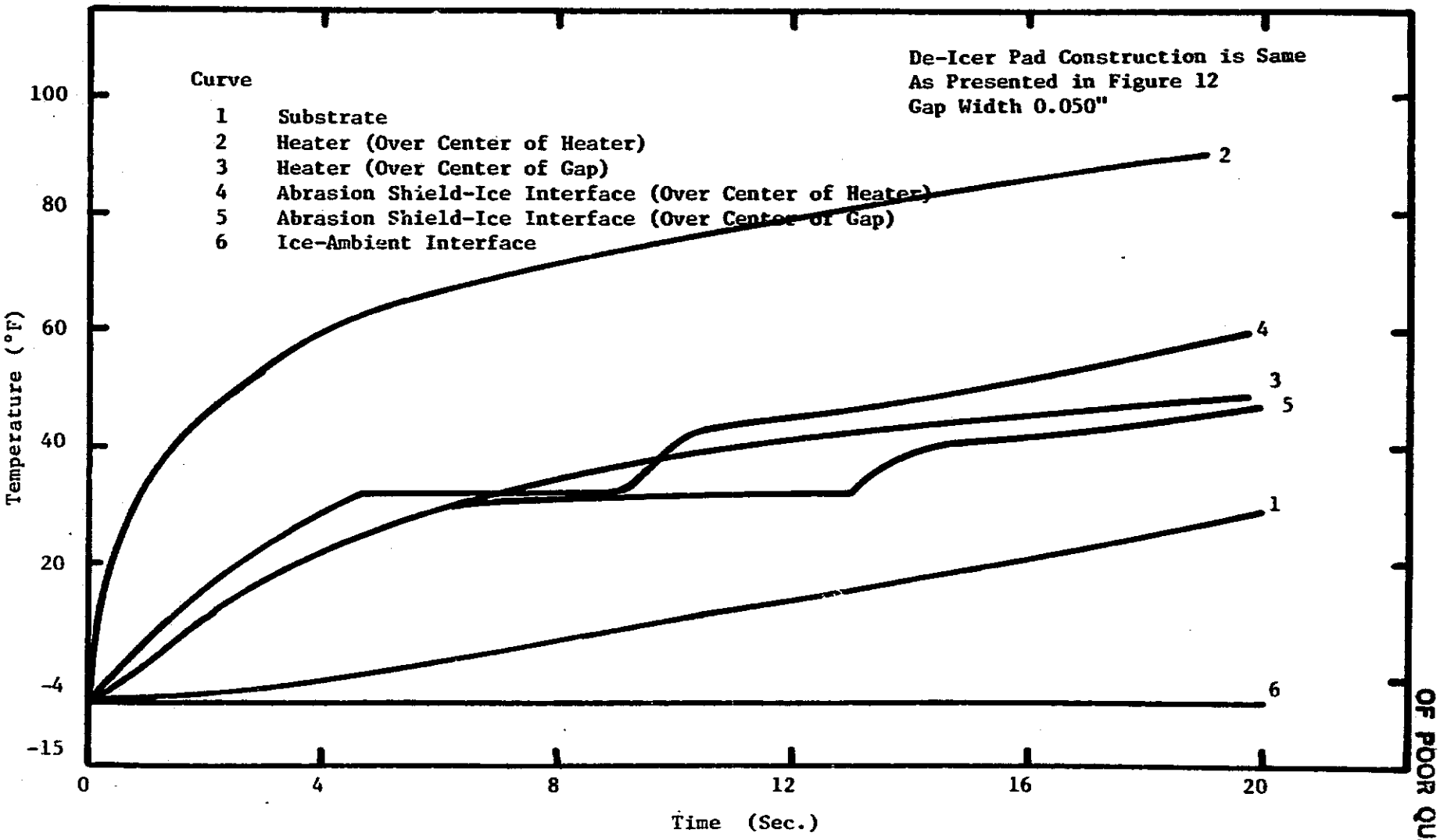

FIGURE 15. TEMPERATURE PROFILES FOR THE TWO-DIMENSIONAL DE-ICER PAD

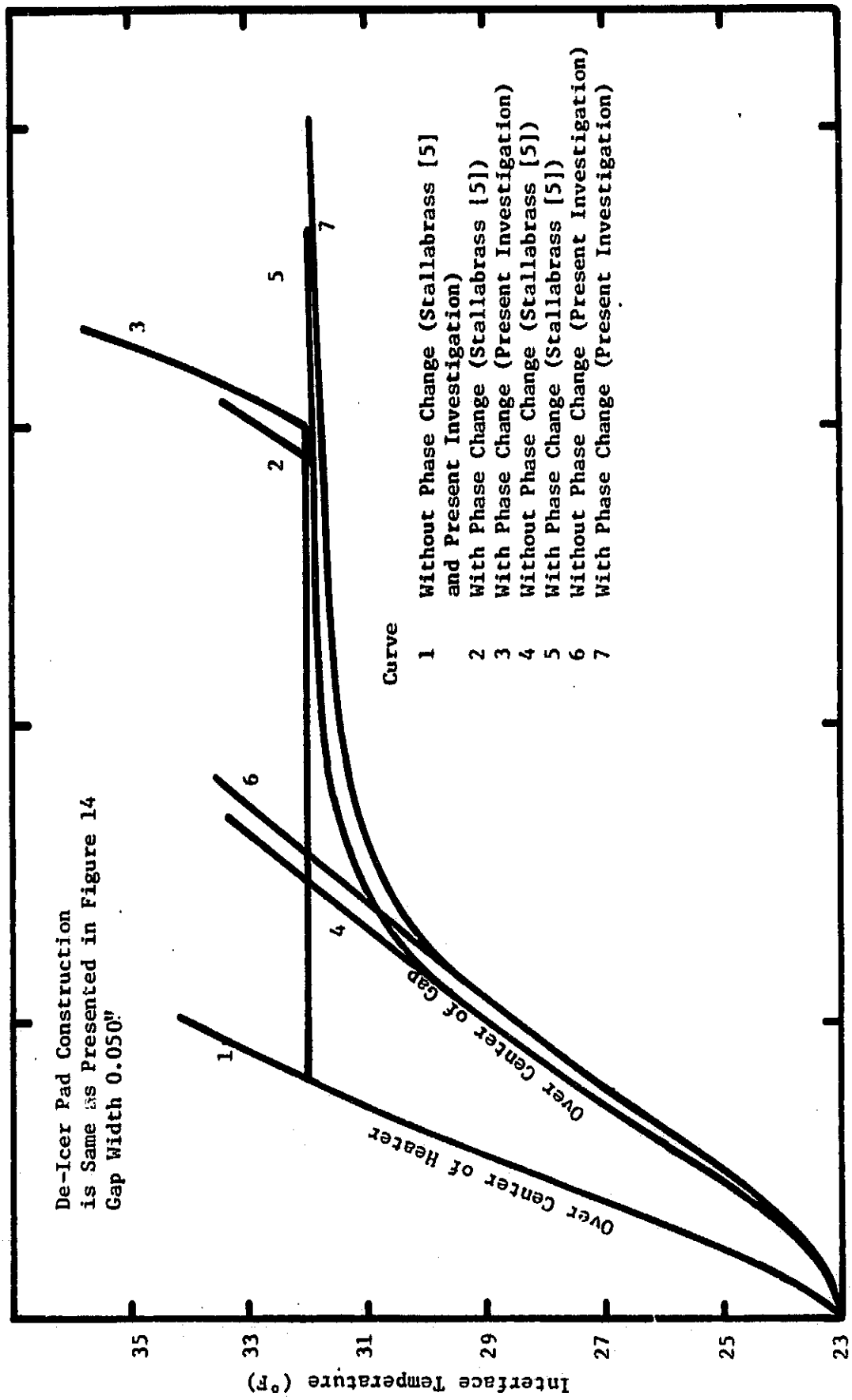

FIGURE 16. EFFECT OF ICE MELTING ON INTERFACE TEMPERATURE

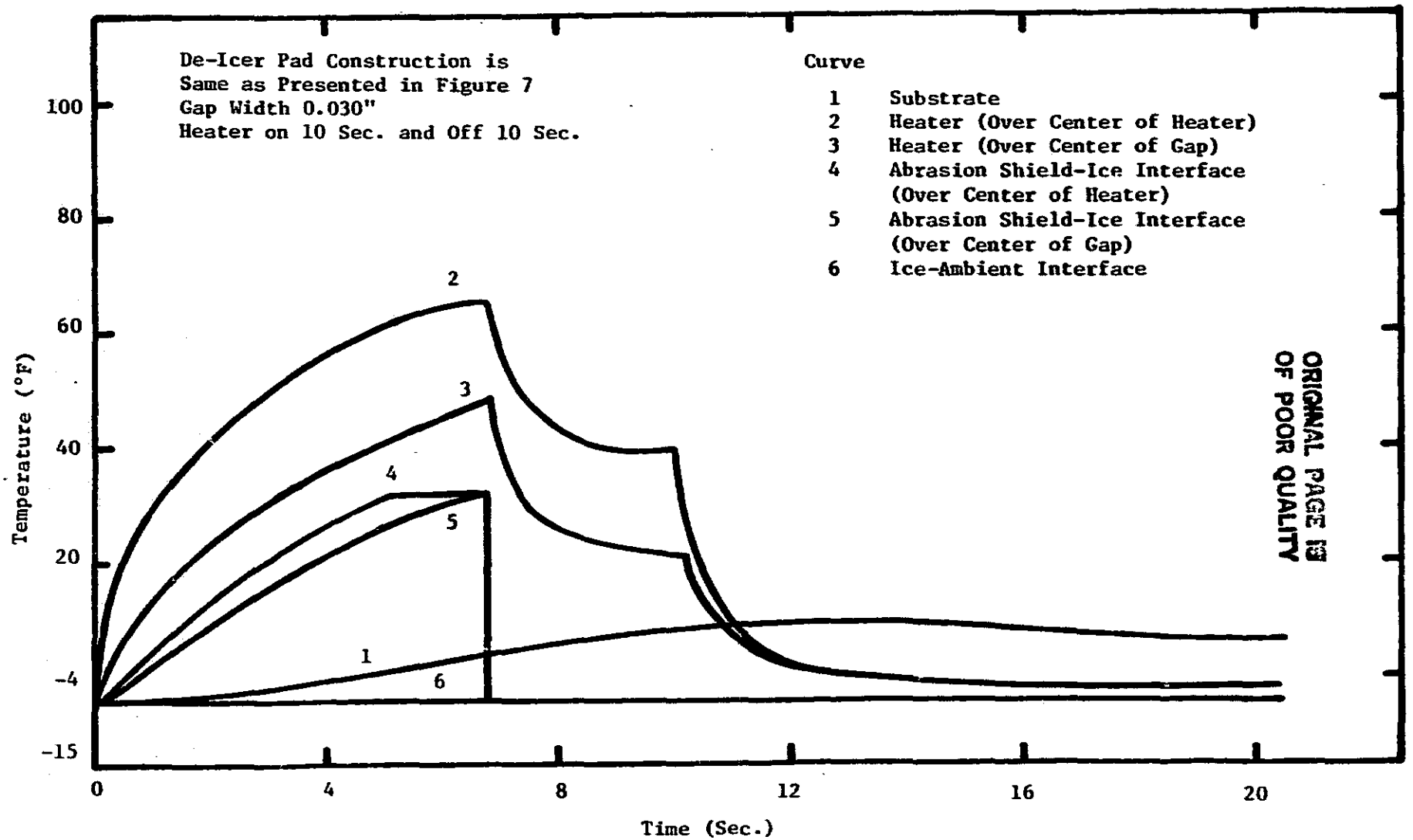

FIGURE 17. TEMPERATURE PROFILES WHEN ICE LAYER IS SHED, 1st CYCLE

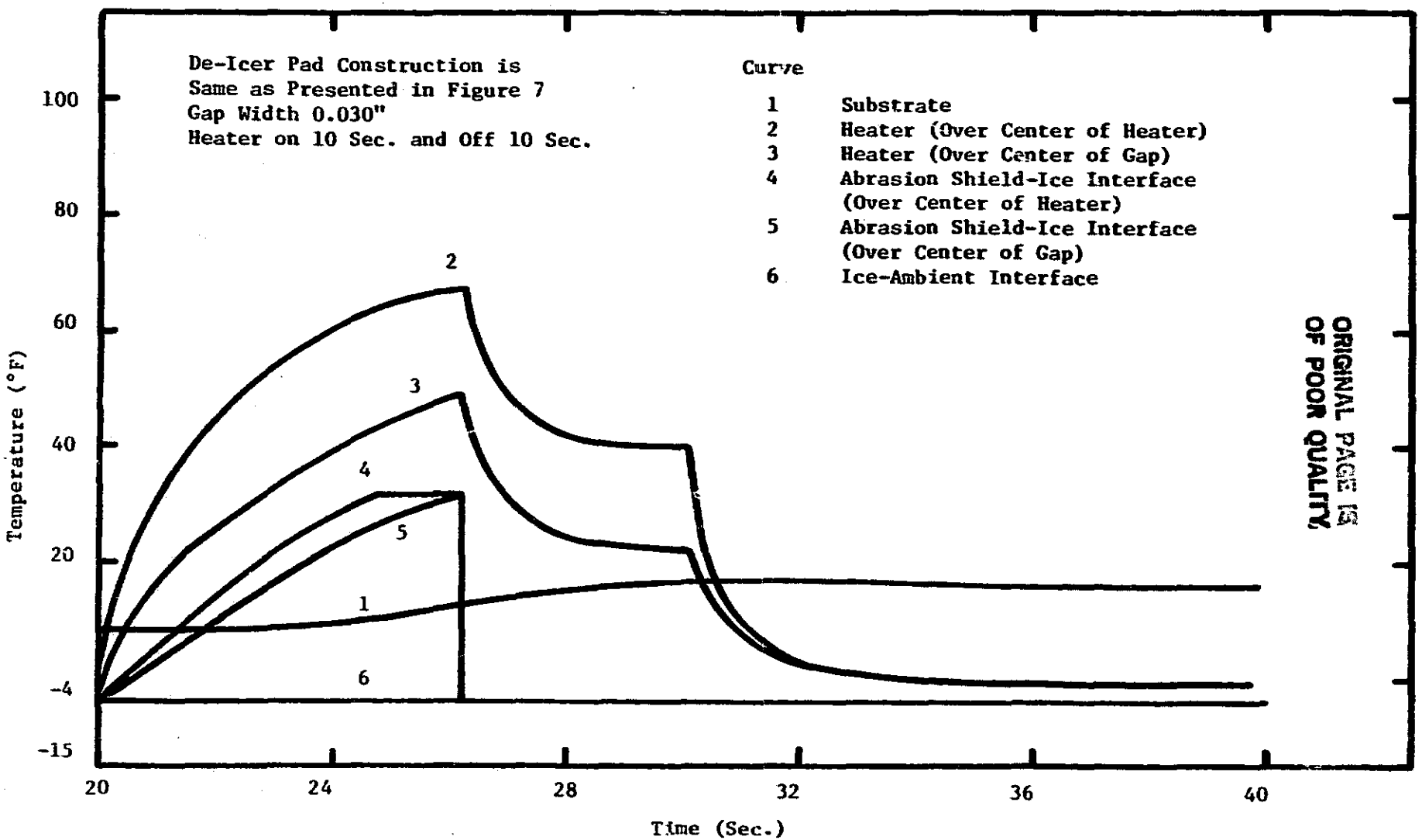

FIGURE 18. TEMPERATURE PROFILES WHEN ICE LAYER IS SHED, 2nd CYCLE

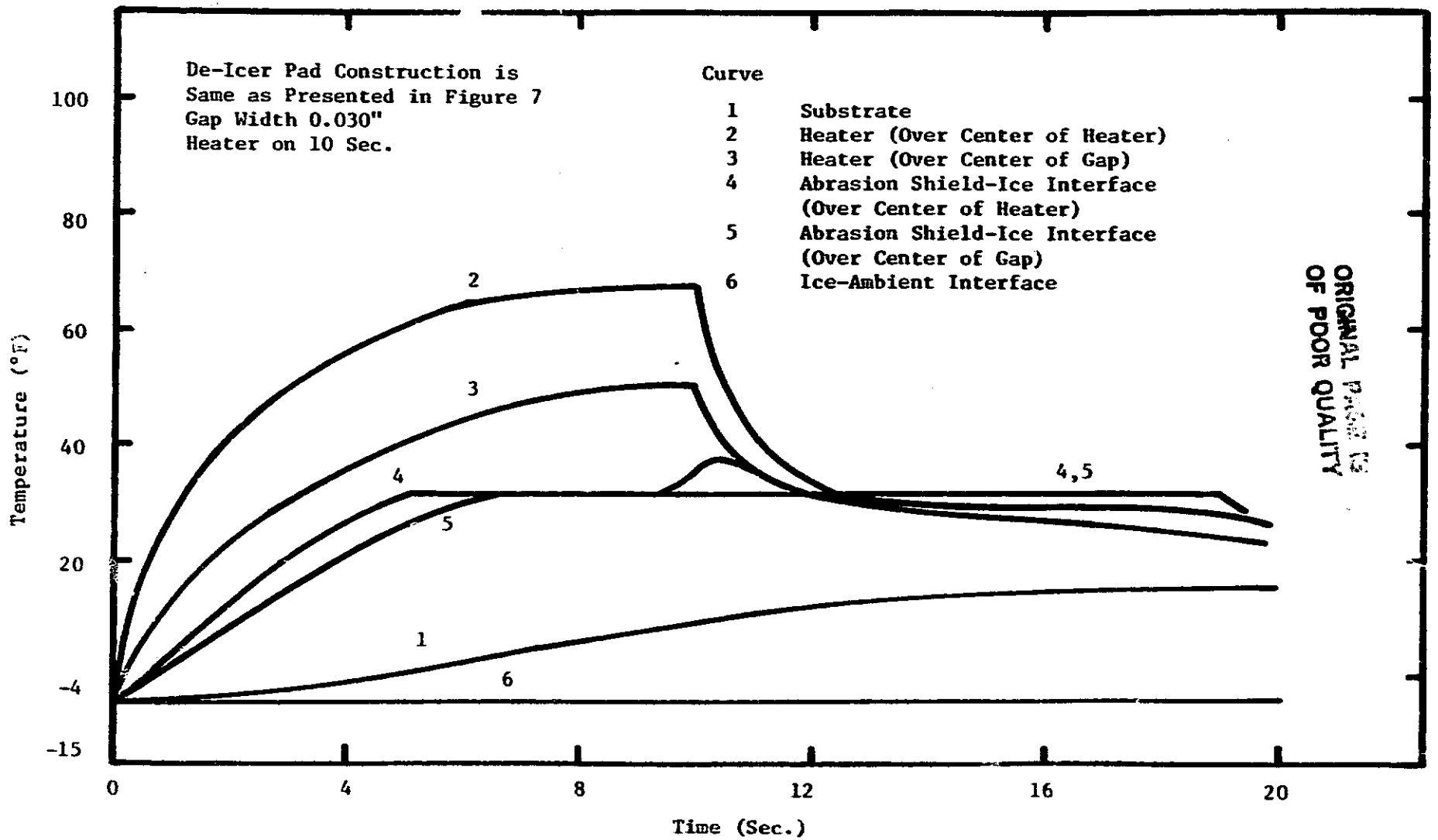

FIGURE 19. TEMPERATURE PROFILES WITH REFREEZING